INFERENCE OF POLYMER ADSORPTION FROM ELECTRICAL DOUBLE LAYER MEASUREMENTS

THE SILVER IODIDE-POLYVINYL ALCOHOL SYSTEM

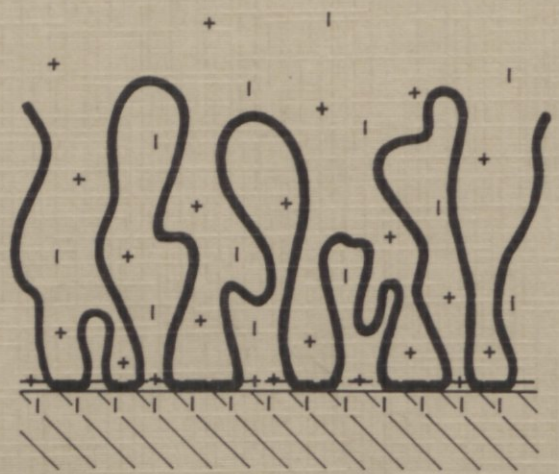

L. K. KOOPAL

Promotor: dr. J. LYKLEMA, hoogleraar in de fysische en kolloïdchemie

546.57'151:541.183.53:541.64:678.744.72

L. K. KOOPAL

INFERENCE OF POLYMER ADSORPTION FROM ELECTRICAL DOUBLE LAYER MEASUREMENTS

THE SILVER IODIDE-POLYVINYL ALCOHOL SYSTEM

PROEFSCHRIFT

TER VERKRIJGING VAN DE GRAAD
VAN DOCTOR IN DE LANDBOUWWETENSCHAPPEN,
OP GEZAG VAN DE RECTOR MAGNIFICUS,
DR. H. C. VAN DER PLAS,
HOOGLERAAR IN DE ORGANISCHE SCHEIKUNDE,
IN HET OPENBAAR TE VERDEDIGEN
OP WOENSDAG 3 MEI 1978
DES NAMIDDAGS TE VIER UUR IN DE AULA
VAN DE LANDBOUWHOGESCHOOL TE WAGENINGEN

H. VEENMAN & ZONEN B.V. – WAGENINGEN – 1978

STELLINGEN

I

De berekening van de dikte van een geadsorbeerde polymeerlaag uit electroforese metingen moet bij voorkeur gebaseerd zijn op de variatie van de zeta-potentiaal met de wand-potentiaal, gemeten rond het iso-electrisch punt.

B.V. KAVANAGH, A.M. POSNER, J.P. QUIRK, Faraday Discuss. Chem. Soc. **59**, 242 (1975).
A. A. BARAN, I. I. KOCHERGA, I. M. SOLOMENTSEVA, O. D. KURILENKO, Kolloidn. Zh. **38**,16 (1976).
M. J. GARVEY, T. F. TADROS, B. VINCENT, J. Colloid Interface Sci. **55**, 440 (1976).
Dit proefschrift, hoofdstuk 6.

II

De bepaling van het specifiek oppervlak van zilverjodide in solen dient te geschieden aan niet gevlokte solen.

Dit proefschrift, hoofdstuk 3.

III

De evenredigheidsconstante, ξ, die aangeeft hoe de hydrodynamische straal van een opgelost polymeermolecuul afhangt van zijn gyratiestraal, houdt nauw verband met het type stroming. De waarde van ξ ligt tussen 0.665 en 1.037.

C. H. TANFORD, 'Physical Chemistry of Macromolecules', J. Wiley and Sons, New York (1967), hoofdstuk 6.
Dit proefschrift, hoofdstuk 7.

IV

Het verdient aanbeveling de Japanse Industriële Standaard voor de berekening van de polymerisatiegraad van polyvinylalcohol uit viscositeitsmetingen te herzien.

Japan Industrial Standard K 6726–1965: 'Testing methods for Polyvinyl Alcohol', zie C. A. FINCH in 'Polyvinyl Alcohol, properties and applications', C. A. FINCH Ed., J. Wiley and Sons, New York (1973), Appendix 3.

V

Bij de verklaring van het adsorptiegedrag van protonen aan actieve kool van het H-type gaan Mattson en Mark er ten onrechte vanuit dat specifieke adsorptie van anionen leidt tot adsorptie van kationen in het diffuse deel van de electrische dubbellaag.

J. S. MATTSON en H. B. MARK jr., 'Activated Carbon, surface chemistry and adsorption from solution', Marcel Dekker Inc., New York (1971), hoofdstuk 5 en 6.

VI

De door Baret gegeven beschrijving van de adsorptie, op basis van de 'significante structuren theorie' van Eyring et al., draagt niet bij tot een beter begrip van een partieel mobiele monolaag geadsorbeerd vanuit oplossing.

J. F. BARET, Kolloid-Z. Z. Polym. **246**, 636 (1971).
H. EYRING, T. REE en N. HIRAI, Proc. Nat. Acad. Sci., U.S.A. **44**, 683 (1958).

VII

De wet van massawerking levert, gezien vanuit didactisch oogpunt, een betere vuistregel voor de omwisseling van kationen in de bodem dan de regel van Gapon.

'Soil chemistry, basic elements', G. H. BOLT, M. G. M. BRUGGENWERT Eds., Elsevier Scientific Publ. Comp., Amsterdam (1976), hoofdstuk 4.
E. N. GAPON, J. Gen. Chem. U.S.S.R. **3**, 144 (1933).

VIII

De door Alian, Sanad en Hassan voorgestelde methode ter bepaling van germanium-lithium detector-efficiëntiecurven voor gammastraling is veel minder nauwkeurig dan de auteurs doen geloven.

A. ALIAN, W. SANAD en A. M. HASSAN, Radiochem. Radional. Letters **22**, 37 (1975).
A. ALIAN, H. J. BORN en J. I. KIM, J. Radioanal. Chem. **15**, 535 (1973).

IX

De door Salvato en Tallandini opgestelde hypothese, dat ureum en calciumionen een soortgelijk effect hebben op de zuurstofbinding van *Octopus vulgaris* hemocyanine, is onjuist.

B. SALVATO en L. TALLANDINI in 'Structure and function of haemocyanin', J. V. BANNISTER Ed., Springer Verlag, Berlin (1977), pag. 217.

X

De door Van Vliet en Van Zelm verrichte metingen vormen een onvoldoende basis voor de vaststelling van de te gebruiken hoeveelheid actieve kool in de zogenaamde Paterson installatie, welke in tijden van rampspoed wordt gebruikt om de Nederlandse militair van drinkwater te voorzien.

A. VAN VLIET en M. VAN ZELM, in 'Sorption and filtration methods for gas and water purification', M. BONNEVIE-SVENDSEN Ed., Nato Advanced Study Institute Series, E, **13**, 425 (1975).
A. VAN VLIET, The Military Engineer **421**, 319 (1972).

XI

Het is te betreuren, dat een niet-onbelangrijk deel van de afgestudeerde Wageningse ingenieurs die een betrekking als leraar aanvaarden, aan een vakspecifieke scholing de voorkeur hebben gegeven boven een vakdidactische scholing.

'De Wageningse ingenieur in functie, verslag van een onderzoek naar de maatschappelijke plaats van afgestudeerden aan de Landbouwhogeschool te Wageningen in de periode 1963–1973.' Rapport Stichting Maatschappelijke Plaats Wageningse Afgestudeerden (1976).
Gegevens afdeling Onderwijs en Wetenschap, sectie studentendocumentatie en statistiek.

XII

Het is onjuist om bij het vaststellen en invullen van de propaedeutische studieprogramma's te veronderstellen, dat zij die het voorbereidend wetenschappelijk onderwijs met vrucht gevolgd hebben, al werkelijk kunnen studeren.

XIII

De 'betere' boer schenkt meer aandacht aan de voeding van zijn stalgenoten dan aan die van zijn huisgenoten.

XIV

Trottoirparkeren is het onrecht van de sterkste.

Proefschrift LIEUWE KORNELIS KOOPAL
'Inference of polymer adsorption from electrical double layer measurements'
Wageningen, 3 mei 1978.

This thesis is also published as Mededelingen Landbouwhogeschool Wageningen 78-12 (1978)
(Communications Agricultural University Wageningen, The Netherlands)

Er zijn twee mogelijkheden om over een zaak met zekerheid te spreken:
Als men er veel en als men er niets van weet.

Aan mijn ouders
Voor Els, Marjan en Heleen

VOORWOORD

Bij het verschijnen van dit proefschrift wil ik graag allen, die direct of indirect bij het tot stand komen ervan betrokken zijn, bedanken. De voldoening, die de afronding van dit stuk wetenschappelijke arbeid mij geeft, bezegelt deze dank.

In de eerste plaats dank ik jullie, vader en moeder die mijn studie hebben mogelijk gemaakt, voor de wijze waarop jullie het fundament gelegd hebben voor mijn vorming. Het ouderlijk huis, waar feiten en meningen getoetst en verwerkt konden worden, is mij altijd zeer dierbaar geweest. Mijn schoonmoeder wil ik in deze dank betrekken voor de manier waarop zij het fundament verbreedde. Ik hoop dat jullie goede zorgen mede zin krijgen, doordat ik werk doe en kan doen dat ik met plezier verricht.

Beste Hans Lyklema, hooggeleerde promotor, jouw voorbeeld en kritische begeleiding hebben veel tot het tot stand komen van dit proefschrift bijgedragen. Plezier in het werk is niet alleen gelegen in het soort werk, maar ook in de structuur waarin het wordt uitgevoerd. Ik prijs me gelukkig dat ik het met beide zo goed getroffen heb en vind dat jij daarin een groot aandeel hebt. Hiervoor mijn dank en waardering.

Jikkie Hibma en Theo Boonman, de nauwgezette manier waarop jullie een groot deel van de experimenten hebben uitgevoerd, is voor mij onmisbaar geweest.

Voor de vriendschappelijke sfeer en goede samenwerking die ik tijdens mijn werk ondervonden heb, ben ik alle medewerkers van het Laboratorium voor Fysische en Kolloidchemie zeer erkentelijk. Enkelen wil ik persoonlijk noemen: Bert Bijsterbosch, jij hebt me ingevoerd in de 'geheimen' van het AgI en de kiem gelegd voor dit onderzoek, het is een stevige plant geworden. Gerard Fleer, de tijd dat we samen rekenden aan AgI of PVA ligt alweer enige tijd achter ons, dit neemt niet weg dat ik er veel van heb opgestoken. Arie de Keizer, hoewel je voor Jikkie en mij eigenlijk wat te laat de afdeling bent komen versterken, heb je er zeker toe bijgedragen dat ook de laatste titraties met grote zorg en nauwkeurigheid zijn voltooid. Henny van Beek en Simon Maasland, jullie deskundige hulp bij de bouw van de titratiecellen maakte betere metingen mogelijk. Willem van Maanen en Ben Spee, ondanks het vele traplopen werd de bevoorrading uitstekend door jullie verzorgd.

Mijn dank geldt ook: Meint Olthof, Ricus Geuze, Martin Geurts van Kessel en Mark Ilsink die in het kader van hun doctoraalstudie aan het onderzoek hebben bijgedragen.

Dear Nobuhiko Onda, I am much indebted to you for the translation of some Japanese articles and remember with pleasure our fruitful discussions about PVA.

Dear Richard Akers, this thesis could not have been submitted in time, if you had not corrected the English text in such a short time,' mijn hartelijke dank hiervoor'.

Hoewel tijdens het persklaar maken van het manuscript het afdelingssecretariaat nogal afwisselend 'bemand' was, is dankzij de goede zorgen van Clara van Dijk, een groot deel van de tekst toch daar getikt door Hetty Wildeboer-van der Klift en Liesbeth Ruyten. Gert Buurman verzorgde het tekenwerk.

Tenslotte Els, jouw bijdrage is het meest veelzijdig geweest, dankzij jou is het dan ook tot stand gekomen.

CONTENTS

1. INTRODUCTION

1.1. General introduction and aim of this study

The adsorption of macromolecules from solution onto solids is not merely of academic interest but it is also a basic phenomenon in many applied processes. For example adsorbed macromolecules can play a decisive role as stabilizers of colloidal dispersions (Lyklema 1968, Vincent 1974), but also as flocculants (Kitchener 1972), they are of great importance for the action of adhesives (Patrick 1967, Schrader and Block 1971) and lubricants (Forbes et al. 1970) and can be used as soil improvers (Greenland 1972). To a large extent, these applications are based upon two characteristic features:

1. The adsorbed molecules are firmly attached to the surface due to their ability to form multiple adsorption bonds, and
2. an adsorbed polymer layer usually has a considerable thickness, giving rise to an interfacial zone with special properties.

To gain insight into these phenomena and in the factors influencing them much work has been done, both experimental and theoretical. See for instance reviews by Patat et al. (1964), Stromberg (1967), Silberberg (1971), Lipatov and Sergeeva (1974, 1976) and Roe (1974).

Although not generally recognized, polymer adsorption from aqueous solution is especially significant. More often than not, particles dispersed in aqueous solution carry a charge on their surfaces. This charge, together with its counterpart in solution around the particle, forms an electrical double layer. Consequently, polymers adsorbed on such particles are as a rule situated in this electrical double layer, which may have important implications for either or both the adsorbed polymer and the electrical double layer. It is this neglected field of study that the present thesis is concerned with. Our aim is to investigate how the double layer properties of charged particles are influenced by the presence of adsorbed polymer molecules and to obtain information on the conformation of the polymer layer from observed alterations in the double layer properties. In particular this latter aspect may conveniently be studied if a neutral polymer is chosen, which does not strongly interact with the charges in the double layer. The basic principle, of such a study lies in the possibility of controlling the thickness of the solution part of the electrical double layer. At high electrolyte concentration (e.g. 10^{-1} M) this layer is very thin. Changes in its properties due to adsorbed polymer molecules are then essentially caused by alterations in this thin region, thus reflecting the presence of segments in direct contact with the surface. On the other hand, at low electrolyte concentration (e.g. 10^{-3} M) the solution part of the electrical double layer is merely diffuse and comparable in thickness with an adsorbed polymer layer. Changes in the double layer properties under these conditions may then be associated

with the presence of loops* and tails* of polymer dangling in the solution phase. The information thus obtained has a relatively wide range of applicability: it is for instance of particular interest of the explanation of polymer induced stability in aqueous dispersions.

1.2. POLYMER ADSORPTION

Unlike the isotherms observed for the adsorption of low molecular weight species, those for polymers are relatively uninformative. In addition to knowing the mass adsorbed, Γ_p, it is also necessary to know how the material is distributed. As the conformation of an adsorbed polymer is continually changing, this can only be expressed in terms of statistical parameters. The best characteristic of a given adsorbed polymer layer is the average segment density distribution, ρ, as a function of the distance, x, from the surface. However, $\rho(x)$ is a complicated parameter, composed of the average density distributions of segments in trains**, loops and tails (see e.g. HOEVE 1965, HESSELINK 1971, 1975). Apart from its compounded character, $\rho(x)$ is not experimentally accessible and recourse has to be made to more available characteristics of an adsorbed polymer layer, such as:

a. the fraction, p, of segments that is in direct contact with the surface,
b. the fraction, θ, of the surface occupied with train segments and
c. some measure of the average thickness, $\bar{\Delta}$, of the adsorbed polymer layer.

Information on these parameters and the factors influencing them can be gained by both theoretical techniques and experiments on model systems.

Important contributions to the theory of homopolymer adsorption have been made by SILBERBERG (1968, 1972, 1975), HOEVE (1971, 1976), ROE (1974), SCHEUTJENS (1976) and others. Although details of the results of these various approaches are different, their predictions are qualitatively similar. All theories conclude that the structure of an adsorbed polymer layer mainly depends on the polymer-surface, polymer-solvent, polymer-polymer and solvent-surface interactions. In addition, the mean molecular weight, the polymer concentration and the chain flexibility play a role. A critical evaluation of these theories requires experimental data on the dimensions and numbers of adsorbed polymer loops, tails and trains and estimates of the magnitudes of the different interactions. However, direct application of the models to practical data is often thwarted by the observed irreversible nature of polymer adsorption, leading to quasi equilibrium states.

Confining our selves to the three important quantities Γ_p, θ (or p) and $\bar{\Delta}$, it is expedient to briefly review what is available in literature.

1. *The amounts adsorbed or the adsorption isotherm.* Literature abunds on this, see for example review articles of PATAT et al. (1964) and LIPATOV and SER-

* A *loop* is a sequence of polymer segments adsorbed at each end, the intervening segments protruding into the solution. A *tail* is a series of segments terminally adsorbed at one end.
** A *train* is an uninterrupted sequence of segments in direct contact with the surface.

GEEVA (1974, 1976). The information is generally obtained from the material balance before and after adsorption. Unfortunately, the interesting initial part of the isotherm, where molecules adsorb in an isolated state, is often difficult to establish experimentally.

2. *The fraction of segments adsorbed in trains, or the degree of occupancy of the first layer.* Spectroscopic techniques can be used to obtain these quantities directly, e.g. IR (e.g. FONTANA and THOMAS 1961, STROMBERG 1967, JOPPIEN 1974, 1975, KILLMANN 1976), ESR (FOX et al. 1974, ROBB and SMITH 1974) and NMR (MIYAMOTO and CANTOW 1972, COSGROVE and VINCENT 1978). Their limitation is that they are applicable only if the chain contains special groups interacting with the surface. Moreover, sophisticated equipment is required. For aqueous media, these techniques seldom work. Other methods are microcalorimetry (e.g. KILLMANN and ECKART 1971, KILLMANN 1976, NORDE 1976) and, as mentioned in sect. 1.1., electrical double layer measurements (MILLER and GRAHAME 1956, KOOPAL and LYKLEMA 1975). These methods are indirect and assumptions have to be made to interpret the results. On the other hand, microcalorimetric data also yield interaction enthalpies. An advantage of the double layer method is that its results not only contain information on the adsorbed polymer layer, but also on for example changes in the surface charge and the displacement of oriented water dipoles and specifically adsorbed ions by train segments. These effects, in turn, lead to changes in the potential, ψ_d, which governs the electrical double layer repulsion between the charged particles in a colloidal system. In other words, such studies are particularly helpful when polymer adsorption and electrostatic repulsion are simultaneously operative in determining stability.

3. *The extent of the adsorbed layer.* To this end ellipsometry provides a powerful tool for adsorption on reflecting surfaces (e.g. STROMBERG et al. 1970, GEBHARD and KILLMANN 1976). The average thickness calculated can be related to actual molecular dimensions (MCCRACKIN and COLSON 1964). Thicknesses can also be determined by hydrodynamic measurements such as: viscometry (e.g. PRIEL and SILBERBERG 1970, FLEER et al. 1972), ultracentrifugation and electrophoresis (GARVEY et al. 1974, 1976, KOOPAL and LYKLEMA 1975) or by measuring the thickness of free polymer films (SONNTAG 1976, VAN VLIET 1977). A disadvantage of this second group of methods is that the physical meaning of the obtained thickness may be ambiguous.

As a special kind of approach, yielding in principle all parameters, Monte Carlo simulations can be mentioned (e.g. MCCRACKIN 1967, CLAYFIELD and LUMB 1974, CLARK et al. 1975, LAL and STEPTO 1976). However, up to now, such methods have only been applied to isolated molecules.

1.3. System used and outline of this study

For our experiments the silver iodide-polyvinyl alcohol (AgI-PVA) system was chosen. A major incentive to use AgI is our interest in polymer induced colloidal stability.

Silver iodide is one of the classical model colloids of the Dutch school (Bijsterbosch and Lyklema 1977). Important parameters such as double layer charge and potential can be determined and controlled. Stability studies have also been carried out in the presence of low (Vincent et al. 1971, De Wit 1975) and high (Fleer and Lyklema 1974, 1975) molecular weight substances. A special study (Van Den Hul 1966) was devoted to the determination of the specific surface area of silver iodide precipitates.

Polyvinyl alcohol is a water-soluble, relatively simple, flexible and uncharged polymer (Finch 1973). Its concentration in solution can be readily determined (Zwick 1965), rendering the determination of, say, the adsorption isotherm relatively easy. This has led to its use in several model studies. An interesting variable, determining to a considerable extent the interfacial activity and the adsorption of polyvinyl alcohol, is the mole fraction of (residual) acetate groups and their distribution along the chain (Scholtens 1977).

The combined AgI-PVA system meets the requirements formulated in sect. 1.1. and preliminary experiments by C. Van Der Berg in our laboratory indicated that double layer measurements are experimentally feasible. For the interpretation of the measurements recourse can be made to similar information already obtained with low molecular weight alcohols (Bijsterbosch 1965, De Wit 1975).

In the first part of this study the materials AgI and PVA are characterized. Previous investigations concerned with the specific surface area determination of AgI showed discrepancies between those determined by electrochemical and non-electrochemical methods of study. As the present investigation is partly based upon double layer measurements and partly on adsorption data of electroneutral species, it is mandatory to reconsider critically the surface area determination. Moreover, as well as *precipitates*, silver iodide *sols* are used, hence, all surface area determinations should also be applicable to such sols.

Of the PVA samples used average molecular weights, molecular weight distributions and solution properties should be known, together with composition data, in particular the mole fraction of acetate groups and their distribution.

The second part of the thesis is concerned with the adsorption of PVA on AgI. Adsorption isotherms and the influence of molecular weight, acetate content and surface charge upon the adsorption are investigated. To obtain insight into the dependence of the surface charge and electrophoretic mobility on the surface potential at various adsorbed amounts of PVA, potentiometric titrations and electrophoretic measurements of AgI in the presence of several PVA's have been carried out. The principles to be used for the interpretation

of these data in terms of coverage of the first layer and thickness of the total layer are outlined. The results to be given, will include the influences of acetate content, molecular weight and surface charge. Finally, a general discussion on the conformation of the adsorbed layer is given. The obtained results will be compared with some theoretical predictions.

2. MATERIALS

2.1. General

All chemicals used were of pro analyse quality, except where states otherwise. Water was destilled and percolated through a column containing silver iodide before use, to remove adsorbing impurities.

All glassware used was high quality borosilicate glass. Before use it was successively cleaned with a solution of potasium dichromate/sulfuric acid, dilute nitric acid and tap water. Finally it was rinsed thoroughly with percolated water.

2.2. Silver iodide

In this study both silver iodide sols and precipitates were used.

2.2.1. *Sols*

The preparation of the silver iodide sols closely followed the procedure given by De Bruyn (1942) and Fleer (1971).

A volume of 0.15 M $AgNO_3$ was added slowly to a volume, twice as large, of 0.0825 M KI under vigorous agitation by a vibrating stirrer, to give a sol of originally 50 mmol dm^{-3}. After one cycle of electrodialysis and electrodecantation the sol was aged in situ for 3 days at 80°C. This was done to prevent coagulation, which did occur in the non-aged sols after the third dialysis cycle. After ageing, the electrodialysis and electrodecantation were repeated twice. Finally the sol was filtered through a glass filter L4 (mean pore diameter 10–20 μm). Several batches were added together to form a stock sol of about 1 mol AgI per dm^3, which was stored at $pI \approx 5$. In this way three stock sols were obtained, differing slightly in surface area. Below, these sols are referred to as sols A, B and C. After dilution, sol A was used for the PVA adsorption and electrophoresis experiments. At the start of each experiment the pI was adjusted.

2.2.2. *Precipitates*

Silver iodide precipitates were made in the dark by addition of 2 dm^3 0.1 M $AgNO_3$ solution to 2 dm^3 of a well stirred equivalent amount of KI. Before the addition both solutions were freed from oxygen by bubbling purified N_2 through them and the preparations were carried out in a N_2-atmosphere. Purification of the nitrogen from oxygen was done using a BTS-catalyst according to the suppliers instructions (BASF 1969). The rate of addition of the $AgNO_3$ solution was about 5 cm^3h^{-1} during the first hours of the experiment, gradually increasing to about 200 cm^3h^{-1}. After addition of the total amount of KI, stirring was continued for about an hour to attain an equilibrium poten-

tial in the supernatant liquid. Several portions of precipitated silver iodide made in this way were mixed together and thoroughly washed with percolated water to remove the salt. The washing was stopped when the conductivity of the washing water and the fresh water were the same. The precipitate was finally aged for 3 days at 80 °C in a solution of initial $pI \approx 5$.

Although the same procedure was used each time when a portion of suspension was made, the specific surface areas of the various batches differed somewhat. A poor control of a. the addition rate of the $AgNO_3$ solution (dripping solution from a funnel) and b. the stirring conditions might have caused this (DESPOTOVIC et al. 1974). The precipitates are numbered from I to VIII.

The ageing of the sols and precipitates was done in order to prevent drastic surface rearrangements (LIJKLEMA 1957, DESPOTOVIC et al. 1974) during the subsequent experiments.

The characterization of the specific surface areas of the samples is given in chapter 3.

2.3. POLYVINYL ALCOHOL

The Polyviol PVA's used in this study were manufactured by Wacker Chemie GmbH., the other samples by Konam N.V., Amsterdam. All samples were obtained by courtesy of Konam and used without further purification. For their characterization and solution properties we refer to chapter 4.

3. SPECIFIC SURFACE AREA OF THE SILVER IODIDE DISPERSIONS

3.1. INTRODUCTION

Adsorption studies measure the amount of material adsorbed per gram of adsorbent. However, a better way to consider the amount adsorbed is per unit area, which can be accomplished only when the specific surface area, S, of the sorbent sample is known. Evaluating unambiguously the absolute value of this quantity for AgI is rather difficult. A discussion of the specific surface area determination of AgI *precipitates* was given by VAN DEN HUL (1966). Although most of the methods described may also be used for AgI *sol* area determination, there is less literature on the latter subject (FLEER, 1971).

VAN DEN HUL (1966) and VAN DEN HUL and LYKLEMA (1968) showed that for double layer studies, the capacitance and negative adsorption areas are to be preferred, a conclusion which is supported by ENGEL (1968) and PIEPER and DE VOOYS (1974). VAN DEN HUL and LYKLEMA criticized nitrogen and dye adsorption, electron microscopy and permeability studies as being sensitive to experimental conditions and disagreeing with capacitance and negative adsorption methods.

Nevertheless in the present study not only capacitance measurements but also nitrogen and dye adsorption studies were included. The latter technique is capable of a good relative indication of the amount of available surface and if reliable values for the surface area covered per molecule become available even more information could be deduced. A more detailed discussion of the problems inherent in the interpretation of dye adsorption measurements is given in sect. 3.4.

Despite the criticism of VAN DEN HUL and LYKLEMA we also used electron microscopy to obtain the specific surface area of sol A. Although the method has its limitations (see sect. 3.5.), its advantage is that it gives a direct visualisation of the particles.

3.2. CAPACITANCE MEASUREMENTS

3.2.1. *Basic principle*

MACKOR (1951) was the first to use the differential capacity for surface area determination. The method was further developed by LIJKLEMA (1957) and VAN DEN HUL (1966, 1967). In essence at low electrolyte concentrations (10^{-3} M) the differential capacity on AgI at the point of zero charge (p.z.c.) in μF cm^{-2} is theoretically estimated and compared with the experimental one in μF g^{-1}. More recently (FLEER 1971, DE WIT 1975) the surface area was obtained

by equalizing the measured adsorption isotherm for potential determining (p.d.) ions in $\mu C\ g^{-1}$ at fixed ionic strength (usually 10^{-1} M KNO_3) with a standard curve in $\mu C\ m^{-2}$ (INTERNATIONAL CRITICAL TABLES 1967). The surface areas of the standard samples are based on negative adsorption and capacitance studies and may be considered as the best presently available. We used this latter technique.

3.2.2. *Experimental method and results*

Adsorption isotherms for p.d. ions were obtained by potentiometric titration as described in sect. 6.3.1. and are expressed in $\mu C\ g^{-1}$ as a function of the *pAg* ($= -\log c_{Ag^+}$). Silver iodide precipitates were titrated in 10^{-1} M KNO_3 as indifferent electrolyte, for the AgI sol two KNO_3 concentrations being used, 10^{-1} M and 10^{-3} M. The titrations were started at about *pI* = 4.5 where AgI has a relatively high negative surface charge. Some characteristic results are given in fig. 3–1. The calculated specific surface areas are collected in table 3–1. As our curves are not exactly identical in shape to one of the standard curves, the calculated specific surface areas depend somethat on the *pAg*-range chosen, leading to an experimental uncertainty of 5 to 10% in the values given.

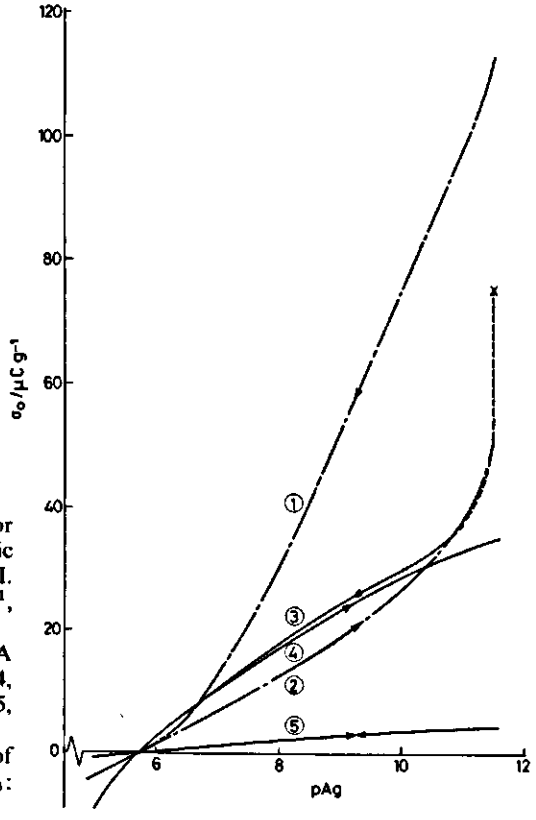

FIG. 3–1. Some typical isotherms for p.d. ions obtained by potentiometric titration of sol A and precipitate VI. The adsorption is given in $\mu C\ g^{-1}$, the concentration in *pAg* units.
1, sol A in 10^{-3} M KNO_3: 2, sol A coagulated in 10^{-3} M KNO_3: 3 and 4, sol A coagulated in 10^{-1} M KNO_3; 5, precipitate VI in 10^{-1} M KNO_3.
The arrows indicate the direction of the titrations. —·—, 10^{-3} M KNO_3: —, 10^{-1} M KNO_3.

TABLE 3–1. Specific surface areas of the AgI samples determined by the capacitance method, S_{cap}.

Sample	S_{cap} m^2g^{-1}	experimental conditions
I	1.4	precipitate in 10^{-1}M KNO_3
II	1.25	
III	2.0	
IV	1.3	
V	0.96	
VI	1.06	
VII	1.7	
VIII	2.6	
A	36	sol in 10^{-3}M KNO_3
A	13	freshly coagulated sol in 10^{-3}M KNO_3
A	18	coagulating sol at $pI = 4.5$ ($pAg = 11.5$) in 10^{-1}M KNO_3
A	8.4	freshly coagulated sol in 10^{-1}M KNO_3
A	4.5	precipitated sol, re-aged (48 h, 80°C) titrated in 10^{-2}M KNO_3
B	9.6	freshly coagulated sol in 10^{-1}M KNO_3
B	5.6	precipitated sol, re-aged (24 h, 80°C), titrated in 10^{-1}M KNO_3
C	7.8	freshly coagulated sol in 10^{-1}M KNO_3

3.2.3. *Discussion*

For silver iodide precipitates the order of magnitude of S_{cap} is the same as those obtained by BIJSTERBOSCH (1965) and VAN DEN HUL (1966). For the silver iodide sols, however, the values given for S_{cap} depend strongly on the salt concentration and titration sequence. For instance, curves 1, 2 and 4 of fig. 3–1, show a quite different adsorption behaviour of the p.d. ions and hence result in a different S_{cap}. Curve 1 is obtained when the sol is not or hardly coagulated. However, close to the p.z.c. the sol coagulates (10^{-3} M KNO_3) and curve 2 is obtained on this freshly coagulated sol. From table 3–1 it may be seen that this coagulation reduces S_{cap} with about a factor three. Curve 4 is also obtained on a freshly coagulated sol, however, here the salt concentration was 10^{-1} M and the reduction in surface area is even greater.

The reduction in adsorption of p.d. ions upon coagulation can be monitored if the coagulation proceeds very slowly, e.g. if to a sol at $pAg = 11.5$ KNO_3 is added up to a concentration of 10^{-1} M and some 10^{-2} M $AgNO_3$. In this case the coagulation process takes about two days. During this period the pAg readings are unstable but a definite decrease in the total amount of adsorbed p.d. ions is observed and the final pAg is only slightly different from the original value (curve 3). Further titration from this point ($pAg < 10.5$) gives reasonably reproducible results: compare for instance curves 3 and 4.

The difference in S_{cap} of a freshly coagulated sol in 10^{-3} M or in 10^{-1} M salt suggest that even lower values for S can be obtained if a precipitated or coagulated sol is subjected to a 're-aging' procedure. Indeed, such a behaviour is observed: re-aging a precipitated sol at the p.z.c. at 80°C for a certain time

gives a further reduction of S, see table 3-1. Another feature of the re-aged precipitated sol is that the titration curve has a better reproducibility than those of a freshly coagulated sol.

For a sol similarly prepared as sol A, FLEER (1971) found $S = 11\ m^2g^{-1}$, using negative adsorption on a freshly precipitated sample and capacitance measurements in 10^{-1} M KNO_3. The average particle size obtained, agreed well with that measured with an I.C.I.-Joyce Loebl disc centrifuge. Although the treatment of the sol was not stated, it is possible that, due to the introduction of the spin fluid and the centrifuging, also in this case coagulation might have occured and that hence the coincidence is fortuitous. The value for S reasonably well agrees with our value found in 10^{-1} M KNO_3. FLEER (1972) also found S much higher (ca. 25 m^2g^{-1}) when the titrations in 10^{-1} M KNO_3 were started with a highly charged sol ($pAg \approx 11.5$) and taking only a short time between the $AgNO_3$ additions, so that complete coagulation did not occur until the p.z.c. was reached. The back-titration resulted again in about 11 m^2g^{-1}

VAN DEN HUL (1966) prepared silver iodide 'sols' (his type C) which are to be compared with our precipitated and re-aged sols. Values for S of these 'sols' obtained from negative adsorption and capacitance measurements lie close to the capacitance areas we find. Moreover, VAN DEN HUL does not report any special behaviour of these 'sols' as compared with the precipitates, so we may assume that the surface area has been stabilized by the re-aging procedure and that such a 'sol' behaves as a precipitate.

In conclusion, for silver iodide *sols* the surface area as determined from capacitance measurements is not well defined, because during titration coagulation and changes in the surface structure occur, resulting in a drastic reduction of area. In view of the fact that a sufficiently charged sol in the presence of 10^{-3} M KNO_3 is stable over a long period of time, we reason that the titration in 10^{-3} M KNO_3 gives the proper specific capacitance area of the stock sol. Further support for this choice is obtained from the dye adsorption studies.

3.3. GAS ADSORPTION

3.3.1. *Evaluation of the method*

Adsorption of gases, especially N_2, has become a standard technique in surface area determination (GREGG and SING 1967). In principle it involves the evaluation of the monolayer volume, V_m, from adsorption data and requires the effective molecular cross section, a_0. The value of V_m is usually obtained from the linearized BET-plot (BRUNAUER, EMMETT and TELLER 1938). Although the choice of a_0 is arbitrary, even in the case of N_2 as the adsorbate (EMMETT and BRUNAUER 1937, PIERCE and EWING 1964, SMITH and FORD 1965, GREGG 1972), much evidence points to a value of 0.162 nm^2 for this gas (MCCLELLAN and HARNSBERGER 1967, GREGG and SING 1967, p. 74).

A disadvantage of the method is that it can only measure the surface area of dry samples, therefore wet samples have to be dried prior to adsorption. For

silver iodide it is very likely that rigorous drying is accompanied by changes in the surface structure and or state of aggregation (see sect. 3.2., CORRIN and STORM 1963, VAN DEN HUL 1966, KRAGH et al. 1966). Outgassing above 146.5 °C gives a phase transition of the silver iodide (DAVIS and ADAMS 1964). VAN DEN HUL and LYKLEMA (1968, 1970) assumed that even mild ways of drying resulted in a loss of area, due to the formation of large aggregates. However, the reproducibility of the BET area of a given silver iodide *precipitate*, determined by various investigators using different adsorbates, is quite good. Comparing BET areas of different silver iodide precipitates with those measured by capacitance shows that the ratio S_{cap}/S_{BET} is reasonably constant, so that S_{BET} is at least a good relative measure. For this reason we used N_2 adsorption to compare the areas of some precipitates and sols.

3.3.2. *Experimental method and results*

Adsorption isotherms were determined with a Perkin-Elmer/Shell sorptometer 212 C. This instrument is based on a continuous flow technique and developed by NELSEN and EGGERTSEN (1958). In its present form it is described by ETTRE et al. (1962) and LUTRICK et al. (1964). VAN DEN HUL and LYKLEMA (1968) showed that there was no significant difference in BET surface area of silver iodide precipitates obtained by this dynamic and the usual static techniques.

Drying of the samples was done at 100 °C or by freeze drying. The dried precipitate was crushed gently with a pestle in a mortar. Degassing was effected in a stream of helium at 110 °C for one night, measurements were done at ca. −196 °C. Ad- and desorption experiments agreed reasonably well, except for sol A. The resulting surface areas are given in table 3–2.

3.3.3. *Comparison with the capacitance areas*

For the *precipitates* the values obtained compare well with those of VAN DEN HUL (1966), who found the same ratio S_{cap}/S_{BET}.

Surprisingly the specific surface areas found for *sols* are rather small. Apparently, drying promotes aggregation of the sol particles and sintering or re-ageing may occur during drying at elevated temperatures or the outgassing

TABLE 3–2. BET-N_2 surface areas ($a_0 = 0.162$ nm^2)

sample	drying conditions	S_{BET} m^2g^{-1}	S_{cap}/S_{BET} [1]	S_{cap}/S_{BET} [2]
precip. VI	100 °C	0.31	3.4	–
precip. VII	100 °C	0.55	3.1	–
sol A	100 °C	0.3	28	15
sol B	freeze dried	1.99	4.8	2.8
sol C	freeze dried	1.35	5.8	–

[1] S_{cap} of the coagulated dispersion (10^{-1}M KNO_3)
[2] S_{cap} of the coagulated and re-aged dispersion (10^{-1}M KNO_3)

procedure (DESPOTOVIC et al. 1974), resulting in a drastic loss of area. The ratios S_{cap}/S_{BET} depend on the value chosen for S_{cap}, but for sample B the second value is close to 3. This supports the idea that drying and outgassing have the same effect as re-aging a precipitated sol, both result in a dispersion very similar to a precipitate. Evidently, gas adsorption cannot be used as a comparative method in case of silver iodide sols.

3.4. ADSORPTION FROM SOLUTION

3.4.1. *General features*

Adsorption from solution is in general conveniently measurable, however, the evaluation of surface areas from it is more problematic than that from gas adsorption. Firstly, adsorption from solution is a competitive process and only if a preferential adsorption takes place from dilute solution, the concentration changes in the bulk solution can be used to measure the adsorption (KIPLING 1965, GREGG and SING 1967, Ch. 7). Secondly, the monolayer coverage and the molecular cross section of the adsorbate molecules depend often on secundary variables, such as: nature of the solvent and supporting electrolyte (KIPLING 1965, PADDAY 1964, VAN DEN HUL 1966), electrolyte concentration, pH, surface charge of the adsorbent (BIJSTERBOSCH and LYKLEMA 1965, DE WIT and LYKLEMA 1973, BOCKRIS et al. 1967, DAMASKIN and FRUMKIN 1972, TRASATTI 1974) and the orientation of the adsorbate molecules. Despite these difficulties in interpretation solute adsorption has been often used and is advocated for the measurement of surface areas (ORR and DALLAVALLE 1959, GILES and NAKHWA 1962, GILES et al. 1970, 1974b) also for silver halides (BOYER and PRETESEILLE 1966, HERZ and HELLING 1966, HERZ et al. 1968, TANI et al. 1967, PEACOCK and KRAG 1968, PADDAY 1970a, b). Due to the above mentioned uncertainties such determinations are relative in nature and standardisation of the experimental technique is necessary. In practice, molecular cross sections of the adsorbate molecules are often found empirically by calibration against other methods e.g. N_2 adsorption or electron microscopy. Especially for AgI such calibrations can be misleading, due to ageing effects caused by drying or outgassing (see above and VAN DEN HUL and LYKLEMA 1968 or PADDAY 1970b). Being aware of these difficulties, we studied the adsorption, first of all to compare the adsorption capacity for low molecular weight solutes on the different silver iodide dispersions. Secondly, a realistic value was assigned to the molecular cross section of an adsorbate molecule and surface areas were eventually calculated.

3.4.2. *Experimental*

Samples of adsorbent (mostly 1 g) were agitated overnight at room temperature in 50 cm^3 dye solutions of the appropriate concentrations. After centrifugation the dye concentrations in the supernatant liquid were determined spectrophotometrically with an Unicam SP 1800 or SP 600. As adsorbates

methylene blue iodide (MB), 1 ethyl, 1' (4-sulfobutyl) 2, 2' cyanine iodide (ESBC)*, 1, 1' diethyl 2, 2' cyanine iodide (DEC)* and paranitrophenol (PNP) were used. ESBC and DEC contained no impurities (HERZ 1974), PNP was recrystallized from aqueous solution, MB was used without further purification. Some properties of these dyes are given in table 3–3. In contrast to VAN DEN HUL's (1966) findings, the absorbance versus concentration curve for MB followed the Lambert-Beer law. Comparison of the molar absorption coefficient, ε, with values reported by HAYDON and SEAMAN (1962) or BERGMANN and O'KONSKI (1963) shows that the MB is reasonably pure. The other dyes also followed the Lambert-Beer law in the limited concentration ranges shown in table 3–3.

3.4.3. *Results and discussion*

Of these adsorbates PNP did not adsorb on silver iodide, which can be due to the fact that the highest PNP concentration used, was only 5×10^{-4} mol dm^{-3}. GILES and NAKHWA (1962) and GILES et al. (1974b) used PNP in the mmol dm^{-3} range for their adsorption studies.

The solubility of DEC (I^-) in water was too small to measure adsorption isotherms, so we tried 40 vol % methanol-water mixtures (HERZ and HELLING 1966). From these solutions DEC (I^-) adsorbed so strongly on silver iodide that no proper adsorption isotherm could be measured. Probably (irreversible) multilayer adsorption occured, because the initial DEC concentrations were close to the saturation value. The precipitated silver iodide had a much greater volume after adsorption because a very loosely packed aggregate was formed. Apparently the particles were connected by DEC aggregated on their surface and not able to slip along each other. In the limit of solubility VAN DEN HUL (1966) also found an anomalous isotherm for DEC (Br^-) on AgI, however, for dilute ethanolic solutions of DEC (Cl^-, Br^- or I^-) normal isotherms were found. The reason can be that in ethanolic solutions conditions favouring aggregation are less likely. Possibly the strong adsorption of DEC in our case is caused by the presence of light, DEC is know as a photographic sensitizer. Working in the dark may be an important condition to obtain better isotherms (HERZ and HELLING 1966, PEACOCK and KRAGH 1968).

The adsorption of MB did not give special problems. Within an uncertainty of $\pm 4\%$ for precipitates and $\pm 3\%$ for the sol the experiments were reproducible and the isotherms had a distinct plateau. The larger absolute error for the sol is due to partial coagulation of the sol after the addition of MB. Using 10^{-1} M KNO_3 as the background electrolyte caused a larger uncertainty ($\pm 15\%$) in the adsorption of MB on the sol. This effect is probably due to coagulation effects (compare the capacity measurements).

At low silver iodide concentrations (< 0.5% w/v) high MB adsorption was

* We gratefully thank Dr. A. H. HERZ of Eastman Kodak Comp., Rochester, New York, for the gift of these dyes.

TABLE 3–3. Some properties of the dyes used.

Dye	structure	wavelength of maximum absorption in λ_{max}		molar absorption coeff. in $10^4\varepsilon$		conc. range $10^5\,c$	supplier
		H_2O	40% MeOH	H_2O	40% MeOH		
		nm	nm	$dm^{-3}mol^{-1}cm^{-1}$		mol dm^{-3}	
MB	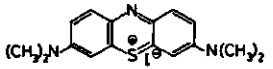	663	663	7.5	8.2	0–1	Baker, analar grade
ESBC	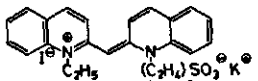	–	522	–	7.6	0–1	Eastman Kodak research laboratory, pure
DEC	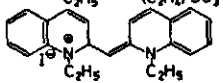	–	522	–	7.6	0–1	Eastman Kodak, pure
PNP	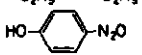	318 (pH <6) 400 (pH >9)		0.92 1.79	– –	0–9 0–5	BDH, laboratory grade recrystallised

sometimes found, suggesting that the adsorbent concentration could affect the adsorption behaviour. However, it was not possible to obtain reproducible data.

For AgI precipitates at $pI \approx 5$ the MB adsorption, measured on six different samples is on average 9% higher than at the point of zero charge. An example of this effect is shown in fig. 3–2a. At $pI < 4$ the adsorption rises steeply, far above the saturation values obtained at $pI \approx 5$, indicating aggregation of MB on the surface. Such behaviour is also found by VAN DEN HUL (1966) and De KEIZER (1977).

The silver iodide sol (A) shows a rather different picture. Isotherms recorded under several conditions are shown in fig. 3–2b. At the p.z.c. and at low surface charges the sol is (partly) coagulated and the adsorption of MB is only about

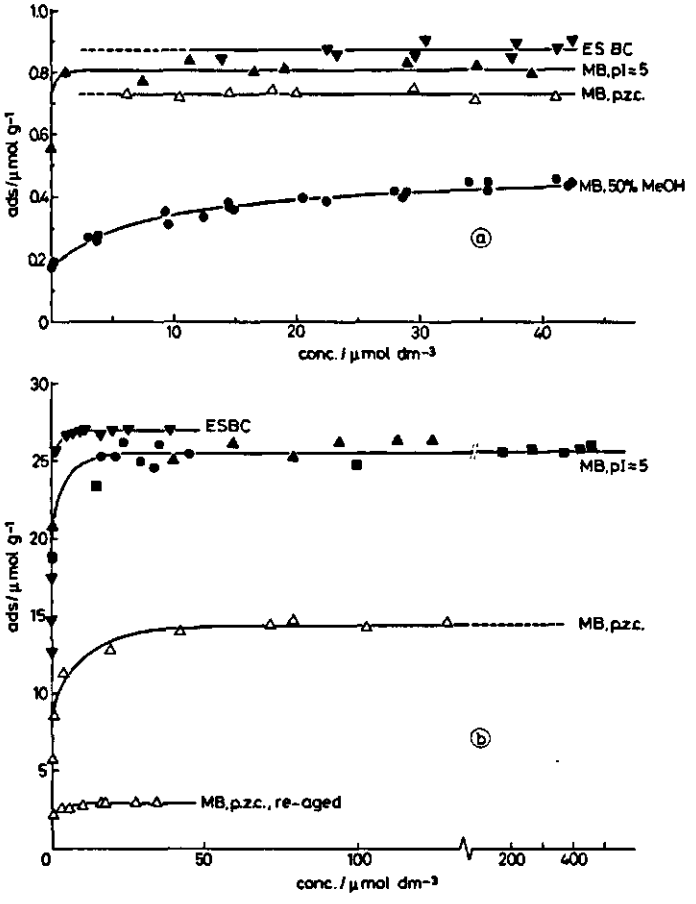

FIG. 3–2. Adsorption isotherms of methylene blue (MB) and 1 ethyl, 1'(4-sulfobutyl) 2,2' cyanine (ESBC) on silver iodide.
a. precipitate VI: b. sol A. At $pI \approx 5$ several silver iodide concentrations were used:
●, ▼, 0.2%; ▲, 0.5%; ■, 2%.

50% of its value at $pI = 5$, indicating a firm decrease in the surface area.

Re-aging a freshly precipitated sol at the p.z.c. at 80°C further reduces the adsorption, depending on the ageing time. Apparently the available surface area decreases due to surface rearrangements. These rearrangements could be similar to the surface diffusional mechanism of sintering. This is not improbable due to the nearness of the experimental temperature to that of a phase transition, which implies that the lattice has an energy close to the activation energy of transition.

The tendency to loose surface area upon coagulation or re-aging was also observed with the capacitance and gas adsorption experiments.

Another variable in the adsorption of MB on silver iodide is the nature of the solvent. Going from water to methanol-water mixtures results in a steady decrease in the adsorption saturation value until in 50 vol % methanol or more it is half that in aqueous solution. An isotherm in a 50 vol % methanol-water mixture is shown in fig. 3–2a. In this case there is no significant effect due to iodide concentration ($5 < pI < 10.5$).

The difference between adsorption from aqueous solution and water-methanol mixtures can in principle be explained by less aggregation of the adsorbed dye molecules or by more adsorption of the solvent. BIJSTERBOSCH and LYKLEMA (1965) showed that lower alcohols adsorb on silver iodide. Although methanol was not studied, one may expect that this alcohol will adsorb at high concentrations. Hence, solvent adsorption cannot be excluded *a priori*. According to VAN DEN HUL (1966) in ethanol or 0.8 M butanol the first saturation values for the MB adsorption on silver iodide are also 50% of the corresponding values in water. This can be explained by assuming either that only 50% of the surface is covered with MB or that MB adsorbs from aqueous solutions as dimers.

Other authors report dimer adsorption of MB e.g. onto mercury (ROFFIA and FEROCI 1973), glass (MARK and RANDALL 1970) and at the air/water interface (GILES et al. 1975). Aggregation in aqueous solution also occurs (HILLSON and MCKAY 1965, MUKERJEE and GOSH 1970, BRASWELL 1972) but at solution concentrations rather higher than our equilibrium concentrations. Yet, in the presence of an interface dimerization may be induced by special interactions with the interface or by orientation of the adsorbed molecules. For dyes adsorbed on silver bromide such behaviour is reported by NYS (1970). It is also known that addition of alcohols to aqueous dye solutions diminishes dye-dye interactions (MUKERJEE and GOSH 1970, HERZ 1975). In view of these arguments it seems realistic to explain the decrease in the adsorption affinity and in the adsorption saturation of MB on addition of methanol by a diminishing of the aggregation of MB. Provided the alcohol concentration is high enough, MB is adsorbed from alcoholic solutions as monomers, whereas in aqueous solutions dimers adsorb.

For the calculation of the specific surface areas of our samples we have to choose a cross sectional area per MB molecule and apart from the presence of

dimers, the orientation and packing density have to be known. As the adsorption isotherms have a high affinity character, a flat adsorption and close packing can be expected (GILES et al. 1974a). A flat adsorption is also suggested by the fact that the adsorption plateau in aqueous solution is just twice that in alcoholic solutions. Taking this into account a reasonable value for a_0 (MB) adsorbed from aqueous solutions is 0.60 nm^2. This value is about half the theoretical value for flat adsorption (KIPLING and WILSON 1960) and close to the experimental one determined from surface pressure – area isotherms and adsorption experiments on BET-calibrated adsorbents (GILES et al. 1970, 1975). Adsorption saturation data, $(x/m)_s$, and calculated surface areas, S_{MB}, are collected in table 3–4.

The adsorption experiments with ESBC were carried out in 40 vol % methanol-water mixtures. In these mixtures ESBC is more soluble than in water and less aggregation occurs in solution (PADDAY 1968, HERZ 1975). Variations in methanol content from 15 – 70 vol % did not influence the adsorption saturation value and probably the adsorption is the same as in aqueous solutions (HERZ and HELLING 1966, HERZ et al. 1968). The experiments were done in the dark, otherwise reproducible isotherms could not be obtained. The presence of 10^{-1} M KNO_3 or 10^{-2} M Borax (buffer, pH = 9.2) had no influence on the isotherm. The absorbance was measured at pH > 4.5, below this value it is pH dependent.

The reproducibility of the isotherms is somewhat better than in the case of MB and amounts to about 4% for precipitates and 0.5% for the sol. The reproducibility of the adsorption on the sol was improved by adding the sol as the

TABLE 3–4. Adsorption-saturation values, $(x/m)_s$, of the adsorption of MB ($pI \approx 5$) and ESBC on AgI dispersions and the surface areas calculated from them.

sample	$10^7(x_{MB}/m)_s$ mol g^{-1}	S_{MB}[1]) m^{2}g^{-1}	$10^7(x_{ESBC}/m)_s$ mol g^{-1}	S_{ESBC}[2]) m^{2}g^{-1}
II	9.3	0.33	9.9	0.37
III	14.7	0.53	–	–
IV	10.5	0.38	–	–
V	7.0	0.25	8.0	0.29
VI	8.1	0.29	8.7	0.31
VII	12.5	0.45	–	–
VIII	19.0	0.69	–	–
A ($pI \approx 5$)	255	9.2	270	9.7
A ($pI \approx 9$)	163	5.9	–	–
A (p.z.c.)	143	5.2	–	–
A (p.z.c., 48 h, 80°C)[3])	35	1.26	–	–
A (p.z.c., 72 h, 80°C)[3])	29	1.05	–	–

[1]) a_0 (MB) = 0.60 nm^2
[2]) a_0 (ESBC) = 0.60 nm^2
[3]) These samples are re-aged at the p.z.c. at 80 °C during the time stated.

last component. The difference between adsorption on precipitates at $pI \approx 5$ or at the p.z.c. is only 5% and hardly significant. Some isotherms are given in fig. 3–2. The adsorption essentially follows the same pattern as found for MB adsorption on the sol and precipitates.

All ESBC isotherms have a high-affinity character, this and the fact that the same dye forms aggregates on silver bromide surfaces (HERZ et al. 1968, p. 179) strongly suggests that aggregation also occurs at the silver iodide interface. In solution di- and polymerization also occurs but generally at higher concentrations than those in the adsorption experiments (GRAVES and ROSE 1975, HERZ 1975), so adsorbate aggregation is promoted by the interface.

The formation of a close-packed array of cyanine molecules on silver halides bonded on their long edge is reasonably well established (HERZ et al. 1968, HERZ 1975, YACYNYCM et al. 1976) although the exact nature of the lateral-overlapping and -interactions between the cyanine molecules is still uncertain (GRAVES and ROSE 1975). As a consequence it is difficult to assess the molecular cross section of the adsorbate molecules very precisely. Calibration studies on silver bromide dispersions with well characterized surfaces point to an experimental value of 0.58 nm^2 for 1, 1' diethyl 2, 2' cyanine and related dyes (HERZ and HELLING 1966, HERZ et al. 1968, PEACOCK and KRAGH 1968, TANI and KIKUCKI 1969 and PADDAY 1970a). HERZ and HELLING also use this value for silver chloride and bromoiodide dispersions. PEACOCK and KRAGH (1968) and TANI and KIKUCKU (1969) differentiate between silver bromide, chloride and iodide, giving about 0.60 nm^2 (AgBr), 0.80 nm^2 (AgCl) and 0.40 nm^2 (AgI) for a_0. However, results for silver chloride and iodide were obtained for less well characterized surfaces. PADDAY and WICKHAM (1966) reported very low values for cyanines adsorbed on silver iodide ($a_0 \approx 0.15\,nm^2$), but they did not give the specific surface area of their AgI dispersion. PADDAY (1964) and VAN DEN HUL and LYKLEMA (1968) measured the adsorption of cyanine dyes from ethanolic solutions on silver iodide and found lower adsorption values than from aqueous solutions. Their values for a_0, calibrated on the basis of BET-areas, depended somewhat on the counterion of the dye: PADDAY found about 0.65 nm^2, VAN DEN HUL 0.75 nm^2. The counterion effect is not found with silver bromide as the adsorbent, using aqueous solutions (PEACOCK and KRAGH 1968).

In conclusion, it is difficult to find a generally accepted experimental value for a_0 (ESBC) when the dye is adsorbed on silver iodide. In order to calculate relative surface areas we have used a_0 (ESBC) = 0.60 nm^2 which is about the theoretical value for edge on adsorption in a close packed array of molecules (WEST et al. 1952). It agrees well with the experimental value of HERZ and HELLING (1966) and is the average of the other experimental values reported.

Adsorption saturation values, $(x/m)_s$, and calculated specific surface areas, S_{ESBC}, are given in table 3–4.

3.4.4. *Comparison with other methods*

The adsorption saturation values for MB and ESBC differ only slightly. Moreover, the surface areas calculated compare well with S_{BET}, lending support

to the values of the molecular cross sections, assuming S_{BET} as a standard.

As with S_{BET}, there is a large difference between S_{MB} and S_{cap}. However, the ratio S_{cap}/S_{MB} is fairly constant and about 3.8. A very interesting and important aspect is that the sol at high negative charge indeed requires a capacitance area of about 36 $m^2\ g^{-1}$ to give the same ratio S_{cap}/S_{MB} as obtained for precipitates. This underlines the ideas put forward in the section on capacitance measurements.

The adsorption capacity of a coagulating sol (e.g. at $pI \approx 9$ or at the p.z.c.) is not very constant. The absence of supporting electrolyte probably explains why relatively high values for S_{MB} were found. Re-ageing the sol for 48 h at 80°C further lowers the adsorption capacity, reaching a more constant value as may be seen from the ratio S_{cap}/S_{MB}.

The ratio S_{cap}/S_{MB} is so high that it is outside experimental order: it is impossible to reduce it to unity by adjustment of a_0 (MB). Hence, even if one considers S_{MB} as a relative value for S, the difference with S_{cap} is real. The same applies for the difference between S_{ESBC} and S_{cap}.

3.5. Electron microscopy

3.5.1. *Introduction*

Electron microscopy is a direct method for determining the size and size distribution of particles in a system. Individual particles are measured and when a great number of particles is inspected an accurate assessment of the distribution is possible. If the shape of the particles is also derived from the microscope image or if an assumption is made about the shape, the external surface area can be calculated. A fundamental problem in microscopy is that normal electron micrographs are two-dimensional and shape and size are essentially three-dimensional quantities so that only the characteristic dimensions of particles with simple geometrics are obtained without assumptions. For irregular particles either a simple geometry has to be assumed or shape factors (Heywood 1947, Herdan 1960) have to be introduced, to obtain the real size or surface area. In line with this lies the choice of the characteristic dimension of an irregular particle. A relatively simple and often used dimension is the projected-area diameter, which is the diameter of a circle equal in area to the profile of the particle as shown in the micrograph. Graticules with circles of increasing diameter are used to obtain this dimension (Allen 1968, Ch. 4), but untrained observers have the tendency to oversize the particle profile, resulting in too large diameters and too small surface areas (Heywood 1947). The extent of the error depends on the measuring technique and the particle shape. Another practical problem is the preparation of a microscope grid containing a representative sample from the particle distribution and/or the selection of the section of the microscope grid that is observed. Errors in sampling can be minimized by using standard procedures to make a mounting film (Allen 1968) and by taking special precautions against e.g. coagulation and

aggregation (IRANI and CALLIS 1963). The choice of a field to be observed can be random or systematic.

Despite all these disadvantages, electron microscopy is an attractive method because of its direct visualisation of the particles and especially in a controversial case it is a valuable comparative technique.

3.5.2. *Experimental*

Silver iodide samples (sol A) were prepared by diluting the stock-sol with 200 mg dm^{-3} PVA 48–98 or with 3% gelatine solutions at $pI \approx 5$, giving a final sol concentration of about 0.3%. A tiny droplet of such a solution was placed on a microscope grid coated with Formvar (polyvinyl formal), drying being done at room temperature. The PVA or gelatine were used as stabilizing agents (FLEER 1971, HERZ and HELLING 1966).

Although both stabilizers work reasonably well, a slight preference was given to gelatine. At high magnifications the silver iodide particles melt and/or evaporate after short exposure times and the silver iodide diffuses into the PVA or gelatine film. Under these conditions gelatine gave the better images of the particles.

Experiments were carried out with a Philips EM 100 electron microscope at three magnifications and fields where no or little aggregation occurred were photographed. Projected-area diameters were obtained with a graticule with circles differing 2 mm in diameter. In total 700 particles were measured.

3.5.3. *Results*

The particle size distribution obtained is rather wide, with a long tail for large diameters, fig. 3–3 shows an electron micrograph and fig. 3–4 a typical histogram of sol A. Whether the tail is caused by aggregation of particles or if it is due to large individual particles cannot be concluded. VAN DEN HUL and LYKLEMA (1968) reported the same phenomenon. Average diameters that can be obtained are D_{10}, D_{32} and D_{63} in which $D_{rs} = \Sigma\, n_i\, D_i^r / \Sigma\, n_i\, D_i^s$, n_i is the number of particles with projected-area diameter D_i.

The specific surface area is calculated with the relation (BARNETT 1970)

$$S_M = \frac{\alpha}{\rho\, D_{32}} \tag{3.1}$$

α is a shape factor, ρ is the solid density i.e. 5.67 g cm^{-3}. For spherical particles $\alpha = 6$, in our case α is approximated following HEYWOOD (1947, 1970) and equals 7.2. The calculated dimensions are given in table 3–5. In view of the possible errors mentioned in the introduction and assuming no artefacts, we may expect these results to be correct within ± 10 to 30%.

D_{10} is the diameter to be used in the electrophoresis studies. The electrophoretic mobility is obtained as a number average. Moreover, in the phase-contrast microscope used in the electrophoresis measurements, intermediate particle sizes were selected, as judged from the scattered light intensity. An

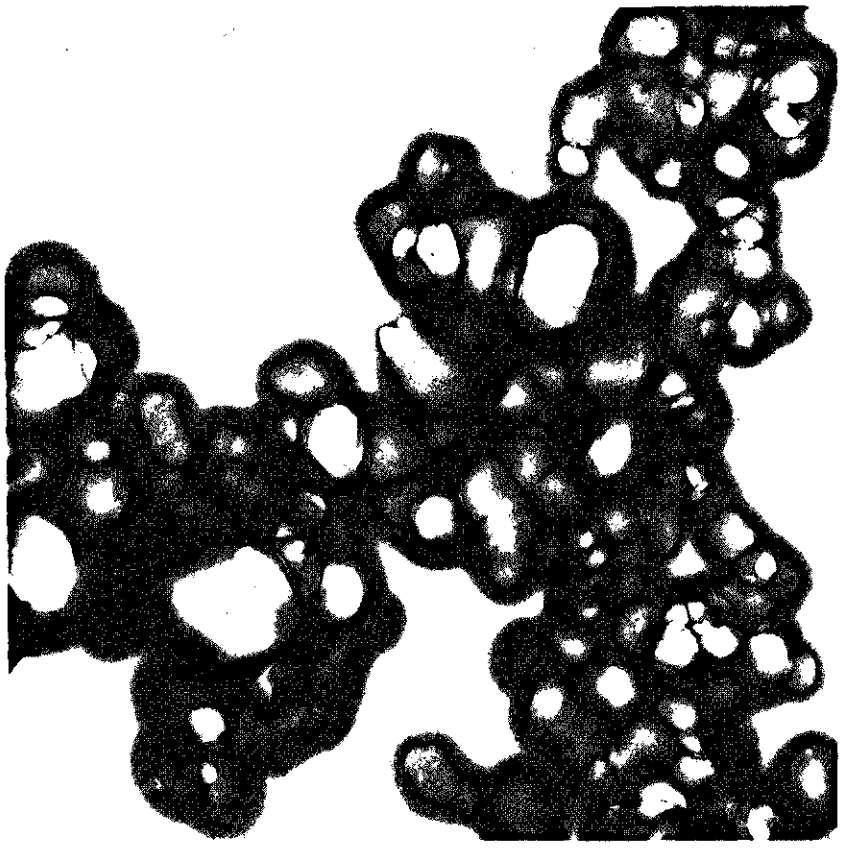

FIG. 3–3. Electron micrograph of silver iodide, sol A. Total magnification 66,600 ×. By courtesy of the Technical and Physical Engineering Research Service, Wageningen.

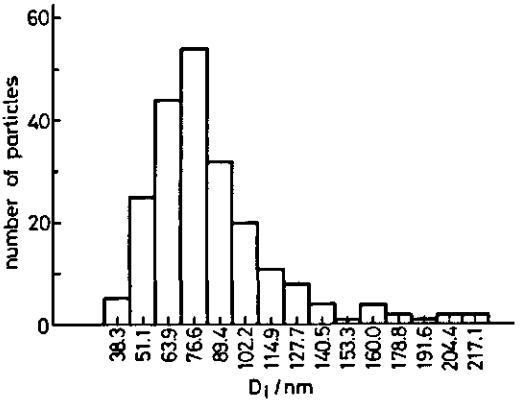

FIG. 3–4. Typical hystogram of silver iodide sol A.

TABLE 3–5. Microscopically determined average diameters and specific surface area of sol A.

D_{10}	D_{32}	D_{63}	S_M [1])
nm	nm	nm	m^2g^{-1}
85	114	151	11

[1]) calculated with eq. (3.1) using $\alpha = 7.2$

average giving more weight to large particle sizes would give erronoues results. D_{63} is merely shown to give an impression of the width of the distribution.

S_M is a measure of the external surface area, however, silver iodide is non porous (VAN DEN HUL 1966, SIDEBOTTOM et al. 1976) so that the external area coincides with the total area.

3.5.4. *Comparison with capacitance areas and discussion*

Comparing S_M and S_{cap} reveals that S_{cap} is again about 3 times as high as S_M. VAN DEN HUL (1966, 1968) found for silver iodide precipitates, using an optical and an electron microscope, an even larger discrepancy: $S_{cap} \approx 6\ S_M$. This may be caused partly by the fact that he redispersed a dry silver iodide powder and assumed the particles to be spherical. Accepting for a moment S_{cap} as the 'true' area, the difference with S_M can be explained only by assuming a large error in the particle size distribution function or in the shape factor, including surface roughness, or in overlooking very small particles. In our experiment a possible error in the size distribution is the long tail for large diameters. Cutting off this tail at its beginning ($D_i > 150$ nm) only increases S_M by about 30%. Another error could be the selection of particles to be sized. However, a random choice would have given more aggregates in the image and apparently a smaller S_M. The fact that for precipitates optical and electron microscopy gave essentially similar results, excludes large systematic errors due to the magnification technique. In conclusion errors in the size distribution cannot account for the discrepancy between S_{cap} and S_M and only possible errors in the shape factor, including surface roughness, or serious artefacts due to sampling are left.

In our opinion normal shape factors also cannot explain the entire difference between S_M and S_{cap}. HEYWOOD (1970) gives for angular particles an average value of $\alpha \approx 12$. The sol particles are rounded and α would be definitely less. For the precipitate particles, which may be regarded as angular, we would need much larger values of α to make S_M and S_{cap} equal. So, higher values of α can only remove a part of the difference. However, it should be noted that $\alpha \approx 12$ would bring a fair agreement between S_{BET} and S_M for the precipitates.

The remaining effect is the surface roughness. In their work on direct capacitance measurements ENGEL (1968) and PIEPER and DE VOOYS (1974) had to introduce a surface roughness factor, $R_f \approx 2$, for AgI surfaces prepared by reaction of silver with iodine vapour, to convert geometrical areas to capaci-

tance areas. ENGEL analyzed electron micrographs taking into consideration primary (100 nm scale) and secondary (5 nm scale) surface roughness. PIEPER and DE VOOYS *i.* calculated the capacitance area according to MACKOR (1951) and compared this area with the macroscopic area and *ii.* counted R_f on a model basis similar to ENGEL, but avoiding secondary roughness (PIEPER 1976 or DE VOOYS 1976). Comparison of electron micrographs given by ENGEL of AgI surfaces made electrolytically and by reaction of iodine vapour with silver shows that considerably higher surface roughness is encountered with less ideal surfaces such as the former. In fact direct capacitance measurements of OOMEN (1965), who used ill defined electrode surfaces in the presence of an AgI precipitate, could be brought in agreement with capacitance values of ENGEL (1968) and LIJKLEMA (1957) only when R_f was given the value 4.5.

Using these concepts for a quantitative analysis of a heterodisperse particle system is nevertheless not so simple. For sol particles, only secondary surface roughness could be taken into account, because the particles themselves are of the order of magnitude of the primary roughness. However, there are two strong arguments against this. Firstly, VAN DEN HUL (1966) found for precipitates agreement between capacitance and negative adsorption areas. However, with the last mentioned method heterogeneities of the order of 50 nm and smaller could not be seen (VAN DEN HUL and LYKLEMA 1968, 1970), so secondary roughness cannot account for the large capacitance areas found. Secondly, if microirregularities of about 5 nm existed, they should have been 'seen' by the N_2 molecules and S_{BET} should be equal to S_{cap} and not smaller.

For precipitates primary roughness could play a role, although it would be difficult to calculate R_f exactly and counting for shape and surface roughness would easily overestimate the effect. Yet, it could help to explain the difference between our results and those of VAN DEN HUL.

Overlooking the discussion we cannot give a decisive conclusion on the difference between S_M and S_{cap}. On the one hand microscopy may give misleading results due to sampling errors. In order to minimize these a standard mounting film was applied and a stabilizer used. On the other hand capacitance areas have an uncertainty due to possible errors in the theoretical estimate of the capacitance and to experimental errors. The capacitance obtained from the adsorption isotherms of p.d. ions is a differential quotient and that from the direct method needs corrections for surface roughness, so neither method is very accurate. However, in spite of the considerable errors that can occur in the microscope and capacitance techniques it is also difficult to concieve of errors accumulating to as much as 300% and we conclude that there is fundamental difference of unknown nature between S_M and S_{cap}.

3.6. Further comparison and discussion

As shown above, there is no simple answer to explain the difference between S_{cap} and the areas obtained with the other methods used. In order to investigate how general this problem is, we collected other data on silver iodide from literature. Table 3–6 gives a survey. Generally the specific surface area obtained from capacitance is 3 to 4 times greater than those calculated with the other

Table 3–6. Specific surface areas of various silver iodide samples, literature values.[1])

author	S				other solutes		
	capacitance	BET	Microscopy	MB[1])	substance	a_0	S
	m^2g^{-1}					nm^2	m^2g^{-1}
Lijklema (1957), Lyklema and Overbeek (1961)	5.8	–	–	1.2			–
Van Den Hul (1966),	1.35	0.38	0.18	0.34	DEC from	0.60	0.29
Van Den Hul and	1.5	0.52	0.32	0.54	ethanol		0.43
Lyklema (1968)	0.85	0.30	0.22	0.36			–
	3.5	0.97	0.45	1.21			0.83
Jaycock et al. (1960)	0.70	0.90 0.66	0.52	–			–
Padday (1970b)	2.96	0.60	–	1.00 0.69	cetylpyridiniumion	0.54	0.92
De Keizer (1977)	0.80	–	–	0.26	TBA[2])	0.80	0.27
	1.00	–	–	0.30			0.32
Koopal, this thesis	1.25	–	–	0.33	ESBC from	0.60	0.37
	0.96	–	–	0.25	40% methanol		0.29
	1.06	0.31	–	0.29			0.31
	1.7	0.55	–	0.45			–
	36	(0.3)	11	9.2			9.7
Padday (1964)	–	0.195	–	–	DEMTC[3])	0.60	0.18
Kragh et al. (1966)	–	0.65–0.52		–	DEC	0.60	0.77
Peacock and Kragh (1968)	–	–	1.75	–	DEC	0.60	2.5
Tani and Kukucki (1969)	–	0.38	–	–	DEC	0.60	0.54

[1]) a_0 values for MB and cyanine dyes were taken from the present study: a_0 (MB) = 0.60 nm^2, a_0 (ESBC) = 0.60 nm^2.
[2]) TBA = tetrabutylammonium.
[3]) DEMTC = 3,3′ diethyl 9 methyl thiocarbocyanine.

methods stated. The only exception is the value of JAYCOCK et al. (1960), regrettedly, the authors did not state experimental details. In a subsequent article JAYCOCK and OTTEWILL (1963) reported an iso-electric point (i.e.p.) (and maximum flotation) of their silver iodide dispersion at $pI = 4$ when the dodecylpyridinium bromide adsorption is 1.2–1.6 μmol g^{-1}. At $pI = 4$ the surface charge, based on a capacitance area, will be about 4 to 5 μC cm^{-2} (BIJSTERBOSCH and LYKLEMA 1966, DE KEIZER and LYKLEMA 1975), corresponding with 0.4 to 0.5 μmol negative sites per m^2. As a consequence, about 3 m^2g^{-1} would be required to give a charge reversal at the noted adsorption. This area is again 3 to 4 times greater than the value given.

Surface areas measured with the other methods (BET, microscopy, solute adsorption) give, within reasonable limits, about the same results. The fact that S_M tends to be a little lower can often be removed by introducing a larger shape or roughness factor.

The areas obtained from solute adsorption are relative, due to the uncertainty in a_0. However, a_0 values used for the calculations in table 3–6 have some theoretical basis and there is a good mutual agreement between the different adsorbates. The tetrabutylammonium ion (TBA) deserves some special attention because of its spherical shape and the fact that TBA does not form micelles (WEN 1972). Due to this, the assignment of a value to a_0 (TBA) is simple and straightforward. The given value is based on the molecular radius (WEN 1972) and the experimental value for adsorption on mercury (KUTA and SMOLER 1975). The close agreement of S_{MB} and S_{TBA} supports the value of a_0 (MB) and underlines the fundamental difference with S_{cap}.

The agreement between S_{BET}, S_M and S_{solute}, independent of the adsorbate used, and the discussions on S_{MB} and S_{cap} and on S_M and S_{cap}, suggest that the difference with S_{cap} is not only a matter of 'wet' or 'dry' measurements as proposed by VAN DEN HUL and LYKLEMA (1968). Nevertheless, drying or outgassing at elevated temperatures of a freshly precipitated dispersion is equivalent to ageing and a drastic decrease in surface area is registered. However, when drying is done under mild conditions, preventing aggregation as much as possible, as is done for the microscopy, a reasonable value of S is found, comparing well with the 'wet' areas from solute adsorption. Another argument is that the strong aggregation tendency of the AgI sols, resulting in a loss of surface area, also occurs in solution, so loosing area is not exclusively to the dry state. Moreover, after re-ageing, the same ratio S_{cap}/S_{MB} is obtained, showing that the loss in area is monitored by both methods.

A final attempt to explain the difference between S_{cap} and S_{solute} or S_{BET} is to assume adsorption on specific sites on the surface. However, in this case S_M and S_{cap} should be close and both greater than S_{BET} or S_{solute}, which is not the case.

Apparently for silver iodide a fundamental difference exists between the electrochemically measured surface areas and those obtained by microscopy or positive adsorption of dyes or other surface active molecules. At the moment

there is no conclusive evidence to decide which type of method gives the preferred value. In order to overcome this difficulty the capacitance areas were chosen for the electrochemical studies, in which field they are well accepted (VAN DEN HUL and LYKLEMA 1966, 1968, ENGEL 1968, PIEPER and DE VOOYS 1974). However, for the polymer adsorption studies we will use S_{MB}, as we believe that in this way more reliable values for the adsorption are found. For example, the adsorption of PVA on AgI would be as low as ca. 0.5 mg m^{-2} when S_{cap} is used. Taking a segmental area of 0.25 nm^2, the maximum adsorption in a flat layer is about 0.3 mg m^{-2}, so less than half of the polymer would be adsorbed in small loops. This is in contradiction with the measured thicknesses (KOOPAL and LYKLEMA 1975) and the protective action of a PVA layer adsorbed on silver iodide (FLEER et al. 1972).

3.7. SUMMARY

Specific surface areas of several silver iodide precipitates and sols were measured by the capacitance method, gas adsorption (BET-N_2), adsorption from solution (methylene blue and 1 ethyl 1′ (4-sulfobutyl) 2, 2′ cyanine) and electron microscopy. Taking an uncertainty margin of 10 to 20% the areas obtained by gas or solute adsorption and microscopy compare reasonably well. However, the capacitance area is always 3 to 4 times greater. This phenomenon was reported in the literature before (VAN DEN HUL 1966). The reason for this difference is not known and cannot be due to e.g. wrong estimates of molecular areas of the adsorbate molecules, shape factors, surface roughness or adsorption on specific sites. It may have to do with the sample preparation, but it would be too simple to attribute the entire effect to the drying of the samples, as is necessary for gas adsorption and electron microscopy.

Surface areas of silver iodide *sols* strongly decrease upon coagulation or precipitation of the sols. A subsequent heat treatment enhances this effect and the original sol probably assumes the surface area characteristics of an aged precipitate.

At this moment there is no evidence to decide which values for the area should be taken. In electrochemical studies the capacitance area is well accepted and we will use it there. However, for the polymer adsorption studies we will use the area based on methylene blue adsorption, otherwise too low adsorptions are found.

4. POLYVINYL ALCOHOL: CHARACTERIZATION AND SOLUTION PROPERTIES

4.1. SYNTHESIS AND PROPERTIES

Polyvinyl alcohol (PVA) is a water soluble polymer of relatively simple chemical structure, its basic unit being $-(CH_2-CHOH)-$. In the preparation, vinyl acetate is polymerized to polyvinyl acetate (PVAc) and subsequently hydrolysed to PVA. For both the polymerization and the hydrolysis several methods are known (HACKEL 1968, NORO 1973b), resulting in different PVA's (ADELMAN and FERGUSON 1975, WINKLER 1973, NORO 1973a, FINCH 1973a, HACKEL 1968). Moreover, in industrial practice complete hydrolysis is seldom achieved and the nature of the catalyst used strongly determines the type of distribution of the residual acetate groups. An alkaline catalyst favours a 'blocky' distribution whereas an acid one promotes a random distribution of acetate groups (HACKEL 1968, NORO 1973b).

The majority of the PVA samples used in this study were manufactured by Wacker, Germany, one of the oldest producers (HERRMANN and HAEHNEL 1927, HERRMAN, HAEHNEL and BERG 1932, BERG 1937). The molecular weight depends on the mode of polymerization. For low molecular weight samples a bulk polymerization process was used, for medium M a solution polymerization and for high M a suspension polymerization (WACKER 1975, HACKEL 1968). The hydrolysis was alkaline catalysed (WACKER 1975, BERG 1937), so we may expect a blocky distribution of residual acetate groups. Further specifications of the samples are listed in table 4–1. We designated the samples by two numbers, the first giving the approximate relative viscosity of a 4% aqueous solution at 20 °C and the second the approximate percentage of hydrolysis. PVA's 16–98 and 60–99 were manufactured by Konam N.V. Amsterdam.

Important physical properties for PVA adsorption studies are: solubility, solution behaviour and interfacial activity. These properties are not only determined by the primary chemical structure but also by secondary effects such as: branching, end-groups, irregularities in the chain, stereoregularity, residual acetate content, distribution of acetate groups and molecular weight. Below we give a short review on these factors. In the later sections a spectroscopic investigation is described, giving insight in the properties of the PVA samples used, followed by viscometry and gel permeation chromatography to determine the average molecular weights and molecular weight distributions. Finally the solution and conformational parameters are calculated, taking into account heterodispersity effects.

Structural irregularities which may be present to very small extents in PVA, are discussed by PRICHARD (1970) and by ZWICK and VAN BOCHOVE (1964). Among them carboxyl and sulphate groups are reported which may yield a

TABLE 4–1. Properties of the PVA samples.

sample code	Trade name Polyviol	type of PVAc polymerization process[1])	hydroxyl content[2]) mole %	acetate content[2]) %	max. ash content %	votile content[2]) %	degree of polymerization[1])
3–98	V 03/20	bulk	98.5	0.27	2.0	4.1	300
13–98	V 13/20	solution	97.6	0.21	1.5	4.7	1000
48–98	W 48/20	suspension	98.7	0.15	1.0	4.6	2000
16–98	–	–	97.5	0.06	–	4.5	1200
60–99	–	–	98.7	0.06	–	4.5	2300
3–88	V 03/140	bulk	87.9	–	0.5	4.1	300
13–88	V 13/140	solution	85.9	0.06	0.5	4.2	1000
40–88	W 40/140	suspension	88.4	0.09	0.5	4.1	2000

[1]) taken from WACKER (1975)
[2]) measured following FINCH (1973b)

charged polymer. However, FLEER (1971) has shown that our PVA samples are essentially *uncharged*, which is of utmost importance for the forthcoming interpretation of the double layer and electrophoresis studies.

An irregularity occurring frequently in PVAc is branching. Fortunately most side chains may split off during saponification and PVA has little branching (HAAS 1973, FINCH 1973a, PRICHARD 1970) or be unbranched (WINKLER 1973, HACKEL 1968).

Stereoregularity affects properties such as crystallinity and solubility. Most probably the crystallinity decreases in the order syndiotactic > atactic > isotactic (FINCH 1973a). Our samples are predominantly atactic (see sect. 2.3.2.), which is normal for industrial samples (SAKURADA 1968, FUJII 1971, FINCH 1973a), so stereoregularity will not be an important factor in this study.

Factors remaining to be considered are the acetate content, its distribution along the chain and the molecular weight. They play an important role in this study and deserve some extra attention, especially in relation to solution and interfacial behaviour.

The rate of dissolution and the solubility of PVA strongly depends upon the degree of hydrolysis. PVA containing 12% acetate groups easily dissolves in cold water, but tends to precipitate at high temperatures. Almost fully hydrolysed PVA (2% acetate) dissolves quickly only at 80°C, and has the tendency to age and form aggregates at room temperature. Completely hydrolysed PVA shows this tendency strongly. The main reason for these phenomena is the intra- and intermolecular hydrogen bonding between the hydroxyl groups, impeding the rate of dissolution and the solubility. On the other hand, residual acetate groups, although essentially hydrophobic, prevent hydrogen bonding of hydroxyl groups (TOYOSHIMA 1973, TUBBS et al. 1968, TUBBS and WU 1973) and improve the solubility characteristics. Clearly, a random acetate distribution is most effective is this respect. To break the internal hydrogen bonds and to dissolve the PVA a temperature above the glass transition point (ca. 75°C) is required. The hydrophobic character of the acetate groups is noticed in the decrease of the critical temperature of phase separation with increasing acetate content (SHAKHOVA and MEERSON 1972).

The extent of the ageing of PVA solutions is monitored from viscosity measurements. At room temperature PVA solutions are reasonably stable if the acetate content is more than 1 to 2% (GRUBER et al. 1974).

An important aspect of the formation of intramolecular hydrogen bonds is the appearance of special chain conformations. FUJII et al. (1964) and FUJIWARA et al. (1966) have indicated that syndiotatic PVA in solution preferably assumes a helix conformation, whereas isotatic PVA prefers a zig-zag structure. Atactic PVA has a more random conformation, although both helix and zig-zag structure can be induced by special agents (BELTMAN 1975). The presence of some helix-like ordering in PVA solutions containing iodine is indicated by a colour reaction (ZWICK 1965, INAGAKI et al. 1972). The colour intensity decreases with increasing isotacticity, 1, 2-glycol content and acetate content (FINCH

1973a, MATSUZAWA et al. 1974). The formation of the PVA iodine complex in the presence of a helix stabilizing agent has been used as a basis of an analytical method for the determination of PVA (ZWICK 1965, LANKVELD 1970, FLEER 1971, GARVEY et al. 1974).

The interfacial properties of PVA have been investigated in many ways. Interfacial tension measurements (e.g. SCHOLTENS 1977, HAYASHI et al. 1964, LANKVELD and LYKLEMA 1972) show that both the acetate content and distribution are important parameters. Raising the acetate content in PVA from 1% to 12% reduces the interfacial activity firmly, an effect which increases when the acetate distribution is blocky. Commercial samples of different origin with the same molecular weights and acetate content exhibit different interfacial activities, reflecting differences in secondary structure. The molecular weight dependence of the interfacial tension, γ, is small and not unequivocal, PVA's from various manufactures behave differently. Low molecular weight PVA of Wacker is slightly more interfacially active than its higher molecular weight analogs (LANKVELD 1971).

Adsorption studies both on solid-liquid (e.g. SUGIURA and YABE 1970, SUGIURA 1971, FLEER et al. 1972, GARVEY et al. 1974, BARAN et al. 1976) and on liquid-liquid interfaces (e.g. LANKVELD and LYKLEMA 1972) show similar trends. The acetate content again is an important parameter, an increase in acetate content from ca. 1 to 12% generally increases the adsorption. The effect of molecular weight on adsorption depends on the acetate content and the nature of the adsorbing surface, these effects being more marked than the dependence of γ on M. Mostly an increase in M is accompanied by an increase in the amount adsorbed, this also being found for Wacker PVA (FLEER et al. 1972, LANKVELD 1970).

Information on the thickness of adsorbed PVA layers is obtained in various ways. SONNTAG (1976) and VAN VLIET (1977) measured thicknesses of free PVA 88 films of about 50–100 nm, but generally thinner layers are found. Ellipsometry of PVA 88 layers in the air-aqueous solution interface gave about 10–30 nm (ZICHY et al. 1973, VAN VLIET 1977), FLEER and SMITH (1976) measured thicknesses of ca. 25 nm on silica's. Various hydrodynamic measurements of PVA adsorbed on solid surfaces showed a layer thickness of 5–30 nm (FLEER et al. 1972, GARVEY et al. 1974, 1976, KOOPAL and LYKLEMA 1975, BARAN et al. 1976). As expected from the adsorption and the interfacial tension studies, the acetate content, its distribution and the molecular weight of the polymer are ruling parameters. Very indirect measures of the layer thickness, such as protection and colloidal stability (HAYASHI et al. 1964, SUGIURA 1971, LANKVELD and LYKLEMA 1972, FLEER et al. 1972, BARAN et al. 1976), reflect qualitatively the same dependencies.

Summarizing, it is worthwile to not only know the acetate content and molecular weight of the samples under study, but also the distribution of acetate groups along the main chain and to have an estimate of the other structural irregularities present.

In the foregoing section it was shown that secondary structural properties affect the interfacial behaviour. In order to obtain more insight into the properties of our samples, ultraviolet and infrared absorption spectra were recorded and analyzed.

4.2.1. *UV Spectroscopy*

Ultraviolet absorption spectra (200–400 nm) were obtained for 0.1% PVA aqueous solutions using a Pye Unicam SP 1800 spectrophotometer. They are reproduced in fig. 4–1.

Main absorption bands are found at 225, 280 and 330 nm. According to HAAS et al. (1963) and MATSUMOTO et al. (1958) these bands should be assigned to $-(CH = CH)_n-CO-$ groups, where $n = 1, 2$ and 3 for $\lambda = 225$, 280 and 330 respectively. Non conjugated carbonyl groups giving an absorption at 265 nm are clearly absent. These groups are thought to arise mainly from the presence of acetaldehyde (HAAS et al. 1963), what may be added or produced as a side reaction during the polymerization (WACKER 1975).

NISHIN (1961), see e.g. PRITCHARD (1970), gives some semi quantitative equations based on the molar absorbance of the equivalent free substances. They relate the absorbance, A, measured in a 1 cm cuvette, with the molarities of the various conjugated groups:

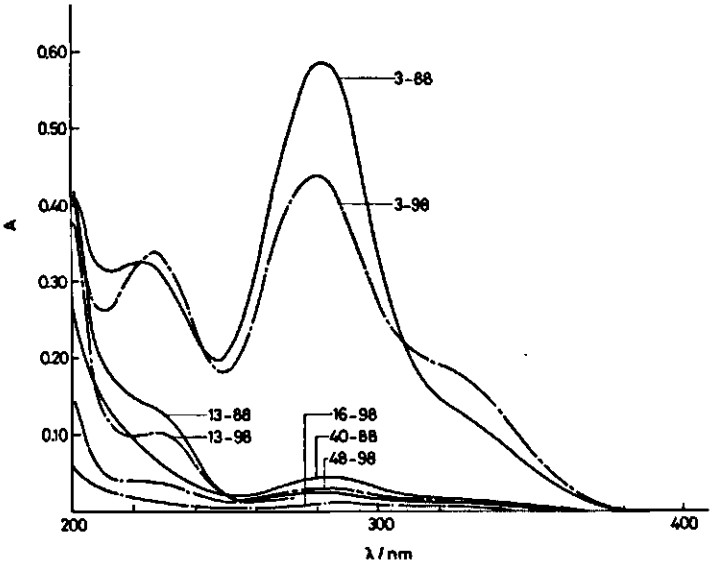

FIG. 4–1. UV absorption spectra of several PVA samples.
The absorbance, A, of 0.1% (w/v) PVA solutions is plotted versus the wavelength, λ.

$$A_{225} = 10{,}000\ [CH = CH - CO]$$
$$A_{280} = 22{,}000\ [(CH = CH)_2 - CO] \qquad (4.1)$$
$$A_{330} = 35{,}000\ [(CH = CH)_3 - CO]$$

Using the average viscometric molecular weights given in table 4–4 the number of conjugated carbonyl containing structures were estimated. The results are given in table 4–2.

Although there is no concensus about the position in the chain where structural elements of this type are present (HAAS et al. 1963, MATSUMOTO et al. 1958), the very fact that the total number of groups per molecule is independent of the molecular weight suggests that the groups are mainly situated at the ends of the PVA chains. The –CH = CH –CO– group is most frequently encountered. Differences in $-(CH = CH)_n-CO-$ content for different molecular weight samples are due to the variations in polymerization conditions for PVA.

4.2.2. *IR Spectroscopy*

Infrared spectra of dry PVA are well known. The main characteristics are given by LIANG and PEARSON (1959), PRITCHARD (1970) and FINCH (1973a).

Fig. 4–2 shows as an example the IR spectra of PVA 48–98 and PVA 40–88 recorded with a Perkin Elmer 237 spectrophotometer. The other samples behave very similarly. Samples were mixed with KBr and compressed into wafers with a hydraulic press.

The bands at 916 and 850 cm^{-1} are characteristic of skeletal vibrations and their intensity may be used as an empirical indication for the extent of stereoregularity. MURAHASHI (1967) proposed the equation:

$$\%\ \text{syndiotactic diads} = 72.4\ (A_{916}/A_{850})^{0.43} \qquad (4.2)$$

TABLE 4–2. Number of $-(CH = CH)_n - CO-$ groups per molecule and stereoregularity.

PVA	number of $-(CH = CH)_n-CO-$ groups per molecule				diads[1])	triads[2])		
	n = 1	n = 2	n = 3	total	syndio %	syndio %	hetero %	iso %
3–98	0.9	0.5	0.2	1.6	44	25	40	35
13–98	1.0	0.1	0.0	1.1	46	28	40	32
48–98	0.7	0.2	0.1	1.0	46	27	40	33
16–98	0.0	0.0	0.0	0.0	46	27	40	33
3–88	0.7	0.6	0.1	1.4	51	34	42	24
13–88	1.3	0.1	0.0	1.4	47	28	41	31
40–88	1.0	0.3	0.0	1.3	45	27	40	33

[1]) Calculated with eq. (4.3)
[2]) Calculated with eq. (4.4)

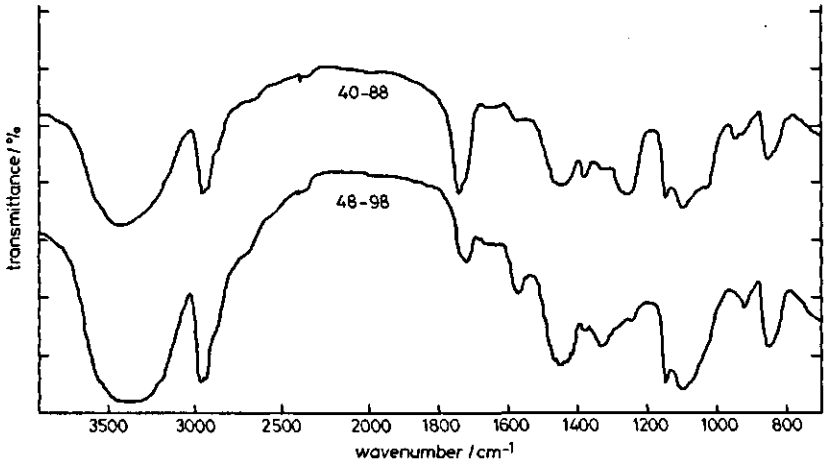

FIG. 4–2. IR absorption spectra of PVA 48–98 and PVA 40–88.

Whereas according to KENNY and WILLCOCKSON (1966)

$$\begin{aligned} \%\ \text{syndiotactic triads} &= 60\,(A_{916}/A_{850}) + 7 \\ \%\ \text{heterotactic triads} &= 18.7\,(A_{916}/A_{850}) + 34 \\ \%\ \text{isotatic triads} &= -78\,(A_{916}/A_{850}) + 59 \end{aligned} \qquad (4.3)$$

A is the absorbance at the indicated wave number. The percentages calculated are collected in table 4–2. It is clear that our PVA samples are atactic.

The band at 1145 cm^{-1} indicates the crystallinity (TADOKORO et al. 1957, MURAHASHI 1967, HAAS 1957), which is an indirect measure for syndio- or heterotacticity since these configurations favour interchain hydrogen bonds. Isotactic PVA merely allows for intramolecular hydrogen bonding, leading to a planar zig-zag conformation of the main chain rather than to crystallinities (FUJII et al. 1964). For PVA 88 the 1145 cm^{-1} band intensity is only slightly less than for PVA 98. However, the crystallinity of PVA 88 would be far less than that of PVA 98 if the residual acetate groups were distributed at random along the main chain (TSUNEMITSU and SHOMATA 1968). So, a distribution in blocks is most probable.

Additional evidence for a blocky distribution in PVA 88 is obtained from the observed shift of the ester-carbonyl band from 1715 cm^{-1} to 1735 cm^{-1}. Such a shift occurs when the forming of a hydrogen bond between the $>C=O$ group with an adjacent hydroxyl is prevented, e.g. due to the fact that the neighbouring group is an acetate group (GULBEKIAN and REYNOLDS 1973, TSUNEMITSU and SHOMATA 1968). The blocklike distribution of the acetate groups corresponds with the distribution as expected from the hydrolysis conditions. PVA 98 exhibited a peak at 1715 cm^{-1} and a shoulder at 1735 cm^{-1}, indicating a more random distribution of acetate groups in these samples.

The small bands appearing at 1630 to 1675 cm^{-1} are due to the conjugated carbonyl structures (DUNCALF and DUNN 1973). Stronger evidence for the presence of these groups was obtained by UV spectroscopy.

MURAHASHI (1967) found that at increasing 1, 2-glycol content the band at 1090 cm^{-1} shifts towards 1060 cm^{-1}. In our spectra, there is no such shift, indicating a low 1, 2-glycol content.

Comparing the IR spectra of PVA 98 with PVA 88 the following main differences are noted: increasing absorption at 945, 1025, 1250, 1380 and 1740 cm^{-1}, decreasing absorption at 1575 and 3450 cm^{-1} if the acetate content rises. The appearing bands correspond fairly well with the absorption bands found in PVAc spectra (FUJII 1967, BEACHELL et al. 1951). The decrease at 3450 cm^{-1} is evidently due to the replacement of hydroxyls by acetate groups. The peak at 1575 cm^{-1} is attributed to acetate ions, showing a relatively higher contamination in PVA 98.

Summarizing the main conclusions from this section we may state that the PVA samples are atactic and contain only few detectable irregularities, such as 1, 2-glycol- and conjugated carbonyl groups. It is suggested that the latter appear as end-group in the polymer chain. We will assume that their influence on the adsorption behaviour is small or absent. The acetate groups in PVA 98 are probably randomly distributed along the main chain, whereas in PVA 88 these groups are predominantly arranged in blocks. Both the higher acetate content and the blocky distribution in PVA 88 may affect the adsorption behaviour of these polymers.

4.3. MOLECULAR WEIGHT AND MOLECULAR WEIGHT DISTRIBUTION

The average degrees of polymerization given by the supplier (see table 4–1) are insufficiently accurate to rely upon. To obtain a better insight in the molecular weights and their distribution, a viscosity and gel permeation chromatography (GPC) study was carried out.

4.3.1. *Viscometry*

Measurements of the viscosity of dilute PVA solutions were made with Ubbelohde precision viscometers (KPG, Jenaer Glasswerk, Schott Mainz) with a flow-time for water of about 250 s. Special attention was paid to good temperature control, cleanliness, vertical alignment and filling of the viscometer. Solutions were filtered before use (see e.g. MCCAFFERTY 1970, p. 25). Couette and kinetic corrections were applied in accordance with the tables supplied with the viscometers. Density and shear corrections were neglected.

Intrinsic viscosities, $[\eta]$, and Huggins constants, k', for each PVA sample were calculated at 25 $\pm$ 0.02°C making use of the equations of Huggins

$$\frac{\eta_{re}}{c_p} = [\eta]_H + k'_H [\eta]_H^2 c_p \tag{4.4a}$$

and Martin

$$\ln \frac{\eta_{re}}{c_p} = \ln [\eta]_M + k'_M [\eta]_M c_p \tag{4.4b}$$

where η_{re} is the viscosity ratio excess, c_p the polymer concentration. The analysis was based on at least four different polymer concentrations in the range 2 to 10 g dm^{-3}, each measured in two different viscometers.

The intrinsic viscosities from the Huggins or Martin plot for the same polymer differed 2% or less, with $[\eta]_M > [\eta]_H$. The difference between the Huggins constants k'_H and k'_M may be as much as 30% and always $k'_H > k'_M$. The largest deviations were found for the highest molecular weights.

SAKAI (1968b) showed in a simulation method that a Huggins plot always underestimates $[\eta]$ and overestimates k'. The Martin equation gives reliable results for poor solvents. In good solvents the arithmetic averages of $[\eta]_M$ and $[\eta]_H$ and of k'_M give an optimal estimate of $[\eta]$ and k'. According to an analysis by GRAUBNER (1967) the difference between k'_H and k'_M should be concentration and molecular weight dependent, giving larger deviations for higher M and/or c. This corresponds with our findings.

As water is only a poor solvent for PVA (see sect. 4.4.3., SCHOLTENS 1977) $[\eta]_M$ and k'_M are the best estimates for $[\eta]$ and k'. Their values are given in table 4–4.

The Huggins constants

Although it is difficult to obtain a rigorous theoretical expression for the Huggins constant (YAMAKAWA 1971 sec. 36, FREED and EDWARDS 1975), k' may serve as a solvent interaction parameter. For Θ-solvents FREED and EDWARDS (1975) predict $k' = 0.76$, other treatments give $0.50 < k' < 0.70$ (SAKAI 1968a, 1970), these values being more in agreement with experimental data. In good solvents k' is found empirically to be between 0.25 and 0.35 (see e.g.: TANFORD 1961 p. 392, ELIAS 1972 sec. 8.9.3, SAKAI 1968a). However, association and branching both tend to increase k' and for polar solvents k' may not be a good measure of the solvent power (MOORE and O'DOWD 1968). For PVA in water k' often exceeds 0.5 (BERESNIEWICS 1959a, MATSUMOTO and IMAI 1959, GARVEY et al. 1974).

Taking in consideration that the values of k' given in table 4–4 are accurate within 10%, it is seen that k' is slightly below 0.5 and hardly dependent on molecular weight and acetate content. The fact that k' is independent of M agrees with GARVEY et al. (1974), but not with FLEER's (1971) results who found k' increasing with molecular weight for the same polymer samples. As k' is independent of molecular weight and identical for PVA 98 and PVA 88, we may conclude that the polymer-solvent interaction and/or state of associa-

tion are roughly equal for the polymer samples used. Judging from k' water is a poor solvent for PVA and no serious branching occurs in our samples.

Viscometric molecular weights

From intrinsic viscosities, viscosity average molecular weights, M_v or M_{va}, can be calculated with the Mark-Houwink-Sakurada (MHS) equation

$$[\eta] = K M_v^a \qquad \text{(MHS)} \tag{4.5}$$

provided the constants K and a are known. The values of the constants depend on the nature of the polymer and solvent and on the temperature. Generally a is a measure for the polymer-solvent interaction, for flexible linear polymers its ranges between 0.5 for Θ-solvents and 0.8–1.0 for very good solvents (FLORY and FOX 1951, KURATA and STOCKMAYER 1963, TANFORD 1961 sec. 2.3.5). K depends mainly on the nature of the polymer.

K and a can be found by calibrating (4.5) with monodisperse polymer samples, or with heterodisperse samples if the molecular weight distribution is known and congruent for the different samples (ELIAS 1972, sec. 8.9.7, TANFORD 1961, p. 411). In the latter case viscosity average molecular weights should be used. If the calibration is done with weight (M_w), or number average molecular weights (M_n) in principle a correction of K and a is necessary. As a is much less than K dependent on the kind of molecular weight used, KURATA et al. (1975) suggest that only K need to be corrected. They tabulate correction factors as a function of M_w/M_n for different molecular weight distributions.

For the PVA-water system many pairs of constants have been reported (KURATA et al. 1975, PRITCHARD 1970, FLEER 1971, LANKVELD 1970, GARVEY et al. 1974, BERESNIEWICS 1959a, b). KURATA et al. (1975) and PRITCHARD (1970) recommend the values of MATSUMOTO and OHYANAGI (1960). These authors determined molecular weights of PVA samples, obtained from low conversion PVAc, by light scattering and end-group analysis, showing $M_w/M_n \approx 2$. Their MHS constants based on M_n agreed with results of NAKAJIMA and FURUTATE (1949) and of MATSUMOTO and MAEDA (1959) obtained by osmometry. The final MHS relation corrected for heterodispersity and recalculated to 25 °C (PRITCHARD 1970) reads:

$$[\eta] = 4.67 \times 10^{-5} M_v^{0.64} \qquad (\mathrm{dm^3 g^{-1}}; 25\,^\circ\mathrm{C}) \tag{4.6}$$

Neglecting the difference between fully and 98% hydrolysed PVA we used eq. (4.6) to calculate M_v for our PVA 98 samples. Results are given in table 4–4.

Using eq. (4.6) for PVA 88 is questionable. BERESNIEWICS (1959b) showed that both K and a depend on the degree of hydrolysis of the PVA samples. He found a rather strong decrease of a and increase of K with increasing acetate content. This is in contrast with the results of FLEER (1971) or LANKVELD (1970)

TABLE 4–3. Original data of BERESNIEWICS (1959b) for the least branched PVA samples with a degree of hydrolysis of about 87%.

Sample code	$10[\eta]^{1})$ dm^3g^{-1}	$10^{-3}\ M_w{}^{2})$ $g\ mol^{-1}$	Hydroxyl content %
C II	0.59	83	87
B II	0.82	145	85
A-1d-II	1.05	(208)	86
A-1c-II	1.29	271	88

[1]) Intrinsic viscosities (25°C), obtained from a Huggins plot.
[2]) Molecular weight determined by light scattering.

who found a only slightly lower for PVA 88 than for PVA 98 and with GARVEY et al. (1974) who reported for PVA 88 a large value for a and a small value for K.

The difference in results between BERESNIEWICS (1959b) and FLEER (1971) or LANKVELD (1970) is largely removed if we select from the data given by BERESNIEWICS those of the least branched samples (see table 4–3) and recalculate the MHS constants on this basis. Taking into account the heterodispersity we calculated for PVA 87

$$[\eta] = 4.97 \times 10^{-5}\ M_v{}^{0.63} \qquad (dm^3g^{-1}: 25^{\circ}C) \qquad (4.7)$$

The value of a in (4.7) is higher than the one ($a = 0.58$) given by BERESNIEWICS (1959b) and about the same as a for fully hydrolysed PVA (eq.(4.6): BERESNIEWICS 1959a). As expected qualitatively, branching decreases the constant a. This trend is also reported for polystyrene (THURMOND and ZIMM 1952) and for dextrans (SENTI et al. 1955, GRANATH 1958).

Another structural effect which influences the intrinsic viscosity of partially hydrolysed PVA is the distribution of residual acetate groups along the main chain (SCHOLTENS 1977). BERESNIEWICS (1959b) applied an alkaline hydrolysis so his PVA 87 samples are probably blocky.

Our PVA 88 samples are blocky and there is no indication of substantial branching. Regarding this and the fact that (4.7) is not too different from (4.6), we prefered to calculate the M_v's for the PVA 88 series with (4.7). Results are given in table 4–4.

The agreement between the molecular weights in both series is good as should be, because comparable PVA 98 and 88 samples have the same parent PVAc. This lends support to (4.7). If we would have used the MHS constants of GARVEY et al. (1974), we would have found the molecular weights of the PVA 88 series considerably smaller than those of the 98 series.

Our values for M_v are about 70% higher than those obtained by FLEER (1971) for the same polymers. FLEER established MHS constants with Kuraray PVA using molecular weight data given by the supplier, who measured

TABLE 4–4. Intrinsic viscosities, Huggins constants and viscometric average molecular weights of the PVA samples (25°C).

PVA	$10\,[\eta]$ dm^3g^{-1}	k'	$10^{-3}M_v$[1]) g mol^{-1}
3–98	0.318	0.50	27
13–98	0.729	0.46	98
48–98	1.037	0.49	170
16–98	0.813	0.44	116
60–99	1.024	0.52	165
3–88	0.277	0.53	23
13–88	0.695	0.45	98
40–88	1.029	0.47	183

[1]) MHS constants for the 98 series: $a = 0.64$ and $K = 4.67 \times 10^{-5}$ dm^3g^{-1}. For the 88 series: $a = 0.63$ and $K = 4.97 \times 10^{-5}$ dm^3g^{-1}.

these according to the Japanese Industrial Standard-K6726 (KURARAY 1976). Essentially this standard is the MHS relation of SAKURADA (1944) based on osmometric average molecular weights. However, using M_n for the calibration of (4.5) leads to systematic errors (KURATA et al. 1975), e.g. for a 'most probable distribution' the Japanese Industrial Standard underestimates M_v by about 80%. This effect explains the large difference between our results and FLEER's.

There is also a great difference between our M_v's and the data given by the supplier, quoted in table 4–1. Probably the MHS constants of DIALER et al. (1952) leading to low molecular weights, were used to calculate M_v (WACKER 1975). These MHS constants deviate seriously from other reported values (KURATA et al. 1975).

4.3.2. *Gel Permeation Chromatography*

To obtain information about the molecular weight distribution and as an additional independent estimate of the molecular weights a GPC study (see e.g.: MOORE 1964, 1967, BILLMEYER 1966, KUBIN 1975) was made.

The instrument used was a Waters Associates model 200 Gel Permeation Chromatograph, located at AKZO Research Laboratory, Arnhem.* Four columns, 122 × 9.7 cm each, packed with 'linear Styragel' (Waters Associates) swollen in a mixture of 2 volumes hexamethyl phosphorotriamide and 1 volume of N-methyl pyrrolidone to which 1% of LiCl was added (HMPT/NMP/LiCl) were employed. The gel was designated by a nominal exclusion limit of 10^5 nm (based on the extended chain length of nearly monodisperse polystyrene). Solution concentrations were about 0.5 g/100 cm^3 (except for PVA 40–88, where the concentration was 0.3%), and 1.25 cm^3 aliquots were introduced in the first column and flushed through with HMPT/NMP/LiCl. The flow rate was 1.03×10^{-2} cm^3 s^{-1} and the operating temperature 80°C. A differential

* We gratefully acknowledge the cooperation of Dr. D. J. GOEDHART.

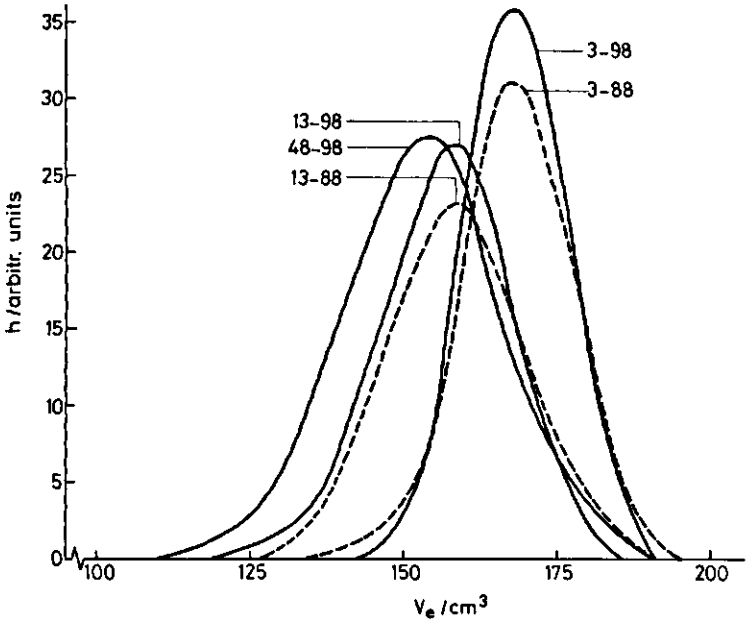

FIG. 4–3. GPC chromatograms, showing detector response, h, as a function of elution volume, V_e, for several PVA samples. For experimental conditions see text.

refractometer (Waters R4) with recorder was used to obtain chromatograms.

Results for several PVA samples are given in fig. 4–3.

Calibration procedure

The area of the chromatogram between two vertical and sufficiently close lines is proportional to the weight fraction, w_i, of the polymer. w_i can be approximated by $w_i = h_i/\Sigma h_i$. The normalized chromatogram gives $w(V_e)$ as a function of V_e with $w(V_e)\mathrm{d}V_e = w_i$. Under the assumption of infinitely high resolution $w(V_e)\mathrm{d}V_e = w(M)\,\mathrm{d}M$ or

$$w(M) = w(V_e)\frac{\mathrm{d}V_e}{\mathrm{d}M} = \frac{\mathrm{d}W(M)}{\mathrm{d}M} \tag{4.8a}$$

where $w(M)$ is the differential and $W(M)$ the integral weight distribution. Eq. (4.8a) can be written also as

$$w(M) = w(V_e)\,M^{-1}\frac{\mathrm{d}V_e}{\mathrm{d}\ln M} \tag{4.8b}$$

$w(V_e)$ is obtained from the normalized chromatogram and computation of $w(M)$ requires either the relation between V_e and M or between V_e and log M.

As there are no well defined narrow molecular weight fractions of PVA avail-

able, a direct calibration curve cannot be established.

GPC work on small molecules has shown that the molecular volume may be regarded as the separation parameter (MOORE 1964, SMITH and KOLLMANSBERGER 1965, DETERMANN 1968). Based on this, the assumption can be made that the polymer size in solution controls the separation. If this assumption holds, a calibration procedure independent of polymer chemical structure can be obtained. The size parameter often chosen is the hydrodynamic volume of the polymer in solution. According to Einstein's viscosity law we can write

$$V_h = [\eta]\, M\, K_E \tag{4.9}$$

where $[\eta]$ and M have their usual meaning, V_h is the hydrodynamic volume of the particles and K_E a constant independent of the nature of the polymer. Hence, a plot of log $[\eta]\, M$ vs. elution volume, V_e, should be the same for all polymers if the above assumption is correct. For a given gel column combination, solvent, elution rate, temperature and elution volume, the relation

$$[\eta]_x\, M_x = [\eta]_{cal}\, M_{cal} \tag{4.10}$$

applies. The index x is for the polymer under research and cal for a well known monodisperse calibration polymer.

Evidence for the correctness of using $[\eta]\, M$ as a calibration parameter is given by GRUBISIC et al. (1967). AMBLER and MCINTIRE (1975) show that $[\eta]\, M$ serves as a universal calibration parameter for polymers with comparable flexibility and extent of branching. A theoretical justification for its use for linear but structurally different polymers is reported by COLL and GILDINGS (1970) and indirectly by DOI (1975). DAWKINS (1972) reports $[\eta]\, M$ as a satisfactory universal calibration parameter for non polar polymers. For polymers considerably more polar than polystyrene (calibration polymer) the applicability remains somewhat uncertain. Although PVA belongs to the latter category, lack of information necessitates us to use the calibration procedures based on $[\eta]\, M$, as outlined above.

However, the intrinsic viscosities in HMPT/NMP/LiCl of the PVA fractions were not measured. Hence, (4.10) is not directly applicable: it should first be converted into a relation between M_{PVA} and M_{cal}. This can be done with an equation relating intrinsic viscosity with molecular weight. In principle two equations are available, the MHS relation (4.5) and the FLORY-FOX (1951) equation. For the moment we will use the latter in a slightly modified form:

$$[\eta] = K_0\, \alpha_\eta^3\, M^{1/2} \tag{4.11}$$

K_0 is a constant characteristic for a given polymer, independent of molecular weight and solvent quality, α_η is the linear viscosity expansion factor (KURATA and STOCKMAYER 1963, YAMAKAWA 1971 p. 364). Substitution of (4.11) into (4.10) and subsequent rearrangement gives:

$$\frac{M_x}{M_{cal}} = \left[\frac{\alpha_{\eta,cal}}{\alpha_{\eta,x}}\right]^2 \left[\frac{K_{0,cal}}{K_{0,x}}\right]^{2/3} \tag{4.12}$$

In practice the GPC solvent should be a good solvent for both polymers and the two polymers are expected to have similar polymer-solvent interactions. Under this condition $\alpha_{\eta,cal} \approx \alpha_{\eta,x}$ and (4.12) reduces to

$$M_x = \left[\frac{K_{0,cal}}{K_{0,x}}\right]^{2/3} M_{cal} \tag{4.13}$$

The use of this type of equation for GPC calibration was forwarded by DAWKINS (1968, 1970, 1972) on the basis of some qualitative arguments and on experimental results with well characterized polymers.

K_0 is obtained from viscometry and tabulated for many polymers (KURATA and STOCKMAYER 1963, KURATA et al. 1975). For a given elution volume, column, solvent and temperature combination, (4.13) gives the relation between M_{cal} and M_x. Taking chromatograms of well-defined monodisperse polymer fractions, the relation between V_e and M_{cal} is found, which is converted to $M_x(V_e)$ with (4.13).

For the calibration nearly monodisperse polystyrene (PS) samples ($M_w/M_n < 1.1$) from Pressure Chemical Company, Pittsburg, were used. Molecular weights, retention volumes in the system used and intrinsic viscosities in HMPT/NMP/LiCl at 80°C of these samples are given in table 4–5 (GOEDHART 1975).

Making use of the BURCHARD (1961)-STOCKMAYER-FIXMAN (1963) equation (BSF) for heterodisperse polymers (see sect. 4.4.2.)

$$[\eta] = K_0 (M_{v.5})^{0.5} + B' M_w \tag{4.14}$$

TABLE 4–5. Molecular weights of PS calibration samples ($M_w/M_n < 1.1$) and their retention volumes and intrinsic viscosities in HMPT/NMP/LiCl at 80°C (GOEDHART 1975).

PS sample code	$10^{-3}M_w$ g mol^{-1}	$10^{-3}M_p$[1]) g mol^{-1}	V_e cm^3	10 $[\eta]$ dm^{3}g^{-1}
16A	0.6	0.6	(200)	0.019
12B	2.1	2.0	192	0.030
8B	10	9.7	179	0.086
7B	37	36	168	0.182
4B	110	106	159	0.402
5A	507	483	143	1.121
13A	670	655	140	1.330

[1]) $M_p = M$ (peak) $\approx (M_w M_n)^{0.5}$ (TUNG 1967, BERGER and SCHULTZ 1965).

(B' is a polymer-solvent interaction parameter) we found for PS $K_{0,PS} = 7.6 \times 10^{-5}$ (dm^3 mol$^{+0.5}$ g$^{-1.5}$) taking a Schultz-Flory distribution of molecular weights (see e.g. ELIAS 1972 Ch. 2.8). This value corresponds reasonably with those reported in literature (KURATA et al. 1975, VAN KREVELEN 1972).

For K_0 of PVA 98 and 88 we analysed our intrinsic viscosity data of PVA in aqueous solution. Assuming that (4.13) is correct, the heterodispersity coefficients, $M_{v,5}/M_{va}$ and M_w/M_{va}, can be calculated with preliminary values of K_0. Using these and M_{va}'s from table 4–4 we obtained

$$K_{0,PVA\,98} = 15.5 \times 10^{-5} \text{ (dm}^3 \text{ mol}^{0.5} \text{ g}^{-1.5}\text{)}$$

$$K_{0,PVA\,88} = 15.8 \times 10^{-5} \text{ (dm}^3 \text{ mol}^{0.5} \text{ g}^{-1.5}\text{)}$$

Literature data and a discussion of $K_{0,PVA}$ are given in table 4–8 and sect. 4.4.3. Substituting the respective values of K_0 in (4.13) we obtain

$$M_{PVA\,98} = 0.60\, M_{PS} \tag{4.15a}$$

$$M_{PVA\,88} = 0.61\, M_{PS} \tag{4.15b}$$

The calibration curves for both PVA series are now readily established from the relation between M_{PS} and V_e. For PVA 98 the result is shown in fig. 4–4. From this graph $dV_e/d \ln M$ is found; substitution in (4.8b) leads to $w(M)$ and average molecular weights and heterodispersity coefficients have been calculated in table 4–6.

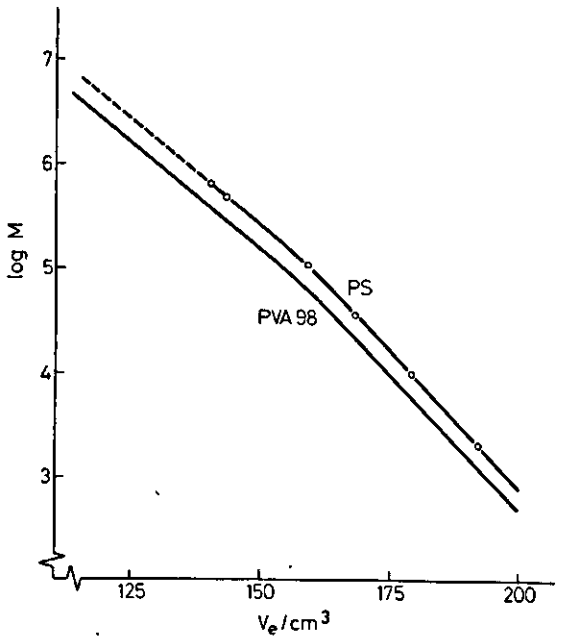

FIG. 4–4. Molecular weight calibration curves for polystyrene and PVA 98 in HMPT/NMP/LiCl at 80°C. Log M is given as a function of the elution volume, V_e. ○, M(peak) polystyrene standards; —, PVA 98 calibration curve, calculated with eq. (4.15a).

TABLE 4–6. Average molecular weights and several heterodispersity coefficients of the PVA samples as calculated from GPC results.

PVA	M_n	M_w	$M_{v.5}$ [1]	$M_{v.64}$ [2]	$\frac{M_w}{M_n}$	$\frac{M_n}{M_{v.64}}$	$\frac{M_w}{M_{v.64}}$	$\frac{M_{v.5}}{M_{v.64}}$	$M_{v.64}$ [4]
	10^3g mol^{-1}								10^3g mol^{-1}
3–98	13	32	26	27	2.41	0.48	1.16	0.94	27
13–98	39	135	101	109	3.49	0.35	1.24	0.92	98
48–98	39	227	160	177	5.83	0.22	1.28	0.90	170

PVA	M_n	M_w	$M_{v.5}$	$M_{v.63}$ [3]	$\frac{M_w}{M_n}$	$\frac{M_n}{M_{v.63}}$	$\frac{M_w}{M_{v.63}}$	$\frac{M_{v.5}}{M_{v.63}}$	$M_{v.63}$ [4]
	10^3 g mol^{-1}								10^3 g mol^{-1}
3–88	11	36	27	29	3.30	0.37	1.23	0.93	23
13–88	28	114	85	92	4.08	0.30	1.23	0.92	98
40–88	52	246	185	200	4.76	0.26	1.22	0.92	183

[1]) Viscometric average molecular weight, $M_{va} = \frac{(\Sigma c_i M_i^a)^{1/a}}{\Sigma c_i}$, $a = 0.5$

[2]) Viscometric average molecular weight $a = 0.64$

[3]) Viscometric average molecular weight $a = 0.63$

[4]) M_v as measured by viscometry, taken from table 4–4.

Results and discussion

The viscometric average molecular weights obtained from viscometry and those calculated from GPC, agree reasonably well. The differences in the dispersity for the different polymer samples may be attributable to differences in polymerization conditions. In order to see the limitations of the GPC results we will end this section with a short discussion of (4.15).

DONDOS and BENOIT (1971) showed that K_0 for polar polymers in polar solvents may be different from K_0 in apolar or slightly polar solvents. Furthermore, K_0 depends on temperature (FLORY 1969, Ch. 2). As far as we know, viscosity data for PVA have been obtained in aqueous solutions (KURATA et al. 1975), alcohol-water mixtures (WOLFRAM and NAGY 1968) and water-dioxane mixtures (DIEU 1954). From these studies we may infer that K_0 depends on the kind of mixture and the temperature. In a theoretical study BLEHA and VALKO (1976) showed that the unperturbed dimensions of isotactic PVA and so K_0 depend on the solvent polarity and temperature. Of these effects probably the temperature effect dominates and a decrease in $K_{0,\mathrm{PVA}}$ of about 30% is possible, resulting in an equivalent increase in M_{PVA}.

To obtain (4.13) we assumed $\alpha_{\eta,x} = \alpha_{\eta,\mathrm{cal}}$, this may be another source of error. HMPT/NMP/LiCl is a polar solvent, capable of forming hydrogen bonds. Hence, we would expect it to be a better solvent for PVA than for PS, and $\alpha_{\eta,\mathrm{PVA}} > \alpha_{\eta,\mathrm{PS}}$ giving a decrease in M_{PVA}. This effect and its dependence on molecular weight is more clearly seen if we substitute in (4.10) the Mark-Houwink-Sakurada equation in stead of the Flory-Fox relation. The result is

$$M_x = \left[\frac{K_{\mathrm{cal}}}{K_x}\right]^q \left(M_{\mathrm{cal}}\right)^p \tag{4.16}$$

$$\text{with } p = \frac{a_{\mathrm{cal}} + 1}{a_x + 1} \text{ and } q = \frac{1}{a_x + 1}$$

Eq. (4.16) will be equivalent to (4.15) only when $p = 1$ or $a_x = a_{\mathrm{cal}}$. A difference in solvent quality is expressed as a difference in a_x and a_{cal}. From table 4–5 we calculated $a_{\mathrm{PS}} = 0.68$. Taking for instance $a_{\mathrm{PVA}} = 0.70$, would lead to a decrease in M_{PVA} of 9 to 15% for the molecular weight range studied. Obviously, both the average molecular weights and heterodispersity coefficients are affected.

In conclusion, the errors in K_0 and α_η or a tend to compensate each other and the calibration procedure will give reasonable results. The heterodispersity coefficients can be used as given in table 4–6, accepting some uncertainty in their numerical values.

Summarizing briefly the results of this section it can be stated that the magnitudes of the Huggins constants, k', indicate that water is a relatively poor solvent for PVA and that no substantial branching exists in the samples. k' is independent of molecular weight and about the same for PVA 98 and 88,

suggesting that the polymer-solvent interaction and/or state of association are about identical for the polymer samples used.

Molecular weights determined by viscometry and gel permeation chromatography agree reasonably. The samples have a rather broad molecular weight distribution varying with the average degree of polymerization as a result of the different polymerization methods used. A summary of the data is given in table 4-6.

4.4. Conformation and solution parameters

The polymer conformation in solution is the initial conformation at the moment of adsorption and we may expect a correlation with the adsorption properties. Moreover, the conformation in solution is to a large extend determined by the solvent quality, which also plays an important role for the conformation at the interface. Although there may be some doubt about its value in the polymer-solvent layer very close to the surface, it is a good measure of the solvent power in the regions where loops protrude into the solution. In view of this the conformational parameters and the solvent quality have been determined.

4.4.1. *Theoretical introduction*

In dilute polymer solutions, quantities such as average molecular dimensions, intrinsic viscosities and second virial coefficients, may be expressed in two basic parameters. One is the mean square end-to-end distance, $<h^2>_0$, of a chain in the theta state, and the other is the excluded volume parameter, z. Although z and $<h^2>_0$ are interrelated, they are generally accepted parameters. The parameter z is proportional to the 'effective' excluded volume for a pair of chain segments at infinite dilution and also to the square root of the number of segments in the chain (Yamakawa 1971, Flory 1975).

Conformational statistics and consideration of the chain structure at atomic level are used to calculate the quantity $<h^2>_0$. Generally for a polymer with bond length l, and number of bonds n,

$$<h^2>_0 = C\,n\,l^2 \tag{4.17}$$

where C is the 'characteristic ratio'. For large flexible polymers, C is independent of n but depends on the nature of the polymer (Flory 1969, 1975). For simple polymer chains C can be calculated from the bond angle and the rotational energies. Usually C is in the range of 4 to 10.

Another molecular dimensions often used is the unperturbed mean square radius of gyration, $<s^2>_0$, (Flory and Fisk 1966, Flory 1969) which for infinitely long chains amounts to

$$<s^2>_0 = \frac{1}{6} C n l^2 \quad (n \to \infty) \tag{4.18a}$$

or

$$<s^2>_0 = \frac{1}{6} <h^2>_0 \tag{4.18b}$$

In order to apply random flight statistics in the development of the theory of polymer solutions, KUHN (1934) postulated the concept of the '*equivalent chain*'. In this picture the real unperturbed chain is replaced by a random flight chain which is composed of N bonds of length L, having the same end-to-end distance at full extension, h_m (the contour length). Its mean square end-to-end distance is equal to that of the chain under consideration, that is

$$<h^2>_0 = NL^2 \tag{4.19}$$

A further specification of N and L is obtained through the contour length

$$h_m = NL \tag{4.20}$$

However, in the two-parameter theory of dilute solutions of flexible polymers N and L never appear separately, and their individual values have no great significance (YAMAKAWA 1971, FLORY 1975). Therefore (4.17) would be equally usefull if for instance $l\sqrt{C}$, as the effective bond length were chosen.

Especially in good solvents a real polymer chain tends to be more expanded than would be expected from the statistics of unperturbed chains. To express the mean square end-to-end distance, $<h^2>$, and the mean square radius of gyration, $<s^2>$, of a real chain we may write

$$<h^2> \equiv <h^2>_0 \quad \alpha_h^2 \tag{4.21}$$

and

$$<s^2> \equiv <s^2>_0 \quad \alpha_s^2 \tag{4.22}$$

The parameter α is the linear expansion factor of the polymer chain. It increases with increasing solvent power. In principle the α's in (4.21) and (4.22) differ slightly (YAMAKAWA 1971, sec. 15), but if we ignore this

$$<s^2> \approx \frac{1}{6} <h^2> \quad (n \to \infty) \tag{4.23}$$

Theoretical approximations of α given by perturbation theory are commonly encountered in terms of the excluded volume parameter, z. YAMAKAWA (1971, Ch. 3) gives an extensive account on this subject. We have chosen a first order equation derived by FIXMAN (1955, 1962) yielding α_s for small values of z

$$\alpha_s^3 = 1 + 2z + \cdots \approx \alpha_h^3 \tag{4.24}$$

The parameter z is defined by

$$z \equiv \left[\frac{3}{2\pi}\right]^{3/2} <h^2>_0^{-3/2} \beta m^2 = 0.330\, BA^{-3}M^{1/2} \tag{4.25}$$

with m the number of segments of the chain,

$$B \equiv \beta M_s^{-2} = v^2(1 - 2\chi)\,(V_1 N_A)^{-1} \tag{4.26}$$

and

$$A^2 \equiv <h^2>_0 M^{-1} = C\, l^2 n\,(mM_s)^{-1} \tag{4.27}$$

M_s = molecular weight of a segment, v = specific volume of the polymer, V_1 = molar volume of the solvent and N_A = Avogradro's number. β is the binary cluster integral for a pair of segments, it represents the effective volume excluded to one segment by the presence of another. β is large in good solvents where preferential attractions occur between the polymer segment and the solvent molecule, zero in the Θ-point and negative in very poor solvents. βm^2 is just twice the total excluded volume between segments (YAMAKAWA 1971, Ch. 3, TANFORD 1961, sec. 12, FLORY 1953, Ch. XII). The interaction between polymer and solvent is more commonly expressed in FLORY's interaction parameter χ. A is a constant characteristic for a given series of polymer homologs.

In order to characterize these properties, an experimental determination of $<h^2>_0$ and α is needed. The most common practice involves determination of the intrinsic viscosities of the polymers in dilute solution as function of molecular weights (STAUDINGER 1960, FLORY 1953, Ch. XVI, YAMAKAWA 1971, Ch. 7).

According to the KIRKWOOD-RISEMAN (1948) theory of viscous flow including hydrodynamic interaction, the intrinsic viscosity of an unperturbed linear flexible chain may be written as

$$[\eta]_0 = \Phi_0 <h^2>_0^{3/2} M^{-1} \tag{4.28}$$

with

$$\Phi_0 = \left[\frac{\pi}{6}\right]^{3/2} N_A\,[X\,F(X)] \tag{4.29}$$

where X is a draining parameter, the poorer the polymer coil is drained, the higher X is. $XF(X)$ is tabulated by YAMAKAWA (1971) p. 269. Φ_0 is the viscosity constant. In the non-free-draining limit (no drainage at all) X becomes infinite and Φ_0 approaches a constant value. In this limit flexible linear polymers in their unperturbed state behave hydrodynamically as rigid spheres and Φ_0 is consider-

ed as a universal constant. The Kirkwood-Riseman theory then gives $XF(X) = 1.259$ (corrected value) leading to $\Phi_0 = 2.87 \times 10^{23}$. A discussion of other theoretical estimates of Φ_0 has been given by YAMAKAWA (1971) sec. 34. The best experimental value of Φ_0 based on viscosity and light scattering measurements is $(2.5 \pm 0.1)\ 10^{23}$ (YAMAKAWA 1971, sec. 39, FLORY 1969, Ch. 2) FLORY suggests use of the value 2.6×10^{23}. Eq. (4.28) is also known in the following form

$$[\eta]_0 = K_0 M^{1/2} \tag{4.30}$$

with

$$K_0 = \Phi_0 <h^2>_0^{3/2} M^{-3/2} = \Phi_0 A^3 \tag{4.31}$$

As A and Φ_0 are constants, $[\eta]_0$ becomes proportional to $M^{1/2}$. All of this applies to Θ-conditions. However, under non-Θ-conditions flexible chains have perturbed dimensions and far more often obey the empirical Mark-Houwink-Sakurada equation (4.5), with an exponent, a, depending on the solvent quality (see sect. 4.3., FLORY and FOX 1951, KURATA and STOCKMAYER 1963). Values of a greater than 0.5 must be interpreted as arising from the excluded volume effect (FLORY 1953).

Replacing $[\eta]_0$ by $[\eta]$, $<h^2>_0$ by $<h^2>$ and Φ_0 by Φ in (4.28) the (empirical) FLORY-FOX (1951) equation for flexible non-free-draining linear polymers is found

$$[\eta] = \Phi <h^2>^{3/2} M^{-1} \tag{4.32}$$

Originally Φ was regarded as a universal viscosity constant. In general, however, Φ depends on the excluded volume effect. Equations (4.32) and (4.28) can be related to each other if the linear viscosity expansion factor, α_η, is defined as

$$\alpha_\eta^3 \equiv [\eta]\,[\eta]_0^{-1} \tag{4.33}$$

Substitution in (4.28) gives the modified Flory-Fox equation

$$[\eta] = \Phi_0 <h^2>_0^{3/2} \alpha_\eta^3 M^{-1} = K_0 \alpha_\eta^3 M^{1/2} \tag{4.34}$$

This equation was already used in sect. 4.3.2. From (4.21), (4.32) and (4.34) follows

$$\Phi = \Phi_0 \alpha_\eta^3 \alpha_h^{-3} \tag{4.35}$$

The viscometric radius of a polymer molecule is less sensitive to a change in solvent power than is the end-to-end distance (YAMAKAWA 1971, sec. 35), so, $\alpha_\eta < \alpha_h$. The approximation $\alpha_\eta = \alpha_h$, although often made, is very poor especially in not too good solvents. KURATA and YAMAKAWA (1958) were the first who developed an expression for α_η^3 for small z

$$\alpha_\eta^3 = 1 + 1.55\, z + \cdots \tag{4.36}$$

Hereafter several other theoretical approximations were reported, giving a different value for the coefficient of z. STOCKMAYER and ALBRECHT (1958) give 1.74, FIXMAN (1966) 1.80 and YAMAKAWA and TANAKA (1971) 1.06. These values may be compared with a value of about 2 for the first coefficient in the series expansion of α_s^3 (or α_h^3), see (4.24).

Experimental light scattering and viscometry results of TANAKA et al. (1970), KAWAHARA et al. (1968) and those collected from literature by YAMAKAWA (1971, sec. 41) suggest that the coefficient of z is between 1.06 and 1.55. Higher values for it overestimate α_η. As the coefficient 1.55 is commonly used, we adopt (4.36), keeping in mind that this may still overestimate α_η or underestimate z.

Eqs. (4.34) and (4.36) provide the tools to calculate the characteristic dimensions of a polymer in solution when $[\eta]$'s are know for a series of polymer homologs with different molecular weights. Following the procedure described by STOCKMAYER and FIXMAN (1963) the BURCHARD (1961) – STOCKMAYER – FIXMAN (BSF) relation is found from (4.36), (4.34) and (4.25)

$$[\eta] = K_0\, M^{1/2} + 0.51\, \Phi_0\, B\, M \quad \text{(BSF)} \tag{4.37}$$

In a slightly different form this equation was presented in sect. 4.3.2. Plotting $[\eta]\, M^{0.5}$ against $M^{0.5}$ for a series of monodisperse polymer homologs should result in a straight line. The ordinate axis intercept equals K_0 and the slope is proportional to the polymer-solvent interaction parameter B, from which χ can be obtained.

A discussion of the BSF relation and the reliability of the derived parameters K_0 and B, also in relation to alternative methods to deduce K_0 and B from viscometry, has been given by INAGAKI et al. (1966), TANAKA et al. (1970) and by YAMAKAWA (1971, sec. 39). Mostly the validity of (4.37) is limited to small expansion factors as expected from the restriction on (4.36). However, STACY and ARNETT (1973) also find in good solvents correct values for K_0 and according to GUAITA and CHIANTORE (1975) the BSF relation can be considered as a satisfactory mathematical tool in theta and good solvents. Other methods offer merely an improvement for large M and/or α. Below molecular weights of about 10,000 the BSF relation breaks down, probably due to the fact that random flight statistics is no longer applicable.

4.4.2. *Heterodispersity effects*

So far the discussion has not included heterodispersity effects. However, in practice almost all polymers are heterodisperse, as are ours. In order to account for the heterodispersity, the derived equations have to be modified. To this end one should know the kind of average the measured parameter is (in our case $[\eta]$), and the way of averaging of other molecular weight dependent quantities should be consistent.

The viscosity ratio excess of a monodisperse polymer solution of concentration c_p reads

$$\eta_{re} = c_p\,[\eta] \quad \text{for } c_p \to 0$$

For a heterodisperse sample containing i monodisperse fractions

$$\eta_{re} = \sum_i \eta_{re,\,i} = \sum_i c_i\,[\eta]_i$$

and

$$[\eta] = \frac{\eta_{re}}{c_p} = \frac{\sum_i c_i\,[\eta]_i}{\sum_i c_i} \quad (c_p \to 0) \tag{4.38}$$

Applying this procedure to (4.30)

$$[\eta]_0 = \frac{\sum_i c_i\,[\eta]_{0,\,i}}{\sum_i c_i} = K_0\,\frac{\sum_i c_i\,M_i^{0.5}}{\sum_i c_i}$$

$$[\eta]_0 = K_0\,(M_{v.5})^{0.5} \tag{4.39}$$

When another molecular weight average is used instead, $[\eta]_0$ becomes $[\eta]_0{}^*$ and contains a heterodispersity contribution. If, for instance, M_{va} is used

$$[\eta]_0{}^* = [\eta]_0 \left[\frac{M_{va}}{M_{v.5}}\right]^{0.5}$$

The Flory-Fox relation, (4.34), reads for heterodisperse polymers

$$[\eta] = K_0\,\frac{\sum_i c_i\,\alpha_{\eta,\,i}{}^3\,M_i^{0.5}}{\sum_i c_i}$$

Assuming that the empirical MHS equation, with constants a and K, holds, the molecular weight dependence of $\alpha_{\eta,\,i}{}^3$ is given by

$$\alpha_{\eta,\,i}{}^3 = k_\alpha M_i{}^{\varepsilon}$$

with $\varepsilon = a - 0.5$ and $k_\alpha = K\,K_0{}^{-1}$, two constants and the FF relation is transformed in the MHS equation:

$$[\eta] = K_0\,k_\alpha\,(M_{va})^{\varepsilon+0.5} = K(M_{va})^a \tag{4.5}$$

Using the definition of $<\alpha_\eta{}^3>$ we find

$$<\alpha_\eta{}^3> \equiv \frac{[\eta]}{[\eta]_0} = k_\alpha\,\frac{(M_{va})^a}{(M_{v.5})^{0.5}} \tag{4.40}$$

If, as generally is done, $<\alpha_\eta>$ is obtained from $[\eta]$ and $[\eta]_0{}^*$, it still contains a heterodispersity effect. Using (4.40) the FF equation becomes

$$[\eta] = K_0 (M_{v.5})^{0.5} <\alpha_\eta^3> \tag{4.41}$$

Another aproach is to insert a theoretical expression for α_η in the FF equation. This leads to the BSF relation, (4.37), which for heterodisperse polymers reads

$$[\eta] = K_0 \frac{\sum_i c_i M_i^{0.5}}{\sum_i c_i} + 0.51\ \Phi_0\ B \frac{\sum_i c_i M_i}{\sum_i c_i}$$

or

$$[\eta] = K_0 (M_{v.5})^{0.5} + 0.51\ \Phi_0\ B\ M_w \tag{4.42}$$

From this equation and the definition of $<\alpha_\eta^3>$ another formula to estimate $<\alpha_\eta^3>$ is obtained:

$$<\alpha_\eta^3> = 1 + 0.51\ BA^{-3} \frac{M_w}{(M_{v.5})^{0.5}} \tag{4.43}$$

Combining (4.43) with (4.36) gives a relation for $<z>$, from which in turn $<\alpha_s>$ can be calculated using (4.24).

Eqs. (4.40) and (4.43) are essentially different, due to the fact that (4.40) is based on the empirical MHS relation and (4.43) on perturbation theory. Mathematically these treatments are incompatible.

The rather unusual molecular weight averages needed in the different equations can be found only when the molecular weight distribution is known. In literature other molecular weight averages are commonly used and the obtained parameters still contain heterodispersity contributions. For instance, using M_{va} instead of $M_{v.5}$ and M_w in the BSF relation would give

$$[\eta] = K_0^* (M_{va})^{0.5} + 0.51\ \Phi_0\ B^*\ M_{va}$$

while the correct equation reads

$$[\eta] = K_0 \left[\frac{M_{v.5}}{M_{va}}\right]^{0.5} (M_{va})^{0.5} + 0.51\ \Phi_0\ B \left[\frac{M_w}{M_{va}}\right] M_{va}$$

When polymers with similar molecular weight distributions are used, the heterodispersity corrections are constants and the magnitude of the errors made, depend on the solvent quality, the molecular weight distribution and the average molecular weights used. In very good solvents K_0^* and B^* differ relatively little from K_0 and B respectively, in nearly Θ-solvents B^* is about B but K_0^* is markedly smaller than K_0 if M_w or M_{va} is used. When M_n or M_z is substituted the errors in K_0 and B become larger.

When the samples differ in molecular weight distribution the errors are very dependent on the differences in heterodispersity. When corrections are not used a straight line BSF plot is due solely to fortuitous compensation.

4.4.3. *Results and discussion*

Using the intrinsic viscosities, heterodispersity coefficients given in table 4–6 and the molecular weights obtained with the MHS equation, BSF plots of PVA 98 and PVA 88 are shown in fig. 4-5. Included also are some earlier results of FLEER (1971), recalculated to 25°C (PRITCHARD 1970), for the same polymers. There is a close agreement with our results. The use of M_v (MHS) introduces an element of circuity into the argument, but we prefer these averages to the GPC molecular weights because of the greater uncertainties in the latter.

Although (4.36) and (4.37) are theoretically valid up to about $|<z>| = 0.15$, the BSF plots give reasonably straight lines over the whole molecular weight range studied. In view of this, we assumed that the dependence of $<\alpha_s>$ on $<z>$ given by (4.24) is also a reasonable approximation and for that reason $<\alpha_s>$ was calculated with it. These and other characteristic parameters together with chain dimensions calculated are collected in table 4–7. The effective length of a segment is $2\_lC^{0.5}$. Values of χ were found by substituting in (4.26) $v = 0.77$ cm^{3}g^{-1} (BRANDRUP and IMMERGUT 1965), $V_1 = 18$ cm^{3}mol^{-1} and $N_A = 6.02 \times 10^{23}$. For Φ_0 the value 2.6×10^{23} (FLORY 1969) was taken.

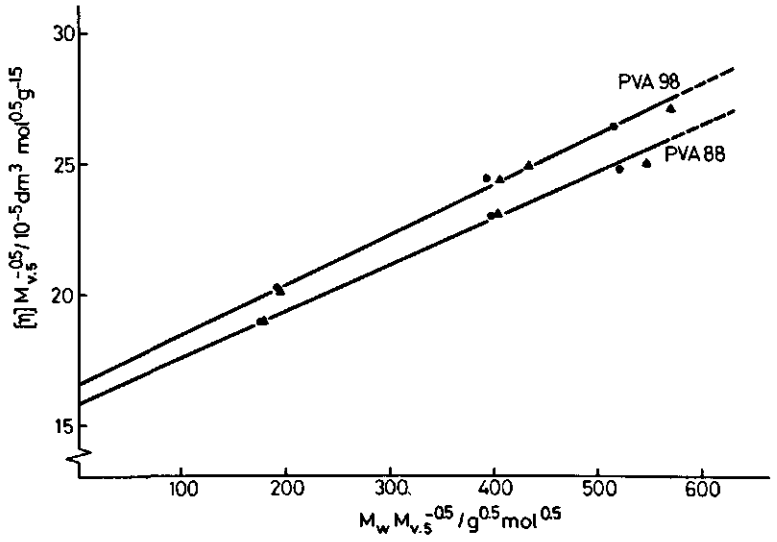

FIG. 4–5. BURCHARD – STOCKMAYER – FIXMAN plot for PVA 98 and PVA 88. ▲, present results, ●, results based on intrinsic viscosity data of FLEER (1971).

Table 4–7. Polyvinylalcohol solution parameters and dimensions.

PVA series	$10^5 K_0$ $dm^3 mol^{0.5} g^{-1.5}$	C	$l C^{0.5}$ nm	$(^1/_2-\chi)$	χ
98	16.5	7.0	0.41	0.0133	0.487
88	15.8	7.4	0.42	0.0123	0.488

PVA sample	$<\alpha_\eta>$	$<z>$	$<\alpha_s>$	$<h^2>_{0,v}^{0.5}$ nm	$<s^2>_{0,v}^{0.5}$ nm	$<s^2>_v^{0.5}$ [1] nm
3–98	1.07	0.14	1.09	14.0	5.72	6.23
13–98	1.14	0.30	1.17	26.8	10.94	12.80
48–98	1.17	0.39	1.27	35.3	14.41	18.30
16–98	1.15	0.33	1.18	29.2	11.92	14.07
3–88	1.06	0.13	1.08	12.8	5.22	5.64
13–88	1.13	0.30	1.17	26.5	10.82	12.66
40–88	1.17	0.38	1.21	36.3	14.82	17.93

[1]) End-to-end distances and radii of gyration were calculated with M_v (MHS), this is indicated with an index v.

For comparison purposes literature data for K_0 and χ of aqueous PVA solutions, complemented with some calculated values, are collected in table 4–8.

In the case of PVA 98–100 the spread of the K_0 values is rather great. The high values of K_0 are all based on very old literature and some of them are calculated using number average molecular weights, which results in large errors. The lower K_0 values are essentially based on the work of MATSUMOTO and OHYANAGI (1960) and BERESNIEWICS (1959a, b). The results of WOLFRAM and NAGY (1968) are based on the uncorrected MHS constants of MATSUMOTO and OHYANAGI.

A brief summary of the work of MATSUMOTO and OHYANAGI was given in sect. 4.3.1. With the extensive data given in their paper, a BSF plot taking into account the heterodispersity, is constructed, see fig. 4–6. It shows linear behaviour up to molecular weights of about 160,000 but for higher molecular weights $<\alpha_\eta^3>$ is overestimated. The values of K_0 and χ obtained may be considered as the best (viscometric) estimates of these parameters for PVA 100 at 30°C. Recalculated to 25°C these values are 15.6×10^{-5} dm^3 $mol^{0.5} g^{-1.5}$ and 0.484 respectively.

The BSF plot easily overestimates K_0 and χ when only a few 'low' molecular weight samples are included. This is shown in the values given in brackets in the second row of table 4–8, based on samples with a molecular weight > 160,000. In contrast, the MHS plot is linear over the whole molecular weight range studied (MATSUMOTO and OHYANAGI) and the spread about the line is less. Evidently, the dependence of $<\alpha_\eta^3>$ on molecular weight as expressed in (4.40) applies over a much wider range of M. GARVEY et al. (1974) found the

TABLE 4–8. $K_{0,PVA}$ and χ for aqueous PVA solutions.

degree hydrolysis %	temp. °C	a	10^5K (MHS) dm^3g^{-1}	10^5K_0 $dm^3mol^{0.5}g^{-1.5}$ exp.	10^5K_0 $dm^3mol^{0.5}g^{-1.5}$ calc.[a])	χ exp.	χ calc.[a])	method	reference
100	30	0.64	4.53	15.1	15.1	0.483	0.484	BSF	(1), (2)
(100	30	0.64	4.53	20.2	20.8	0.492	0.492	BSF	(1)[b]))
98	25	0.64	4.67	16.5	15.6	0.487	0.484	BSF	(2)
–	25	0.64	4.28	14.8	14.3	0.499	0.485	KS	(3)
99	25	0.63	5.95	–	18.3	–	0.483		(4)
99	25	0.60	14.0	28.4	33.8	0.475	0.480	FFS	(5)
99	0			33.7				FFS	(5)
99	50			23.8				FFS	(5)
–	–			22.5 ± 2.5					(6)
–	–			19 ± 3				–	(7)
–	30			–		0.494		–	(8)[c])
88	25	0.71	2.70	15.2	15.7	0.462	0.470	BSF	(9)
88	25	0.63	4.97	15.8	15.3	0.488	0.486	BSF	(2)
88	25	0.63	4.97	16.0	15.3	0.488	0.486	BSF	(4), (2)
99[e])	0			34.9				FFS	(5)
99[e])	25			28.7				FFS	(5)
99[e])	50			22.2				FFS	(5)
–	25			15.5–28.3				KS	(3)

Literature references
(1) MATSUMOTO and OHYANAGI (1960)
(2) this thesis
(3) WOLFRAM and NAGY (1968)
(4) BERESNIEWICS (1959a, b)
(5) DIEU (1954)
(6) KURATA and STOCKMAYER (1963); KURATA et al. (1975)
(7) VAN KREVELEN (1972)
(8) NAKAJIMA and FURUTATE (1949), SAKURADA et al. (1959)
(9) GARVEY et al. (1974)

[a]) Calculated with simulated molecular weights after substitution of the MHS relation in the BSF relation. $M_1 = 25{,}000$ $M_2 = 175{,}000$
[b]) Incorrect molecular weights were used. Calculation is done with $M_1 = 500{,}000$ $M_2 = 400{,}000$
[c]) From osmotic and vapour pressure data.
[d]) In water – 10% dioxane mextures.
[e]) In 'Θ-mixtures' of water-alcohol for 5 different alcohols.

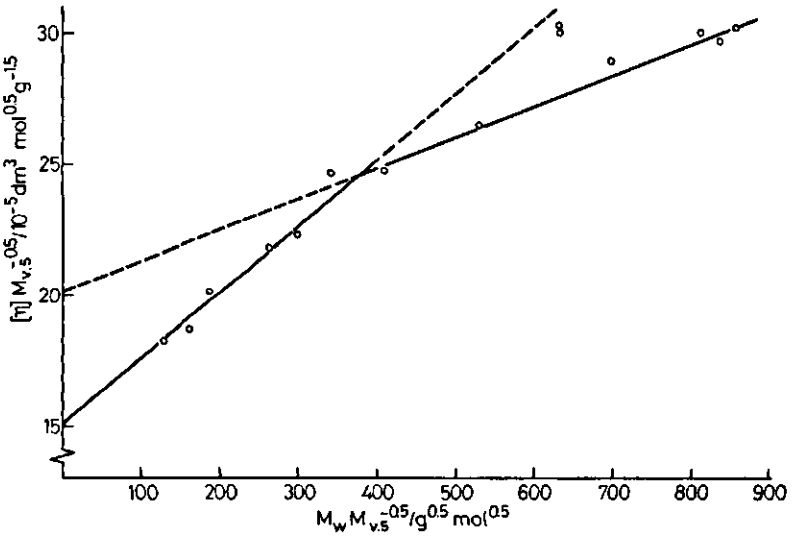

FIG. 4–6. BURCHARD – STOCKMAYER – FIXMAN plot for PVA, covering a wide molecular weight range; based upon results of MATSUMOTO and OHYANAGI (1960).

same for PVA 88.

Comparing the experimental values of χ one should take into account that its value depends on the chosen relation between α_η and z, and on the value of Φ_0. To avoid the last difficulty the experimental values given in table 4–8 are all (re)calculated with $\Phi_0 = 2.6 \times 10^{23}$. A theoretical inspection of the relations between α_η and z, shows that χ (KS) (KURATA and STOCKMAYER 1963) and χ (FFS) (FLORY-FOX-SCHAEFGEN, see FLORY and FOX 1951) should come out larger than χ (BSF). This should be taken into account also when the experimental and calculated values are compared.

Our experimental values of PVA 98 are slightly higher than those of MATSUMOTO and OHYANAGI. This may be due to the weight given to the highest molecular weight samples in the BSF plot.

For PVA 88 only a small quantity of material is available and it is difficult to assign a best value. GARVEY et al. (1974) measured weight average molecular weights of several samples and established MHS constants without heterodispersity corrections. The resulting equation was used to obtain the molecular weights of the remaining samples. Correcting for heterodispersity would probably lead to slightly higher values of K_0 and χ. The remaining difference with the other values quoted could be due to differences in secondary structure, for instance the distribution of the residual acetate groups.

In combining the MHS relation with known constants and the BSF equation, it is possible to calculate K_0 and χ with given molecular weights. However, mathematically the two equations are incompatible and values of K_0 and χ still depend somewhat on the molecular weights used. Taking reasonable

values for M the difference between the calculated and experimental values of K_0 is within 5% and for χ about 1%. An empirical equation proposed by VAN KREVELEN (1972) relating K and a with K_0 gives about the same values for K_0. In conclusion, if a MHS equation is used to calculate molecular weights, then values of K_0 and χ are determined within narrow limits by the values of a and K.

Our experimental values are slightly higher than the calculated ones, due to the weight given to the higher molecular weight samples in the BSF plot.

A check on $<\alpha_\eta>$ was made by calculating it using (4.40). The difference with the original $<\alpha_\eta>$ was small, about 2.5% for PVA 98 and 1.5% for the 88 series.

In comparison with other simple vinylpolymers such as polyethylene or polypropylene K_0 and C are relatively large (KURATA and STOCKMAYER 1963, FLORY 1969 Ch. II, DONDOS and BENOIT 1971). A relatively large steric hindrance can be due to interactions between chain segments, but also to water association with the hydroxyl groups. This would give rise to an increase in apparent molar volume which is equivalent to a larger steric hindrance. An argument against polymer-water association is the magnitude of the polymer-solvent interaction parameter, χ. In Θ-solvents $\chi = 0.5$, in better solvents χ decreases with solvent quality (FLORY 1953). The values obtained for χ show that water is only a poor solvent for PVA and that the difference between PVA 98 and 88 is neglectible. The same kind of information was gained from the Huggins constants (see sect. 4.3.1.). Probably the higher content of hydrophilic groups in PVA 98 as compared with PVA 88 is compensated by more intramolecular interactions. Evidence for some structuring in PVA chains in solution is given by FUJII et al. (1964), FUJIWARA et al. (1966), ZWICK (1965) and INAGAKI et al. (1972). Taking into account that polymer-solvent and polymer-polymer interactions are competitive, we conclude that the large values of K_0 and C suggest intersegmental interactions in the polymer chain.

4.5. SUMMARY

Several PVA samples differing in molecular weight and hydroxyl content were studied. Emphasis was given to properties such as: structural irregularities, stereoregularity, the acetate content and its distribution and molecular weight, which can be related to solution and interfacial behaviour of PVA.

From UV and IR spectra it was concluded that the samples used were atactic, contained no or very little 1, 2-glycol units and one or two conjugated carbonyl groups per molecule, probably present as end-groups. The acetate groups in the series of PVA with an hydroxyl content of about 88 mol %, PVA 88, are predominantly distributed in blocks along the chain. The PVA 98 samples have a more random distribution of these groups.

The magnitude of the Huggins constants, obtained from viscometry, suggest that no serious branching occurs in the samples and that water is a relatively

poor solvent. k' is independent of molecular weight and about the same for both types of PVA.

Viscometric molecular weights were calculated using the Mark-Houwink-Sakurada equation. For PVA 98 the constants $a = 0.64$ and $K = 4.67 \times 10^{-5}$ dm^3g^{-1} of MATSUMOTO and OHYANAGI (1960) were used, whereas for PVA 88 new constants were calculated ($a = 0.63$, $K = 4.97 \times 10^{-5}$ dm^3g^{-1}), based on the data of BERENIEWICS (1959b), taking into account the least branched samples only. The molecular weight distribution was found from gel permeation chromatography, GPC, using the unperturbed viscosity constant, K_0, as a characteristic dimension and nearly monodisperse polystyrene samples for the calibration. The distributions are rather broad and vary with the degree of polymerization, due to the differences in the polymerization methods. Average molecular weights obtained by GPC and viscometry agree reasonably.

Viscometry is also used to obtain the properties of the PVA samples in solution. Unperturbed dimensions, linear expansion factors and polymer-solvent interaction parameters were calculated, taking into account heterodispersity effects. The differences between PVA 98 and 88 are small. Again, the solvent quality is found about the same for both kinds of PVA, water being a relatively poor solvent. For PVA 88 a slightly greater value is found for the steric hindrance or characteristic ratio. The relative magnitude of this parameter, combined with the fact that water is a poor solvent for both PVA 98 and PVA 88, suggests that intersegmental interactions occur in the polymer chain.

A literature review of the solution parameters shows that our values for PVA 98 agree well with the best literature data. For PVA 88 such a conclusion is not possible due to the limited number of data.

5. ADSORPTION OF POLYVINYL ALCOHOL ON SILVER IODIDE

5.1. INTRODUCTION

In the last twenty five years much work, both experimental and theoretical has been devoted to adsorption of polymers and considerable insight into its mechanism has been gained. An extensive review of the early work has been given by PATAT et al. (1964) and more recent literature is included in review articles by STROMBERG (1967), SILBERBERG (1971), VINCENT (1974), ROE (1974) and LIPATOV and SERGEEVA (1974, 1976). One of the principle concerns in the study of polymer adsorption is the conformation of the adsorbed layer. As shown in chapter 1. at least three parameters are necessary to characterize such a layer:

1. the total adsorbed amount, Γ_p,
2. the amount, Γ_A, adsorbed in the first layer or the degree of occupancy, θ, of that layer
3. the segment density distribution, $\rho(x)$, or alternatively some insight into the effective layer thickness, $\overline{\Delta}$.

In this chapter we shall treat the adsorption isotherm, Γ_p as a function of the polymer concentration, c_p. In the next chapter electrical double layer and electrophoresis measurements are invoked to obtain θ or Γ_A and $\overline{\Delta}$ as a function of the adsorbed amount Γ_p. Finally a description of the adsorbed layer is given.

5.2. THE ADSORPTION ISOTHERM

5.2.1. *General features*

Of the three above mentioned parameters the adsorption isotherm is generally the easiest to establish. On solid adsorbents, the total adsorption is readily found from the difference in the polymer concentration before and after adsorption. The amount adsorbed is generally observed to remain almost independent of the bulk concentration over a large part of the range that is studied in practice. When several orders of magnitudes of bulk concentrations are investigated often a slight increase is noticed in the adsorption plateau, such an increase being theoretically expected. The rise to the plateau value is very steep and occurs often at so dilute a concentration that its experimental determination is impossible. This is a serious disadvantage, as the intial part of the isotherm where molecules can adsorb in an isolated state, is especially interesting for comparison with adsorption theories (e.g. SILBERBERG 1967, 1972, HOEVE 1965, 1971, 1976, MOTOMURA et al. 1971b, RUBIN 1966).

Another problem in relation to adsorption theories is that complete desorption upon washing with pure solvent or dilution is seldom achieved. It follows

that in this respect the adsorption is (partially) irreversible. The reason is that an adsorbed polymer molecule has many segments in contact with the surface. For desorption of the whole molecule to occur, all of these attachments have to be broken simultaneously, which makes the probability of complete desorption extremely small. However, this does not mean that polymer adsorption as such is irreversible. Addittion of competitive adsorbates or changing the solvent power often leads to desorption (PATAT et al. 1964, LIPATOV and SERGEEVA 1974).

5.2.2. *Effect of molecular weight*

A variable frequently investigated, also in the present study, is the molecular weight, M, of the adsorbing polymer. The general trend for non porous adsorbents is that for not too high molecular weights the mass adsorbed increases with molecular weight (see e.g. LIPATOV and SERGEEVA 1974). For very high molecular weights this increase levels off and finally the adsorption becomes independent of M. The relation between Γ_p and M is often expressed in an empirical form first proposed by PERKEL and ULLMAN (1961):

$$\Gamma_p = K_\Gamma < M >^{a_\Gamma} \tag{5.1}$$

where a_Γ and K_Γ are constants, $< M >$ is an average molecular weight. The magnitude of a_Γ is a rough indication of the conformation of the molecules at the interface. If $a_\Gamma = 0$, the adsorption is independent of M suggesting a flat conformation, or a distribution of segments in the adsorbed layer independent of M. The opposite, $a_\Gamma = 1$, corresponds to a fixed number of attachments per molecule independent of M, e.g. terminally bound chains. Adsorption as a random coil of unperturbed molecules would result in $a_\Gamma = 0.5$. Clearly, a_Γ also depends on parameters influencing the conformation at the interface such as solvency and the nature of the interface or the net adsorption energy. According to current adsorption theories, better solvency and higher affinity result in flatter conformations, thus a_Γ should be smaller under these conditions.

In practice the use of (5.1) is complicated by the fact that K_Γ and a_Γ depend not only on the above mentioned parameters, but also on the polymer concentration and on the heterodispersity of the samples. The first problem is often circumvented by applying (5.1) to the plateau region only (also because of lack of information on the intitial part of the isotherm). The hetero-dispersity problem is similar to the one described in sect. 4.3.1. for the Mark-Houwink-Sakurada equation. However, the appropriate kind of average to be used in (5.1) is not known. To obtain this, one should know the dependence of Γ_p on c_p for a monodisperse sample. Moreover, adsorption can have a fractionating effect due to preferential adsorption of the higher molecular weight molecules (FELTER and RAY 1960, FELTER 1971, LIPATOV and SERGEEVA 1974, STROMBERG 1967). In conclusion, (5.1) has only a limited importance and a meaningful comparison of a_Γ is only possible for well-defined systems, including monodisperse polymers.

Theoretically it has also been predicted that Γ_p increases with molecular weight, except at very high values of M (SILBERBERG 1968, HOEVE 1966, 1971, SIOW and PATTERSON 1973, ROE 1974). This trend becomes more pronounced in not good solvents. In a Θ-solvent Γ_p should be roughly proportional to $M^{0.5}$, for better solvents the dependence is less. This suggests that in practice values of $a_\Gamma > 0.5$ may not be expected often.

5.2.3. *The silver iodide – polyvinyl alcohol system*

In the system under study, AgI-PVA, three main variables will be considered. First the molecular weight, second the acetate content of the polymer and third the surface charge of the silver iodide. As shown in sect. 4.1. the first two parameters have a relatively large influence on the adsorption of PVA. The surface charge of the AgI is important in considering double layer effects.

Experience of other authors on the adsorption of PVA shows that the effect of molecular weight on the adsorption of PVA depends on the acetate content and the nature of the adsorbing surface, the adsorption generally increasing with increasing M (GREENLAND 1963, 1972, SUGIURA and YABE 1970, SUGIURA 1971, FLEER et al. 1972, GARVEY et al. 1974, 1976, BARAN et al. 1976, FLEER and SMITH 1976a, b).

Experimental values of a_Γ for PVA adsorbed from aqueous solutions (close to Θ-conditions, see sect. 4.4.3.) are in the range 0.5 to values < 0.1. For PVA containing 0.5 to 2% acetate groups the adsorption on negative silver iodide is relatively independent of M (SUGIURA and YABE 1970, FLEER et al. 1972), whereas for PVA 88 a much stronger M effect is found (BARAN et al. 1976).

LANKVELD and LYKLEMA (1972) show that for the paraffin-water interface the effect of molecular weight on the amount adsorbed is markedly greater than on the interfacial tension. This might suggest that the number of train segments in the interface is less dependent on M than is the total adsorption.

In general, acetate groups have a marked effect on the physical properties of PVA, including its interfacial behaviour (see sect. 4.1.). Increasing the percentage of these groups from 0.5 or 2% to about 12% drastically increases the adsorption. This increase in adsorption can be explained only partly by a decrease in the solvent quality. As pointed out in sect. 4.4.3. the polymer-solvent interaction parameter, χ, is only slightly smaller for PVA 98 than for PVA 88. Another contribution could be a somewhat larger gain in adsorption free energy by the replacement of adsorbed solvent molecules by a polymer segment containing an acetate group. However, this contribution is also small (SILBERBERG 1968). An important factor may well be the distribution of acetate groups, which is found to determine the interfacial behaviour of PVA drastically (SCHOLTENS 1977). This is probably due to the fact that in an adsorbed *blocky* copolymer loops (or tails) and trains can be of different nature.

Theoretical treatments of copolymer adsorption are scarce (MOTOMURA et al. 1971a, CLAYFIELD and LUMB 1974a, b) and have a limited applicability.

Apart from variations in the natures of the polymer samples used, we also have to deal with some factors introduced by the use of silver iodide. Silver iodide may be present as a sol or a precipitate. In the precipitate individual particles adhere and form aggregates, which can lead to a smaller adsorption per unit weight or unit area if, for instance, pores in these aggregates become inaccessible to the polymer molecules, thus complicating the interpretation of the adsorption experiments. Another disdavantage of the precipitated silver iodide samples is that their specific surface areas are rather small, leading to relatively inaccurate adsorption measurements. At first sight, these considerations are good reasons to use only the silver iodide sol. However, for double layer studies a precipitate is required as sols would coagulate during the experiments, resulting in a decrease in the specific surface area and a poor reproducibility (see sect. 3.2.). Moreover, the surface charge of the silver iodide is an important variable and with a sol only a very limited range can be studied.

Thus, to be able to make a proper comparison between the results of the double layer studies and the adsorption measurements, isotherms on both sols and precipitates have to be investigated. For similar reasons, the salt concentration was also included as a variable.

Finally the silver iodide concentration itself is varied. Both particle aggregation and partial flocculation due to polymer bridging can lead to a decrease in the effective surface area. Changing the silver iodide concentration affects both factors, so that their influence, if any, can be studied.

In conclusion, earlier studies on the adsorption of PVA are of interest but except for the work of FLEER et al. (1972), the characterization of the adsorbed layer is limited to the determination of one or two of the essential parameters: Γ_p, Γ_A (or Θ) and $\rho(x)$ (or $\bar{\Delta}$). In the present study all three parameters are investigated and the influence of molecular weight, acetate content and surface charge on each of them is examined. In this chapter a description is given of Γ_p (c_p). Some complications due to the use of silver iodide will attract special attention. Chapter 6, deals with Γ_A (or Θ) and $\bar{\Delta}$.

5.3. EXPERIMENTAL PROCEDURES

5.3.1. *Adsorption measurements*

Adsorption isotherms were measured at $pAg \approx 5.6$ and $pAg \approx 11$ ($pI \approx 5$) on a silver iodide sol (A) and on precipitates, III, VI and VIII. The pAg values stated are initial values, due to adsorption a shift up to one pAg unit might occur.

The *general procedure* was that to a stoppered flask containing a known amount of silver iodide a quantity of freshly prepared PVA solution was added from a burette. The wet precipitate was weighed in a flask having a precisely known volume. From the known volume of the flask and the weight of it filled with water, W_w, or silver iodide slurry, W_{AgI}, the amount of silver iodide, x, is found as

$$x = \frac{W_{AgI} - W_w}{1 - \rho_w/\rho_{AgI}} \quad (\text{g AgI}) \tag{5.2}$$

ρ_w and ρ_{AgI} are the densities of water and silver iodide respectively. For the introduction of the sol a pipette was used.

To prevent irregular mixing and adsorption, a sharp boundary was maintained between the silver iodide phase and the PVA solution before the flasks were shaken by hand. Thereafter the bottles were rotated end-over-end for at least 48 h at room temperature. Subsequently the samples were centrifuged sols at 20,000 r.p.m. for 20 min., precipitates at 5,000 r.p.m. for 15 min. The concentration of PVA in the supernatant liquid was determined spectrophotometrically as described in sect. 5.3.2.

Loss of PVA 98 or 88 by *adsorption on the glassware* was checked by measuring isotherms on 5 g powdered glass (0.5 m^2g^{-1}). The adsorption turned out to be negligible.

The *time dependence of adsorption* was studied over a period of 160 h, during which PVA 48–98 was adsorbed onto silver iodide precipitate III at $pAg \approx 5.6$, using a AgI concentration of 2% (w/v). The equilibrium concentration of PVA was about 30 mg dm^{-3}.

A *desorption study* was made with PVA 48–98 and PVA 40–88 by redispersing into water several centrifuged silver iodide sol samples on which PVA was adsorbed. The samples were again rotated for 48 h and the supernatant analyzed for PVA.

The adsorptions of PVA 48–98 and PVA 60–99 as a function of the *silver iodide concentration* were investigated at sol concentrations ranging from 0.05 to 1.4% (w/v) by measuring adsorption isotherms at $pAg \approx 11$. On silver iodide precipitates this dependency was studied at $pAg \approx 5.6$ using PVA 48–98. The adsorption was measured at one equilibrium concentration PVA (50 mg dm^{-3}) only. The solid content was varied from 1 to 8% (w/v).

The influence of the *presence of KNO_3* was investigated at $pAg \approx 11$ both with sols and precipitates, using PVA's 48–98, 40–88 and 13–88. Variable solid concentrations were also considered here.

5.3.2. *Determination of the PVA concentration*

The concentration PVA was determined spectrophotometrically in a Unicam SP600 with 1 cm cells at 670 nm. To do this, 4 cm^3 of a reagent containing 0.64 M H_3BO_3, 0.006 M I_2 and 0.018 M KI were added to 6 cm^3 of PVA solution (0–40 mg dm^{-3}) (HORACEK 1962, FLEER 1971). Both the addition of the reagent and the mixing were done carefully to avoid the formation of 'blue specks' in solution, which form on excessive agitation. The green complex formed was placed in the dark in a thermostatted room for at least half an hour to obtain a stable colour and to ensure that the absorbance was measured at constant temperature. This is necessary as the colour intensity is temperature dependent (ZWICK 1965).

Calibration curves were measured at the same temperature, using calibrated flasks and pipettes. They appeared to be good straight lines. Despite these precautions, the error in the analysis is about $\pm 2\%$. The slopes of the lines depend on molecular weight and acetate content, a behaviour already described by ZWICK (1966) and FLEER (1971).

At $pAg < 8.5$ some silver iodide sol is formed on addition of the reagent to the polymer solution, due to the iodide concentration in the former solution. However, under these conditions the blank also contains some sol and the calibration lines at pAg 5.6 and pAg 11 were identical within the experimental accuracy.

Addition of some KNO_3 to the PVA solutions increased the absorbance a little. Therefore for every salt concentration a new calibration line was established.

5.4. RESULTS AND DISCUSSION

5.4.1. *General*

Adsorption isotherms of five PVA samples adsorbed on sol A and precipitate III are shown in figs. 5–1 and 5–2 respectively. The adsorption is expressed in mg m^{-2} using the specific surface areas based on methylene blue adsorption, for reasons given in sect. 3.4. The reported isotherms on *sol* A are obtained at $pAg \approx 11$ ($pI \approx 5$) and a sol concentration of 0.5% (w/v). For PVA 48–98 the effect of the pAg is shown in the inset. The adsorption on *precipitate* III is measured at $pAg \approx 5.6$ and a solid concentration of 2% (w/v). In the inset in fig. 5–2 the effect of the pAg on the adsorption of PVA 48–98 is shown, these isotherms were measured on precipitate VI.

Generally the isotherms have a high-affinity character, adsorption saturation values being attained at equilibrium concentrations of 75–120 mg dm^{-3}. The concentration range studied does not permit one to decide whether or not the saturation adsorption is definite or a pseudo plateau.

In comparing the results shown in figs. 5–1 and 5–2 one should keep in mind that 1. the accuracy and reproducibility in the case of a sol is much better due to the larger total surface area available, 2. the absolute amount adsorbed on different dispersions may differ by about 10–15% due to the inaccuracy of the specific surface areas and 3. the two sets of isotherms are recorded at two different pAg values, namely 5.6 and 11. Within these limits of uncertainty the adsorption of PVA onto silver iodide sols and precipitates is essentially the same. This result is based on specific surface areas calculated from the methylene blue adsorption. However, the conclusion would be principally the same if capacitance areas were used, if for sol A at $pAg = 11$ $S = 36$ m^2g^{-1} would have been taken.

The values obtained for the adsorption correspond reasonably with other literature data (SUGIURA and YABE 1970, BARAN et al. 1976). However, in comparing absolute adsorption data the specific surface areas of the silver

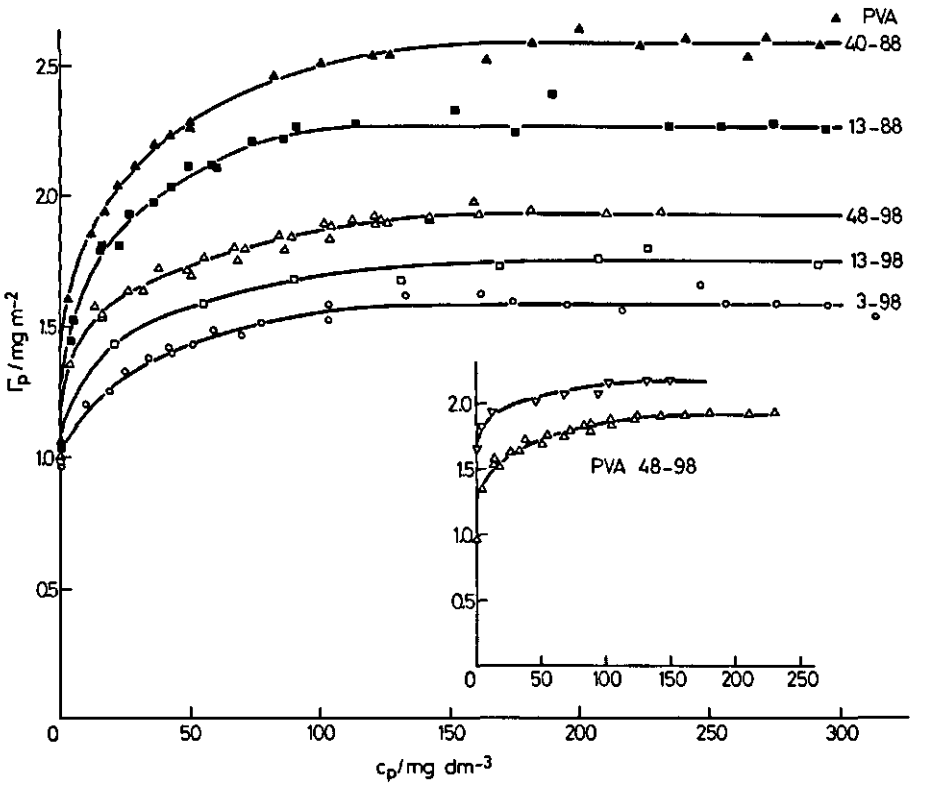

FIG. 5–1. Adsorption isotherms of PVA on AgI sol A.
c_{AgI} = 0.5% (w/v); adsorption time 48 h: $pAg \approx 11$; △, PVA 48–98; ▲, PVA 40–88; □, PVA 13–98; ■, PVA 13–88; ○, PVA 3–98.
In the inset the effect of the pAg upon the adsorption is shown for PVA 48–98; ▽, $pAg \approx 5.6$; △, $pAg \approx 11$.

iodide dispersions are needed and neither one of the above mentioned articles reports on them, hence the correspondence may be fortuitous. Values found by FLEER et al. (1972) are somewhat lower, due to the fact that the samples were agitated for one hour only. Moreover, another method was used to determine the surface area which may have led to the different result.

Indirectly some information on the conformation of the adsorbed polymer can be obtained by comparison of the total adsorption with the adsorption in a flat monolayer. Assuming a surface area per segment of 0.25 nm^2 (LANKVELD 1970, BARAN et al. 1976b) the amount adsorbed in a close-packed monolayer would be about 0.30 mg m^{-2}. Thus, at the saturation adsorption the major amount (5/6 to 7/8) of PVA is located in loops and tails dangling in the solution phase, giving the PVA adsorbate layer its spatial extension. At a lower amount adsorbed a relatively higher portion of the segments can be adsorbed at the surface, giving a thinner layer. In chapter 6. we shall discuss this matter in more detail.

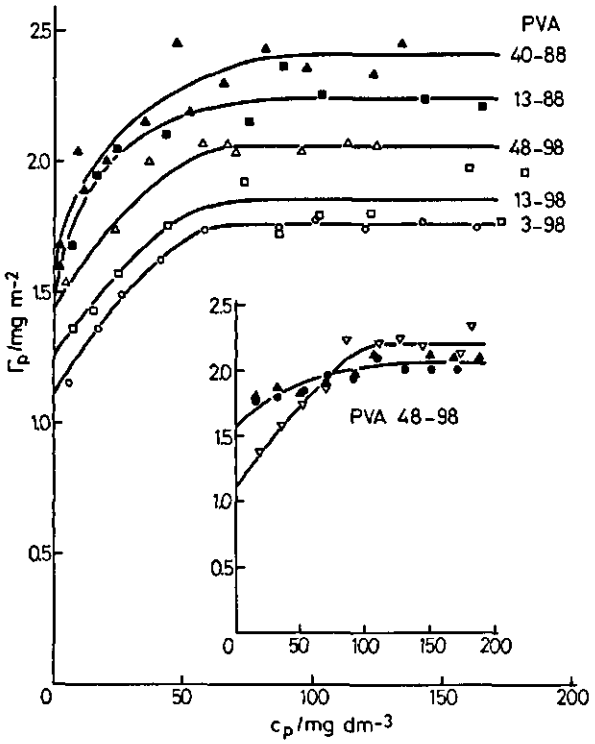

FIG. 5–2. Adsorption isotherms of PVA on AgI precipitate III.
c_{AgI} = 2% (w/v): adsorption time 48 h: $pAg \approx 11$; △, PVA 48–98; ▲, PVA 40–88; □, PVA 13–98; ■, PVA 13–88; ○, PVA 3–98.
In the inset the effect of the pAg upon the adsorption is shown for PVA 48–98 on AgI precipitate VI. △, $pAg \approx 5.6$; ●, $pAg \approx 7.5$; ▽, $pAg \approx 11$.

The effects of surface charge, molecular weight and acetate content upon the adsorption will be discussed later.

The study of *adsorption versus time* showed an increase in the adsorption of about 40% over a period of 1 h to 40 h. An extension of the time to 160 h increased the amount adsorbed by only 5%, see for instance fig. 5–3. It seems reasonable to assume that the isotherms shown in figs. 5–1 and 5–2 are close to the limiting adsorption values. The increase can be explained either by a rearrangement of the molecules in order to enable more material to adsorb, or by displacement of initially adsorbed lower molecular weight molecules by higher molecular weight species. As shown in sect. 4.3.2. the molecular weight distribution of the PVA samples is rather broad.

Desorption of PVA's 48–98 and 40–88 could not be detected with the present technique. However, this may not be interpreted in terms of the segments being irreversibly bound, indeed the increase of adsorption with time pleads against

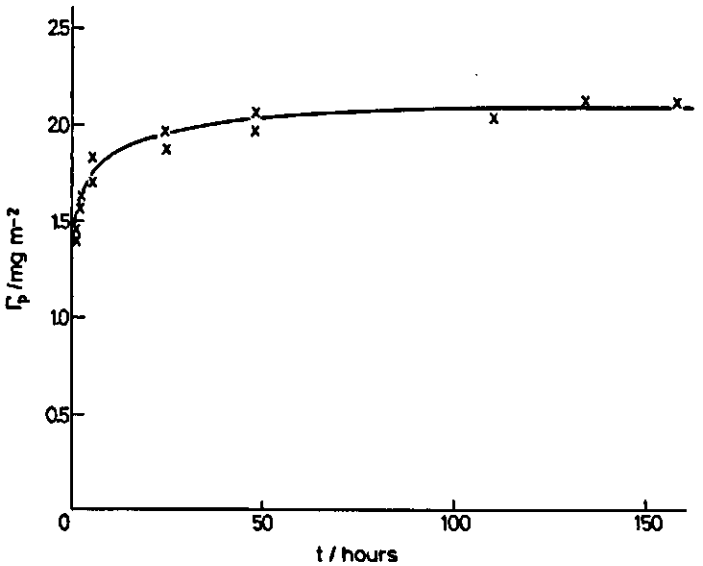

FIG. 5–3. Adsorption of PVA 48–98 on AgI precipitate III as a function of the time. $c_{AgI} = 2\%$ (w/v); $c_p \approx 50$ mg dm^{-3}.

this. More conclusive evidence for the reversibility of the segmental adsorption is given in chapter 6. Entire molecules do not desorb in the time given due to the negligible probability of simultaneous desorption of several tens or hundreds of segments.

5.4.2. *Effect of surface charge*

Adsorption studies were carried out at *pAg* 5.6 and 11. The first value coincides with the p.z.c. of the uncovered surface and at *pAg* = 11 the surface charge is −3 to −4 μC cm^{-2}. The results for PVA 48–98 are shown in the insets in figs. 5–1 and 5–2, other PVA's behave similary.

On precipitates at *pAg* = 11 the isotherms are often somewhat less accurate than at *pAg* = 5.6 and generally saturation adsorption is reached at a higher polymer concentration. However, the isotherms on the sol measured at both *pAg* values differ hardly in shape nor accuracy.

As noticed in sect. 5.4.1. close comparison of the results is difficult. Moreover, at *pAg* = 5.6 the sol is precipitated and only a very approximate estimate of the surface area is available, which may well account for the observed difference between the adsorption levels at both *pAg*'s. Taking all of this into account, we may say that the total adsorption at *pAg* 5.6 and 11 is the same.

For positive silver iodide SUGIURA (1971) reports a decreasing adsorption with increasing acetate content in contradistinction to the behaviour on negative silver iodide. Also the adsorption plateau is much lower, both for PVA 100 and PVA 90. The authors offered no explanation for this behaviour. The present

study, although done over a more limited surface charge range, seems not to confirm these results.

In conclusion, we find no significant dependence of the adsorption on pAg or surface charge. For further comments we shall base ourselves on the (more accurate) isotherms shown in fig. 5–1.

5.4.3. *Effect of molecular weight and acetate content*

The adsorption increases with molecular weight (fig. 5–1) with a proportionality to $M_v^{0.1}$ for PVA 98 and to $M_v^{0.2}$ for PVA 88. This feature is in qualitative agreement with adsorption theories, but quantitatively the increase is less than predicted. Water is nearly a Θ-solvent for both types of PVA (see sect. 4.4.3.) which should make the adsorption proportional to about $M^{0.5}$. An exact comparison is however not possible, the heterodispersity of the PVA samples is substantial (see sect. 4.3.2.) and the use of a wrong average molecular weight could lead to an error in the exponent of M. Moreover, PVA 88 and to a lesser extent PVA 98 are copolymers, while the theoretical prediction is based on the behaviour of homopolymers.

The differences in the adsorption level as a function of M are found most clearly with the sol at $pAg = 11$. On the precipitated sol at $pAg = 5.6$, or on the precipitates these differences are somewhat less pronounced.

Experimentally, SUGIURA and YABE (1970) found for the adsorption of PVA 99 on AgI even a lesser dependence on M_v. On the other hand BARAN et al. (1976) measured for PVA 88 on AgI a proportionality to about $M_v^{0.5}$. Although the trends are the same the agreement with our results is poor. However, we may not expect much more because (1) the viscometric molecular weights of the samples used were obtained with different coefficients in the MHS equation and the heterodispersities were unknown, (2) the number of experimental data is small.

The fact that the saturation adsorption depends only little on molecular weight indicates that the conformation of the adsorbed layer is not strongly dependent upon M. Probably preferential adsorption of higher molecular weight molecules occurs, especially in case of PVA 3–98. Knowing that ca. 85% of the segments is adsorbed in loops and tails we can exclude a flat conformation. Thus, the increase in saturation adsorption with M takes place because of a somewhat greater adsorption in loops and tails, whereas the adsorption in the first layer is relatively constant. In chapter 6. we return to this matter.

The maximum adsorption increases with acetate content by about 30% at fixed molecular weight. Qualitatively similar results have been obtained by SUGIURA and YABE (1970) and by BARAN et al. (1976). The difference between the adsorbed amounts PVA 88 and PVA 98 at the plateau adsorption is greater than could be accounted for in a complete monolayer. Thus, although θ_{max} can be slightly different for both types of PVA, the contribution of the first layer to this difference is small. The increase in adsorption with increasing acetate content must be largely attributed to a greater adsorption in loops and

tails. As shown before (sect. 5.2.3.) χ (PVA 98) and χ (PVA 88) are only slightly different and we cannot fully explain the difference in adsorption behaviour with this parameter. The difference in free energy created by the replacement of some water molecules by a polymer segment on the adsorbent surface, is also unlikely to produce a convincing explanation. From the double layer studies, especially from the position of the common intersection point and the magnitude of the shift of the point of zero charge, to be discussed in chapter 6, we infer that relatively many segments containing an acetate group are adsorbed in case of PVA 88. This is possible by virtue of the fact that the distribution of the acetate groups in PVA 88 is blocky, whereas that in PVA 98 is more random (see sect. 4.2.). Once a segment with an acetate group in PVA 88 is adsorbed, the neighbouring segments easily follow. This preference of adsorption of acetate containing segments will have some important consequences. a. The first layer consists of relatively many acetate groups. In this situation χ_1, the χ-parameter for the first layer, will be definitely much larger than χ_1(PVA). Due to the fact that χ_1 is to be multiplied by a factor counting the number of interactions (SILBERBERG 1968) this may give an important contribution to the gain in free energy of adsorption. b. A second difference is that the restrictions which accompany the transition from train to loop and vice-versa can be different for both types of PVA. It is not unrealistic to assume that PVA 88 has a relatively lower flexibility, which could perhaps set constraints to the minimum loop size. Due to the preferential adsorption of acetate groups, the train size is limited by the length of the acetate blocks. The result of a. and b. would be that adsorbed layers of PVA 88 contain more material than those of PVA 98 both for enthalpic (interactions between trains) and entropic reasons (long loops).

5.4.4. *Influences of the silver iodide concentration and the presence of salt*

Figures (5–4) show that there is a pronounced effect due to the silver iodide concentration For both PVA's the curvature of the isotherms is affected: the smaller the silver iodide sol concentration, the steeper the isotherm. For PVA 48–98 there is also a decrease in adsorption noticed at high silver iodide concentrations.

On silver iodide *precipitates*, the results are ambiguous due to the poorer reproducibility, but within experimental error the solid content does not affect the adsorption.

The addition of KNO_3 up to 10^{-1} M decreases the adsorption on the sol by 20–25%. The solid content is again reflected in the shape of the isotherm. Results for PVA 48–98 are shown in fig. 5–5. Similar behaviour is observed for PVA's 40–88 and 13–88. On silver iodide precipitate VIII the adsorption of PVA's 48–98, 40–88 and 13–88 was measured at 10^{-3} M and 10^{-1} M KNO_3. At low silver iodide concentrations ($\leqslant 4\%$) the saturation adsorption is almost independent of the presence of salt, whereas in 10^{-1} M the adsorption is only 5% lower than without salt. However, increasing the silver iodide concentration to 10% in the presence of 10^{-1} M KNO_3 decreases the adsorption by 20%.

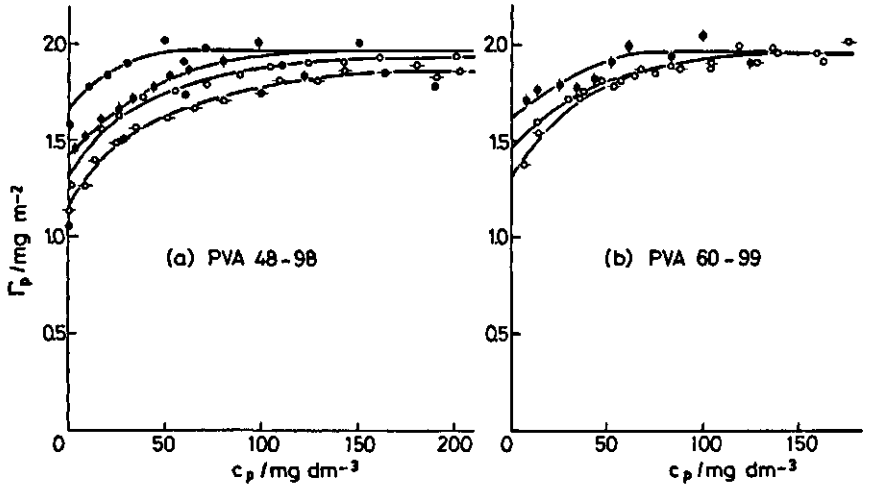

FIG. 5–4. The effect of the AgI sol (A) concentration upon the adsorption of PVA 48–98 (a) and PVA 60–98 (b). Sol concentrations (%, w/v): ●, 0.05; ♦, 0.2; ○, 0.5; ⊖, 1.1; ◆, 1.3.

A further increase in the solid content to 40% gradually decreases Γ_p by another 10%.

The effect of 10^{-1} M KNO_3 is different for the sol and the precipitate. With a sol a drastic decrease in adsorption is found, whereas for the precipitate such a strong decrease occurred only at high silver iodide concentrations. This suggests that in the presence of 10^{-1} M salt the sol partially coagulates, resulting in a decrease in the area available for adsorption. For the sol such an effect was demonstrated in sect. 3.2.2. and 3.4.3. Moreover, a satisfactory explanation of the decreasing adsorption on the basis of solvency or double layer effects is not unambiguous (FLEER 1971, BARAN et al. 1976).

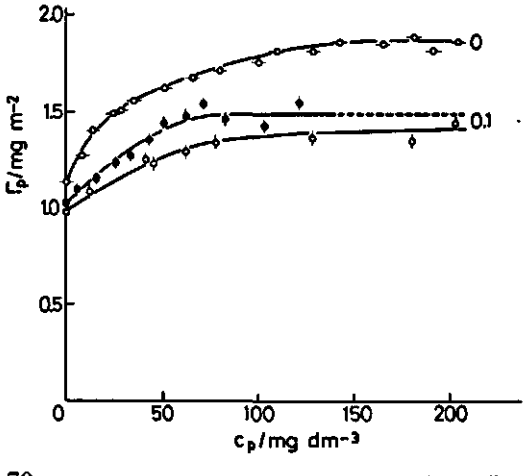

FIG. 5–5. The influence of the KNO_3 concentration upon the adsorption of PVA 48–98 on AgI sol A. The salt concentration in mol dm^{-3} is indicated.
Sol concentrations (%, w/v): ⊖, ⌽, 1.1; ●, 0.2.

With precipitates the situation is somewhat different. Before adsorption large aggregates of particles are already present, which could redisperse upon adsorption, resulting in a much better dispersed precipitate. However, in the presence of 10^{-1} M KNO_3 the aggregates become more stable and complete redispersion is difficult. Moreover, polymer molecules may adsorb on different particles in the aggregate, leading to a stable floc and a decrease in effective area, especially at high silver iodide concentration.

In conclusion, we presume that the lower adsorption in the presence of 10^{-1} M KNO_3 is due to a decrease in the effective surface area.

The change in the shape of the isotherms upon an increase of the silver iodide concentration is probably also due to a reduction in the effective area. FLEER and LYKLEMA (1976) showed that at very low silver iodide concentrations (1 mmol dm^{-3}) in the presence of some electrolyte partial flocculation occurred upon addition of PVA to a silver iodide sol. This was explained by the formation of polymer bridges between the sol particles. This bridging mechanism occurs only at low polymer concentrations. It reduces the total adsorption somewhat due to the fact that an already adsorbed polymer again adsorbs on a second particle, thereby blocking some area. In the present study we found a change in the curvature of the isotherm as a function of the solid content, also in the absence of salt. However, the silver iodide concentration is in our case much higher and some bridging could occur due to the much greater particle collision frequency. Increasing the silver iodide content increases the possibility of bridging, leading to smaller adsorption at low polymer concentrations. In other words the slope of the isotherm is affected, not the saturation adsorption. Assuming that this explanation is correct, the ideal adsorption isotherm of PVA on silver iodide is best approached at low silver iodide concentrations. Hence, the ideal isotherms will be somewhat steeper than those shown in fig. 5–1, but the saturation values are correct.

5.5. SUMMARY

Adsorption isotherms of polyvinyl alcohol on silver iodide sols and precipitates are essentially the same and in qualitative agreement with previous experimental findings. As a function of the polymer concentration, the adsorption rises steeply to a plateau value and then remains independent of the bulk concentration up to at least 300 mg dm^{-3}. At the saturation about 85% of the polymer is located in loops and tails, indicating a layer thickness far beyond the thickness of a segment. Within the time given (48 h) the adsorption approaches closely its limiting value. However, experiments in which the silver iodide concentration was varied, suggest that at low polymer concentrations some bridging occurs, resulting in too low adsorption values. It was concluded that the ideal isotherms will rise more steeply to their sturation values than the measured isotherms do.

Changing the surface charge of the silver iodide from ca. 0 μC cm^{-2} to ca. -3 μC cm^{-2} has no measurable influence on the total adsorption.

Increasing M increases the adsorption with a proportionality to $M_v^{0.1}$ for PVA 98 and to $M_v^{0.2}$ for PVA 88. These low proportionalities suggest that the conformation in the adsorbed state is only little dependent upon M. Probably preferential adsorption of higher molecular weight molecules occurs, especially in the case of PVA 3–98. The amount adsorbed in the first layer is expected to be less dependent on M than Γ_p.

The adsorption rises also with increasing acetate content, resulting in both longer loops and longer tails. This increase is explained by a preferential adsorption of acetate containing segments. Due to this, in the first layer polymer-polymer interactions are favoured over polymer-solvent interactions. leading to a stronger adsorption in this layer. Moreover, the lower flexibility in PVA 88 favours an increase of the average loop length, which, in turn, leads to an increase in adsorption.

No desorption of the polymer could be detected, but the increase in adsorption with time shows that the segments are reversibly bound, at least to some extent.

The reduction in adsorption by the addition of KNO_3 up to 10^{-1} M is explained by a decrease in the available surface area due to partial coagulation of the silver iodide.

6. CHARACTERIZATION OF THE ADSORBED POLYMER LAYER BY DOUBLE LAYER MEASUREMENTS

6.1. INTRODUCTION

In chapter 5. the total adsorption, Γ_p, as a function of the polymer concentration was discussed. It was shown that Γ_p depends on molecular weight and acetate content, but not significantly on the surface charge. Indirectly it is shown that the conformation of the adsorbed layer is not very dependent on M. In the present chapter we shall examine the conformation in more detail. Double layer measurements in conjunction with electrophoresis studies will be used to obtain the degree of occupancy of the first layer, θ, and the effective thickness, $\bar{\Delta}$. Preliminary work with the AgI-PVA system (KOOPAL 1970, FLEER et al. 1972) has shown that the obtained information, combined with direct adsorption data, can be used to assess $\rho(x)$.

Besides this, the double layer studies reveal interesting aspects of the behaviour of a charged substrate in the presence of an adsorbed polymer. Both the conformation of adsorbed polymers and the effect of a neutral polymer on the properties of a double layer are important for e.g. colloid stability (FLEER 1971, VINCENT 1974).

6.2. BASIC PRINCIPLES AND OUTLINE OF THE DOUBLE LAYER STUDIES

Silver iodide particles, dispersed in aqueous solution generally have a charge on their surface. This surface charge, together with the counter charge in the solution around that particle forms the electrical double layer. Usually the solution side of the double layer is thought of as being in two parts (see e.g. OVERBEEK 1952, SPARNAAY 1972): (1) a non-diffuse molecular condensor or Stern-layer (STERN 1924) and (2) a diffuse or Gouy-layer (GOUY 1910, 1917) in which charge and potential obey the Poisson-Boltzman distribution. The Stern-layer is the site of specific interactions with the surface and is sometimes further subdivided (GRAHAME 1947), whereas the diffuse layer is entirely non-specific. Although the division is an abstraction of the physical reality, experience over several decades has shown (see e.g. OVERBEEK 1952, SPARNAAY 1972, BIJSTERBOSCH and LYKLEMA 1977) that it works satisfactorily.

With polymer adsorption, the situation is similar. The actual nature of the average segment density as a function of the distance to the surface, $\rho(x)$, generally depends on many factors, e.g. the amount adsorbed, Γ_p, the net adsorption energy per segment, the quality of the solvent, chain flexibility, the presence of long tails, etc. (e.g. SILBERBERG 1968, 1972, 1975, HOEVE 1965, 1971, 1976, HESSELINK 1969, 1971, 1975, ROE 1974, CHAN et al. 1975a, b). However, the direct influence of the surface is most strongly felt by the segments in

actual contact with it, the train segments. Again as a first approximation, a division can be made into two regions: 1. that under direct influence of the surface which contains the train segments and 2. the region in intimate contact with the solution, containing loops and tails.

Geometrically, the Stern-layer and the train segment layer, having about the same thickness of ca. 0.4 nm, may be thought of as coincident. The diffuse layer and the layer of loop and tail segments then both start from the Stern-plane and extend into the solution. However, their thicknesses are not sharply defined because both the number of counterions and segments in loops and tails decay gradually with distance. Generally, the thickness of the diffuse layer is expressed as the reciprocal Debije length, κ^{-1} (see e.g. OVERBEEK 1952). This thickness depends on the concentration and valency of the ions present in solution. For example, in 10^{-3} mol dm^{-3} KNO_3 it is 10 nm, but in 1 mol dm^{-3} KNO_3 it is only 0.1 nm. For the 'effective' polymer layer thickness at a given adsorption no general measure exists because of the complexity of the segmental distribution and the interpretational difficulties of thickness measurements. Actual values reported in literature (SILBERBERG 1962, 1975, HOEVE 1966, STROMBERG 1967, LIPATOV and SERGEEVA 1974) vary widely, but are usually of the order of one to several tens of nm. They depend on the factors mentioned above for the density distribution and on the experimental method.

The overall situation of a neutral polymer adsorbed on a charged interface with its electrical double layer is illustrated in fig. 6–1. The figure is schematic especially with respect to the distribution of segments over trains, loops and tails. Summarizing the picture, the following important conclusion can be made:

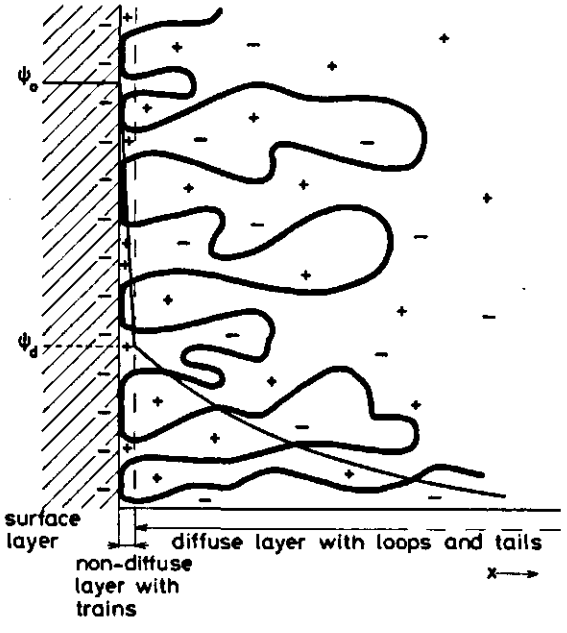

FIG. 6–1. Schematic representation of a polymer adsorbed at a charged interface. The course of the potential, $\psi(x)$, is indicated.

Upon adsorption of a neutral polymer on a charged surface any modification of the Stern-layer is only attributable to adsorption of train segments, whereas modification of the diffuse layer is essentially attributable to the presence of loops and tails.

Thus, an investigation of the Stern-layer properties will give valuable information on the adsorption in the first layer, the train segments. As the double layer is essentially non-diffuse in concentrated electrolyte solutions, this condition is favourable for study of the Stern-layer properties. On the other hand information on the diffuse layer properties, reflecting the presence of loops and tails, is preferably obtained at low electrolyte concentrations because an extended diffuse layer is needed. However, for the determination of $\psi(x)$ in the diffuse part, the Stern-layer properties also have to be known. In fig. 6–1 a potential distribution is drawn representing approximately the situation for a highly charged silver iodide particle in 10^{-3} M KNO_3. It should be noted that the potential at the Stern-plane, ψ_d, is substantially lower than the surface potential, ψ_0. The potential decay over the Stern-layer depends not only on the salt concentration, but also on the amount of polymer adsorbed in trains. For the interpretation of the experimental data this last factor should be taken into account. In literature this point is often not properly recognized, not only in electrophoretic thickness studies but also in work on colloid stability.

In the study to be described, double layer charges on AgI are measured in 10^{-1} M KNO_3 in the presence of varying amounts of different types of PVA. As PVA is uncharged (see sect. 4.1.) the only charge on the particle + adsorbed polymer is that of the AgI surface. The results reflect Stern-layer properties, especially θ and the orientation of segments. Electrophoresis in 10^{-3} M electrolytes gives similar information and in combination with the double layer studies, a measure for an effective polymer layer thickness, $\bar{\Delta}$, is obtained.

Comparing the properties of low molecular weight alcohols at the silver iodide/solution interface (BIJSTERBOSCH 1965, BIJSTERBOSCH and LYKLEMA 1965, VINCENT et al. 1971, DE WIT and LYKLEMA 1973, DE WIT 1975) with those of PVA reveal a number of striking analogies which are very useful for the interpretation of the present data.

Double layer studies on mercury in the presence of polymers (MILLER and GRAHAME 1956, WOJCIAK and DUTKIEWICS 1964, CRAIG et al. 1967, YOSHIDA et al. 1972a, b, c, MARSZALL 1974, MILLER 1971, MILLER and BACH 1973) are somewhat difficult to compare with those on the AgI-PVA system because of time effects inherent to the capacitance measurements on growing droplets and the fact that it was not always properly recognized that the Stern-layer properties reflect the behaviour of the train segments only.

6.3.1. *Surface charge versus pAg curves*

The starting point for double layer analyses is a set of surface charge, σ_0, against pAg curves in the presence of varying amounts of PVA. These curves have been obtained by potentiometric titration of AgI precipitates with potential determining ions (I^- or Ag^+), following essentially the procedure described by BIJSTERBOSCH and LYKLEMA (1965, 1977). The surface charge is defined by

$$\sigma_0 \equiv F(\Gamma_{Ag^+} - \Gamma_{I^-}) \tag{6.1}$$

where F is the Faraday and Γ_{Ag^+} and Γ_{I^-} are the surface excesses of the two p.d. ions. Relative values of σ_0 thus obtained are plotted as a function of the pAg, which according to Nernst's law is a measure of the surface potential, ψ_0

$$\psi_0 \equiv -\frac{2.303\,RT}{F}(pAg - pAg^0) \tag{6.2}$$

where pAg^0 is the value of the pAg in the point of zero charge. The definition of ψ_0 implies that ψ_0 is the Galvani potential difference across the interface with reference to the same at the p.z.c. An extensive description of the underlying thermodynamics is given by LYKLEMA (1977) and BIJSTERBOSCH and LYKLEMA (1977). The $\sigma_0(pAg)$ curves obtained by the titration technique agree satisfactorily with those from directly obtained double layer capacitances on AgI, using an AC-bridge (ENGEL 1968, PIEPER and DE VOOYS 1974, 1975).

Titration gives only the shape of $\sigma_0(pAg)$ curves, not their actual positions. In order to locate them, a reference point is needed. In the absence of polymer, but with KNO_3, the p.z.c. is used, being $pAg^0 = 5.67$ (BIJSTERBOSCH 1965, VINCENT and LYKLEMA 1970). In the presence of PVA we have used the fact that curves at different PVA additions passed through a common intersection point (c.i.p.), see figs. 6–5 to 6–9, a phenomenon already observed before with low molecular weight alcohols. By carrying out separately short titrations around these points at various amounts of PVA, it was possible to locate them within 0.2 $\mu C\ cm^{-2}$ for all PVA's. These c.i.p.'s (see table 6–1) were used to fix the positions of the long titration curves. The same procedure was applied by DE WIT and LYKLEMA (1973) to locate titration curves in the presence of ethylene glycol.

The adsorbed amounts in $\mu C\ g^{-1}$ were converted into values in $\mu C\ cm^{-2}$ with the specific surface areas given in table 3–1. For a discussion of the specific surface area we refer to chapter 3. The should be repeated that the surface charge expressed in $\mu C\ cm^{-2}$ is based on a surface area differing from that for polymer adsorption. Arguments for this have been given in sect. 3.6.

The elctrochemical cell

The electrochemical cell consisted of a silver iodide precipitate in 10^{-1} M

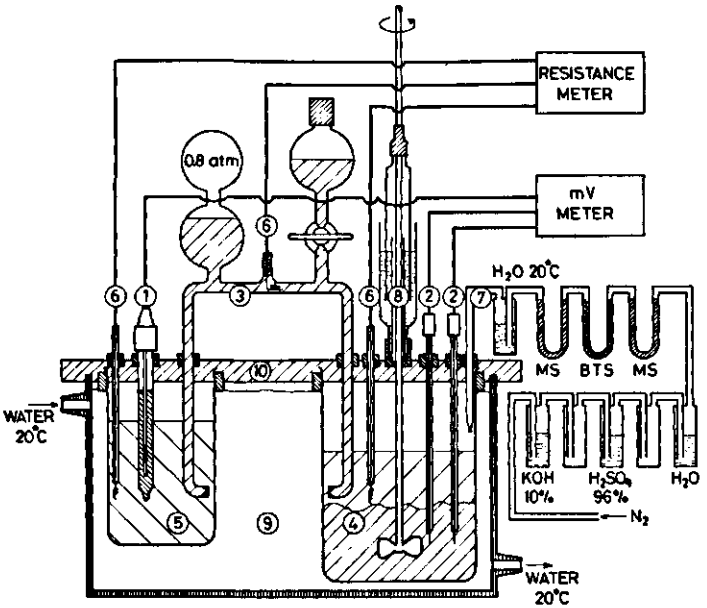

FIG. 6–2. Titration set up.
1. Saturated KCl calomel electrode.
2. AgI electrodes (5 ×).
3. Salt bridge with 1.75 M KNO_3 + 0.25 M $NaNO_3$ and two Van Laar-capillaries, overpressure 0.8 atm.
4. Measuring cell with AgI precipitate in 10^{-1} M KNO_3.
5. Vessel with saturated KCl.
6. Electrodes for the resistance measurement.
7. N_2 inlet and purification set up (BTS = reductor, MS = molecular sieve).
8. Stirrer with water lock.
9. Thermostatted bath, 20.0 ± 0.1 °C.
10. Perspex cover.

The whole cell is placed in a Faraday cage (not shown in the figure).

KNO_3 in which a set of at least five AgI electrodes and a reference electrode were placed. Fig. 6–2 shows a sketch of the experimental set-up. The large number of AgI electrodes is used for sake of mutual control: although between the different electrodes the potential may differ by 0.5 mV, the relative changes with the solution composition usually remained to within 0.1 mV. The electrodes were prepared following BROWN (1934) and AGAR (1961), and aged before use.

As the reference electrode for the earlier experiments a 0.1 M calomel electrode (DE WIT 1975) was used, later a saturated calomel electrode (Electrofact R111). The latter is more stable at constant temperature. In order to avoid contamination of the measuring solution with KCl the reference electrode is linked to the measuring solution through a salt-bridge filled with 1.75 M KNO_3 + 0.25 M $NaNO_3$, which is known to suppress liquid junction potentials (VAN

LAAR 1952). The two liquid junctions are realized in so-called VAN LAAR (1955)-capillaries through which the liquid is dispensed at an overpressure (0.5–0.8 atm) to ensure that the junction between PVA containing liquid remains outside the capillary. Because of the high electrical resistance of this bridge, good insulation of the cell is necessary. The absence of blocking impurities in the liquid junctions was frequently checked by measuring the electrical resistance over them which should not exceed 0.8 MΩ.

The cell potential is measured with an Electrofact mV/pH-meter, type 36,200/N or with a Knick mV/pH-meter, type 34. Both instruments have an imput impedance $> 10^{12}\ \Omega$.

To prevent evaporation the titration vessel, the electrodes, capillaries, etc. are placed in a gas-tight perspex cover: the stirrer being sealed with a water-lock. Because of the long duration of each titration and to obtain more stable readings, purified nitrogen, saturated with water at 20°C, is led over the solution under some overpressure. The nitrogen is purified to remove trace amounts of O_2, CO_2 and organic gases by bubbling it successively through a 10% aqueous KOH, 96% H_2SO_4 and water, followed by passage over a molecular sieve (MS, type 4A, 1/16) and a reductor (BTS, BASF 1969). The gas stream is finally dried over silica gel and led over a further molecular sieve. The complete cell is placed in a perspex box and thermostatted at 20.0 ± 0.2°C by pumping water from a Colora Ultrathermostat through the box. The cell is placed in a Faraday cage.

Standardization

Silver or iodide ion concentrations are determined after each addition of p.d. ions from the cell-EMF using the relations

$$E_{cell} = E_0'\,(\mathrm{Ag}) - 58.16\,pAg \tag{6.3a}$$

in the presence of excess Ag^+, or

$$E_{cell} = E_0'\,(\mathrm{I}) + 58.16\,pI \tag{6.3b}$$

in the presence of excess I^- (BIJSTERBOSCH and LYKLEMA 1977). E_0'(Ag) and E_0'(I) are standard potentials at given temperature depending on the ionic strength, solution composition and liquid junctions. Before and after each titration the E_0''s are determined by measuring the cell-EMF of a solution of known *pAg* or *pI* (generally 10^{-4} or 10^{-5} M) in the presence of 10^{-1} M KNO_3, so that the ionic strength can be considered to be constant. Adding PVA to the calibration solution at concentrations up to 50 mg dm^{-3} did not significantly affect the E_0' values. During the titrations the PVA concentration was always lower than 50 mg dm^{-3}, so further calibrations were carried out without PVA.

From (6.3) it is obvious that at a given temperature, ionic strength and solution composition the solubility product of AgI, *L*, can be calculated:

$$pL \equiv -\log L = pAg + pI = [E_0'\,(\mathrm{Ag}) - E_0'\,(\mathrm{I})]/58.16 \tag{6.4}$$

Once the pL is established, (6.4) offers a means to check the standard potentials. Generally the E_0' values, measured over a period of several weeks, are constant within 1 to 1.5 mV. Sometimes, however, they differed by 3 or 4 mV when measured before and after a titration. Such values were only accepted if the pL remained constant. If not, the titration results were discarded, the Van Laar-capillaries were cleaned and/or the AgI electrodes renewed. The reference value of the pL in 10^{-1} M KNO_3 was 16.15 $\pm$ 0.02. This is close to the value given by DE WIT (1975).

Titration procedure

The actual experiments are usually done with about 10 g of AgI precipitate and started at $pAg \approx 7$. After addition of a known volume of 10^{-2} M KI with a calibrated micropipette or -syringe and equilibration, the cell-EMF is measured. The criterium for equilibrium is that the average potential of the five electrodes changed less than 0.1 mV per 15 min. The procedure is repeated ca. 15 times untill a pAg of about 11 is reached, after which successive additions of 10^{-2} M $AgNO_3$ bring the pAg up to 4. From here again 10^{-2} M KI is added and so on.

PVA was added at around $pAg = 11$ for PVA 16–98 and around $pAg = 8$ for PVA's 13–98, 13–88, 48–98 and 40–88. The polymer is then allowed at least 18 hours adsorb before the titration is continued. Each full titration in the presence of PVA was preceded by a titration of the bare silver iodide. All curves are taken both with increasing and decreasing pAg.

The equilibration period after each addition of p.d. ions is 15 min. to 1.5 h in the case of bare silver iodide. However, in the presence of PVA this period sometimes increased to more than 12 h. These long times may have to do with the irreversible character of polymer adsorption, since in the presence of low molecular weight substances the equilibration period is of the same order as that for bare silver iodide. In order to reduce the time required for a complete titration, the equilibration period was cut off after 5 h, if slow equilibration occurred. The changes in potential become small after such a time and any errors incurred in neglecting them are comparable with the errors introduced by an extremely long duration of a titration.

Reproducibility and accuracy

In order to obtain a good reproducibility experimental factors such as: discrepances between the five electrodes, electrical cell resistance, temperature, addition of standard solution, evaporation and attainment of equilibrium were carefully controlled. When the average of the standard potentials, measured at the beginning and the end of the titration, differed by 3 mV or more, the E_0' values were adjusted within the experimentally observed range to avoid 'swinging' of the ends of the curves. Yet, in the presence of polymer it was difficult to obtain readings reproducible within 0.1 $\mu C\ cm^{-2}$ over the whole pAg range. Fig. 6–3a gives a good impression of the overall reproducibility. The experimental errors accumulate at the ends of the curves. The isotherms in the presence

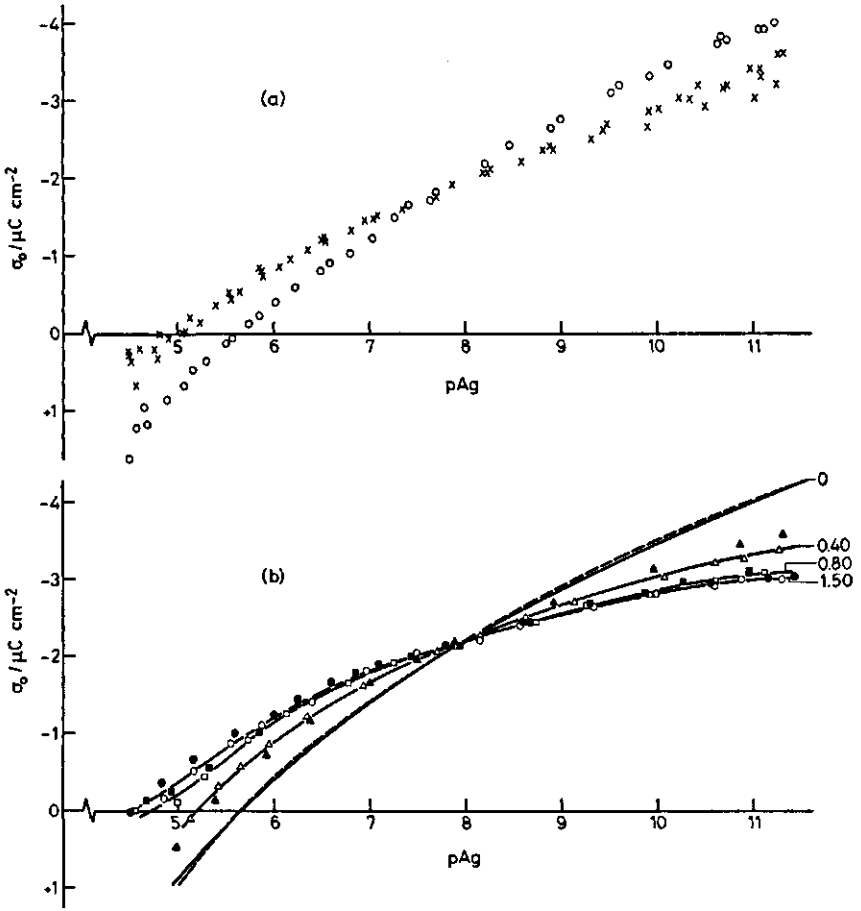

FIG. 6–3. Reproducibility of the $\sigma_0(pAg)$ curves.
(a) Reproducibility of successive titrations in 10^{-1} M KNO_3, all measured at increasing *pAg*. ○, bare AgI precipitate I; x, AgI precipitate I covered with 1 mg m^{-2} PVA 16–98.
(b) Relative accuracy of independent titrations in 10^{-1} M KNO_3, measured at decreasing *pAg* with various amounts of PVA 40–88 adsorbed. The figures indicate the adsorption in mg m^{-2}. Open symbols: AgI precipitate II, cell 1; closed symbols: precipitate III, duplicate cell (2).

of PVA's 13–98 and 13–88 have a slightly better reproducibility due to a better control of the cell and the use of a microsyringe instead of a -pipette.

To obtain the relative accuracy and the reproducibility, two complete sets of titration curves have been measured in the presence of PVA 40–88 on different silver iodide precipitates and in different cells. The capacitance areas of these precipitates were chosen such that the two curves, measured in the absence of polymer were largely coincident. The results for three PVA additions, obtained at decreasing *pAg*, are shown in fig. 6–3b. The discrepency between two

equivalent curves amounts to about the maximum experimental error as shown in fig. 6–3a. It may be concluded that the relative accuracy is satisfactory. The absolute accuracy is mainly determined by the experimental error in the specific surface area and to a lesser extent by the error in the position of the p.z.c. and will be in the order of 10 to 20%.

So far the discussion has not included the effect of the direction of the titration, viz. measuring at in- or decreasing the *pAg*. We return to this point in sect. 6.4.1.

6.3.2. *Electrophoretic mobilities*

Measurements of electrophoretic mobilities were carried out at 20.0 ± 0.2°C in a Rank Bros MK II microelectrophoresis apparatus, equipped with a thin-walled closed cilindrical cell, platinum black electrodes and a constant current source. Particle velocities were measured at the two depths in the cell at which the solvent is calculated to be at rest (VAN GILS and KRUYT 1936, SHAW 1969). The direction of the field was reversed after each measurement and in total 40 readings were taken at a preset *pAg* value and PVA adsorption. The 20 measurements at each depth were averaged and from the thus obtained values one final velocity, U, is calculated. If the first two velocities of any set measured differed substantially the readings were repeated with a freshly cleaned cell. Except for the usual cleaning (sect. 2.1.) the cell was rinsed daily with a 2% HF solution. This improved the reproducibility and stability of the readings. Silver iodide sticking to the glass wall was removed by rinsing with acetone saturated with KI.

The field strength, X, is calculated from the cell dimension, the current flowing through the cell and the specific onductance of the sample. The electrophoretic mobility is expressed as UX^{-1}.

The reproducibility of UX^{-1} depends on the extent of coagulation of the sol and the particle velocity and is within 5 to 10%.

The measurements are done with sol A diluted to 5×10^{-5} mole dm^{-3} AgI. As carrier electrolyte a 10^{-3} M HNO_3 solution is prefered to a KNO_3 solution. This is done to keep the solubility of silicates down and to attain a *pH* close to the p.z.c. of glass (TADROS and LYKLEMA 1968, 1969), thus minimizing any interference of adsorbing silicates (DOUGLAS and BURDEN 1959).

The use of 10^{-3} M HNO_3 and the cleaning with a HF solution enabled us to find the isoelectric point of uncovered AgI sol at $pAg = 5.6$, a value very close to the p.z.c. (sect. 6.3.1). This is in agreement with the fact that in 10^{-3} M HNO_3 specific adsorption is very low (LIJKLEMA 1957).

PVA was adsorbed onto the sol at a sol concentration of 0.5% and a mixing time of 48 h. These conditions are equivalent to those at which the isotherms (sect. 5.4, fig. 5–1) are recorded. From this stock sample dilutions were made at several *pAg* values. As the PVA adsorption is irreversible (sect. 5.4.) this does not affect the adsorbed amount. Due to the dilution the solution viscosity becomes virtually identical to that of water. After dilution the *pAg* was adjusted

in a titration cell (see sect. 6.3.1.). To prevent strong coagulation at *pAg* values <8, the *pAg* was given only one hour to establish. In samples of $pAg > 8$ the *pAg* was equilibrated over night. Due to the stabilizing effect of the adsorbed polymer, coagulation is less and a better reproducibility is reached when PVA is present.

The specific conductance of each sample was measured separately with a Philips 9501/01 conductance meter at 20.0°C making use of a Philips PW 9510 cell.

6.4. Results and discussion

6.4.1. *Surface charge versus pAg curves*

The obtained $\sigma_0(pAg)$ curves for AgI precipitates in the presence of PVA's 13–98, 13–88, 48–98, 40–88 and 16–98 are shown in figs. 6–5 to 6–9. For sake of clarity, measuring points are shown only in fig. 6–5. For most PVA's two sets of curves are given, one set measured at decreasing *pAg*, the other at increasing *pAg*.

Before discussing the general features, it is mandatory to compare the curves obtained at in- and decreasing *pAg*. Fig. 6–4 shows some typical results. Especially at *pAg* values smaller than 6 or 7 there is a small but measurable

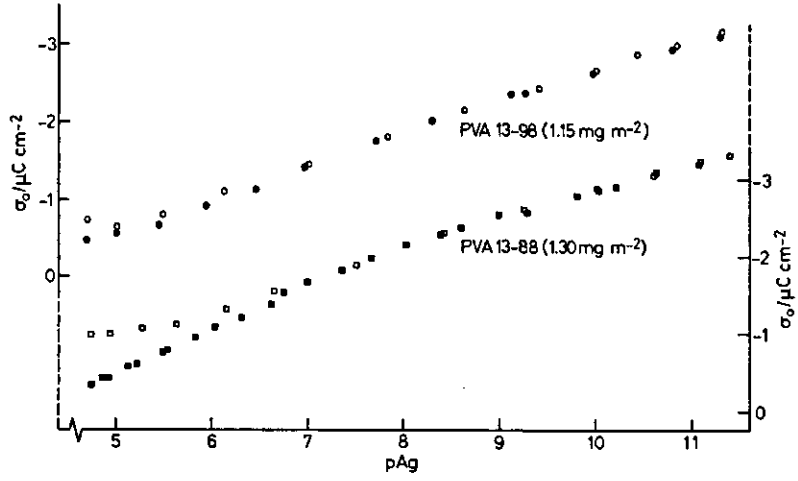

Fig. 6–4. Influence of the direction of the titration. Open symbols: measurements at increasing *pAg*: closed symbols: measurements at decreasing *pAg*.

irreversibility, which increases with increasing acetate content. For bare silver iodide a small irreversibility is (sometimes) found, but only for pAg's < 5. The large deviations in the presence of PVA indicate that the effect is dependent on the adsorbate. According to table 4–1 all PVA samples contain minor amounts of impurities, which may react with Ag^+ or release I^- ions. However, in general PVA 88 is more pure than PVA 98, making it improbable that the effect is caused by contaminants. Moreover, repeated titrations of the same AgI + PVA sample still show the effect (i.e. irreversible Ag^+ consumption occurred in each cycle), though it decreases somewhat. At present we cannot offer a satisfactory explanation for this irreversibility.

Besides this effect, there is a small 'hysteresis', occurring especially when relatively much polymer is adsorbed. It is usually less than 0.1 $\mu C\ cm^{-2}$. This 'hysteresis' probably reflects the long adaption times of the polymer conformation, in particular that of the trains, to alterations in the pAg, so that, strictly speaking, it is not hysteresis but a very slow relaxation.

Hysteresis or phenomena involving long relaxation times have also been reported for polymers adsorbed on mercury (MILLER and GRAHAME 1956, FLEMMING 1973).

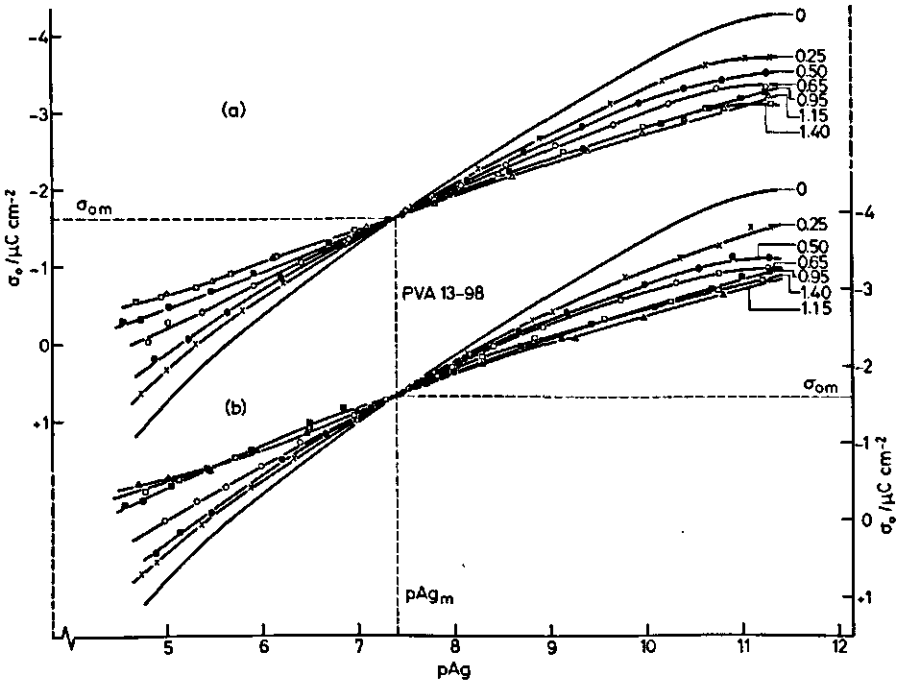

FIG. 6–5. Surface charge as function of pAg for AgI precipitates in the presence of adsorbed PVA 13–98. The adsorbed amounts in mg m^{-2} are indicated.
$\sigma_{0m} = -1.6\ \mu C\ cm^{-2}$; $c(KNO_3) = 10^{-1}$ M; $T = 20.0°C$: AgI precipitate VI. (a) Measured at increasing pAg, (b) at decreasing pAg.

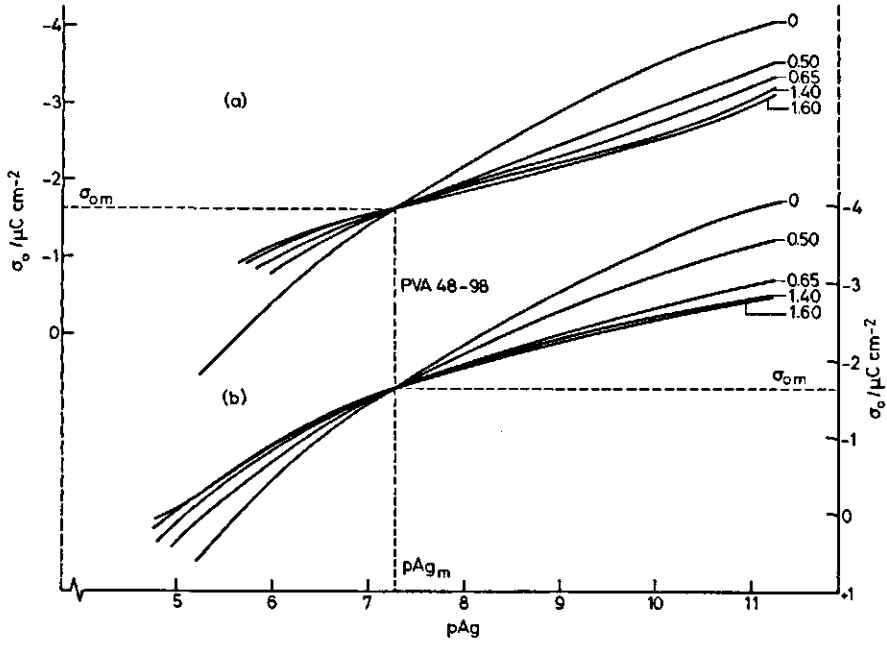

FIG. 6–6. Surface charge as function of pAg for AgI precipitates in the presence of adsorbed PVA 48–98. The adsorbed amounts in mg m^{-2} are indicated.
$\sigma_{0m} = -1.6$ μC cm^{-2}; $c(KNO_3) = 10^{-1}$ M; $T = 20.0$°C; AgI precipitate III. (a) Measured at increasing pAg, (b) at decreasing pAg.

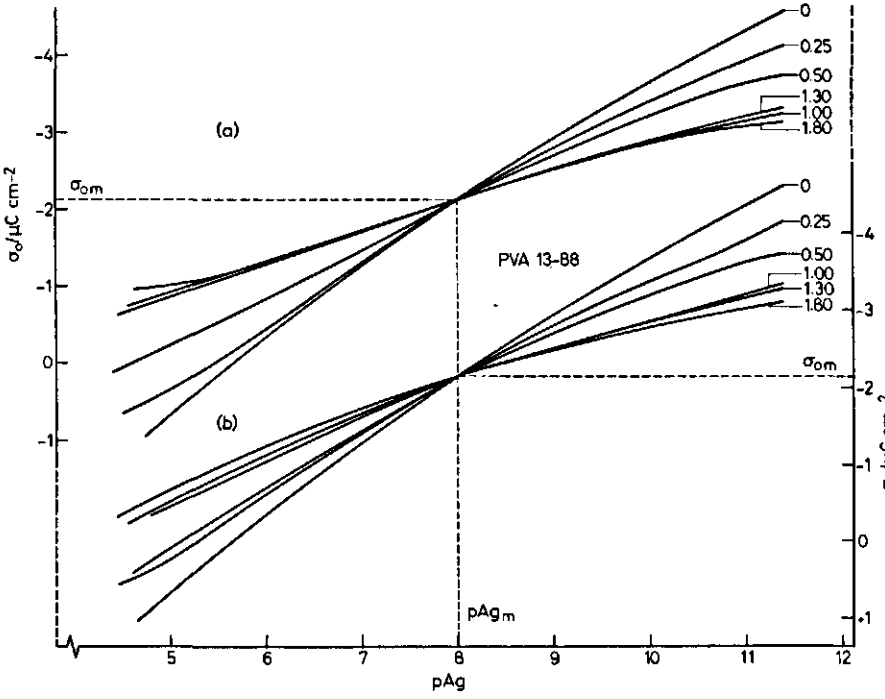

FIG. 6–7. Surface charge as function of pAg for AgI precipitates in the presence of adsorbed PVA 13–88. The adsorbed amounts in mg m^{-2} are indicated.
$\sigma_{0m} = -2.1$ μC cm^{-2}; $c(KNO_3) = 10^{-1}$ M; $T = 20.0$°C; AgI precipitate VI. (a) Measured at increasing pAg, (b) at decreasing pAg.

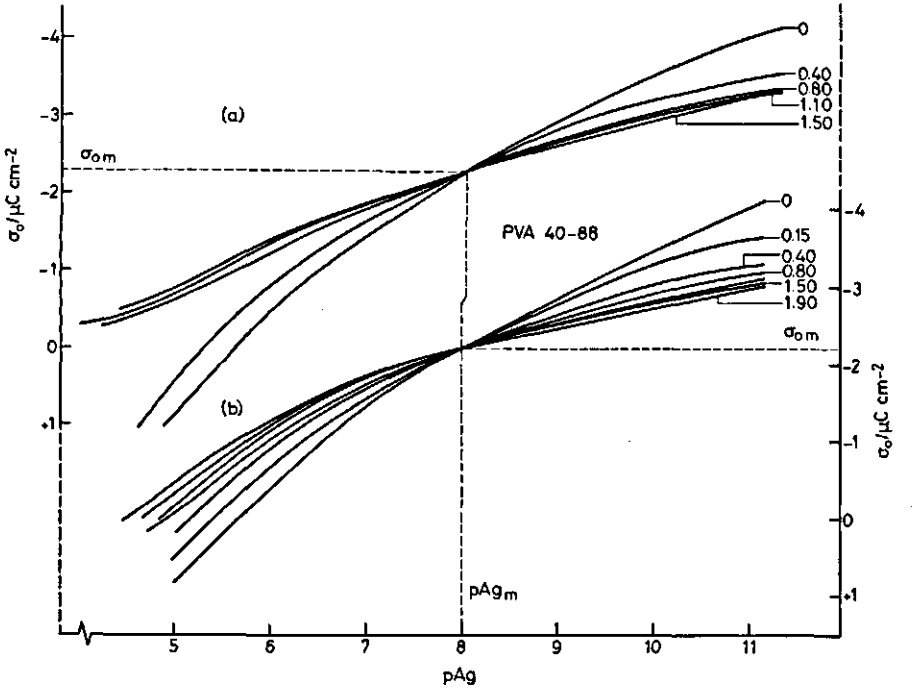

FIG. 6–8. Surface charge as function of pAg for AgI precipitates in the presence of adsorbed PVA 40–88. The adsorbed amounts in mg m^{-2} are indicated.
$\sigma_{0m} = -2.2\ \mu C\ cm^{-2}$; $c(KNO_3) = 10^{-1}$ M; $T = 20.0°C$; AgI precipitate II, III. (a) Measured at increasing pAg, (b) at decreasing pAg.

6.4.2. *General features*

Irrespective of the direction of the titration, the following qualitative features are always observed.

1. Adsorption of PVA reduces the slopes of the curves,
2. it moves the point of zero charge to more positive values.
3. All curves pass through a common intersection point at $\sigma_0 = \sigma_{0m}$.

Quantitatively, the extents of these shifts depend on the nature of the PVA, 88 being more effective than 98. The effect of molecular weight is small.

Lowering the slope is virtually equivalent to decreasing the differential capacitance, C, of the Stern-layer. This can be attributed to either or both of two causes, the displacement by polymer segments of originally specifically adsorbed counterions and the lowering of ε_s/d upon the replacement of water by polymer segments. Here ε_s is the average relative static permittivity of the Stern-layer, and d the average thickness of this layer. In the case of low molecular weight alcohols (BIJSTERBOSCH 1965, DE WIT and LYKLEMA 1973) the same trend is observed. Moreover, the lowering of the differential capacitance is also observed with PVA on mercury (WOJCIAK and DUTKIEWICZ 1964).

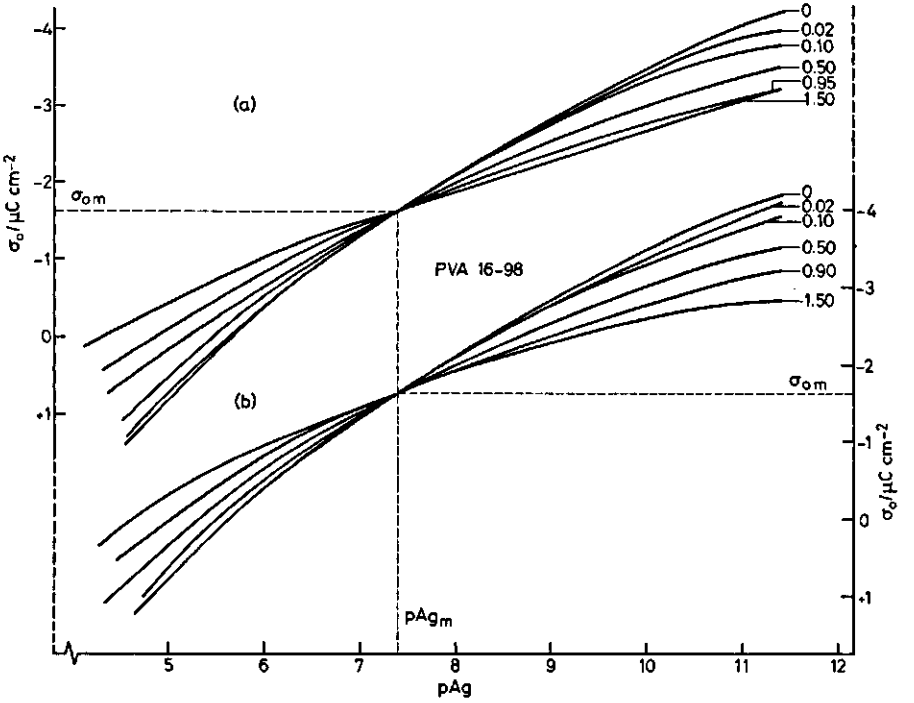

FIG. 6–9. Surface charge as function of *pAg* for AgI precipitates in the presence of adsorbed PVA 16–98. The adsorbed amounts in mg m^{-2} are indicated.
$\sigma_{om} = -1.6\ \mu C\ cm^{-2}$: $c(KNO_3) = 10^{-1}$ M: $T = 20.0°C$: AgI precipitate IV. (a) Measured at increasing *pAg*, (b) at decreasing *pAg*.

The shift of the p.z.c. can be due to either or all of three causes: (*i*) change in specific ion adsorption, (*ii*) change in activity coefficient of p.d. ions and (*iii*) change in the χ-potential upon the replacement of water dipoles by polymer segments. The last-mentioned effect is the dominant factor, because standard potential measurements in the presence of PVA indicated only negligible activity coefficient shifts (sect. 6.3.1.), whereas specific adsorption of NO_3^- ions at the p.z.c. is small, though not entirely absent: upon increasing the KNO_3 concentration from 10^{-3} to 10^{-1} M the p.z.c. on bare silver iodide shifts only a few mV (BIJSTERBOSCH and LYKLEMA 1977).

In previous papers (BIJSTERBOSCH and LYKLEMA 1965, 1968, DE WIT and LYKLEMA 1973) for low molecular weight adsorbates these positive shift of the p.z.c. has been interpreted in the following way. In the absence of adsorbate the water dipoles are oriented with their negative end towards the surface (BIJSTERBOSCH and LYKLEMA 1977). In the case of butanol (BuOH), which adsorbs with its hydrocarbon moiety towards the surface, water dipoles are replaced by a virtually apolar layer. This causes of a large positive shift (maximum +190 mV). A very similar shift is to be expected for apolar adsorbates. On mercury a similar trend is observed (though the shift is larger) and the same model has

been proposed (BLOMGREN et al. 1961, BOCKRIS et al. 1963). In ethylene glycol (EG) upon complete occupancy Δp.z.c. = +89 mV of which +64.5 mV has been attributed to $\Delta\chi$, the remainder being due to changes in the activities of the p.d. ions (DE WIT and LYKLEMA 1973). It was concluded that EG adsorbs on AgI with a net normal dipole moment component, the negative side pointing to the surface. On mercurry, EG adsorbs in a different way (TRASATTI 1970). It would be logical to approximate the effect of PVA (repeating unit $-CH_2-CHOH-$) on the p.z.c. as if the segments of PVA behaved for 50% like BuOH (or like all other substances, adsorbing with their hydrocarbon moiety towards the surface) and for 50% like EG. Upon maximum coverage with no voids, Δp.z.c. would then be $^1/_2(190 + 64) = +128$ mV. Such a maximum shift can be expected for PVA 98, having only a few acetate groups distributed randomly along the main chain (sect. 4.2.). However, in the case of PVA 88 with 12 mole % acetate groups in a blocky distribution, a larger shift is to be expected, especially if the segments containing an acetate group adsorb preferentially. In that case, water dipoles are replaced by almost apolar segments, resulting in a large value of $\Delta\chi$. Assuming that the normal component of the dipole moment of the acetate group is negligible, a shift comparable to $\Delta\chi_{max}$ (BuOH) is to be expected. Even in the case the carbonyl group is oriented with its positive side toward the surface, as is the case with acetone ($\Delta\chi_{max} = +225$ mV: OVERBEEK et al. 1957, DE WIT and LYKLEMA 1973), only a slightly greater shift can be expected. Thus it seems reasonable to expect for PVA 88, with preferentially adsorbed segments containing the acetate group, and no voids on the surface, $\Delta\chi_{max} < +205$ mV. Random adsorption of acetate and hydroxyl group containing segments would give the much smaller shift of about +135 mV.

Quantitative comparison of these calculated shifts with Δp.z.c. from titrations is not feasible because of the uncertainty in the $\sigma_0(pAg)$ curves at low pAg values. However, the effect of PVA 88 is substantially greater than that of PVA 98 indicating a preferential adsorption of the segments with the acetate group. A more quantitative comparison is possible with Δi.e.p. from electrophoresis which we shall discuss in sect. 6.4.4.

It is characteristic that Δp.z.c. as a function of the adsorbed amount is concave. At low Γ_p, the molecules adsorb in a relatively flat conformation, but loops are formed at greater values of Γ_p and these loops do not contribute to Δp.z.c.

The common intersection point at $\sigma_0 = \sigma_{0m}$ is also observed with low molecular weight adsorbates, both on AgI and on mercury. For these substances this point has a very definite physical meaning, viz. it is the surface charge where the surface excess, Γ_A^w of the organic substance A with respect to water is a maximum as a function of σ_0 (BIJSTERBOSCH and LYKLEMA 1965, DE WIT and LYKLEMA 1973, BLOMGREN et al. 1961, TRASATTI 1970, 1974). For AgI the following relation holds (BIJSTERBOSCH and LYKLEMA 1977)

$$\Gamma_A^w(pAg) - \Gamma_A^w(pAg_m) = -\frac{RT}{F}\int_{pAg_m}^{pAg}\left[\frac{\partial\sigma_0}{\partial\mu_A}\right]_T \mathrm{d}pAg \qquad (6.5)$$

where pAg_m is the pAg of the common intersection point. The RHS of (6.5) is < 0 for $pAg \neq pAg_m$. Eq. (6.5) follows from the Gibbs equation, i.e. from reversible thermodynamics. The very occurrence of the intersection point with polymers therefore leads to two conclusions: 1. Train segment adsorption is also reversible as a-function of pAg. In sect. 5.4.1. time effects were described supporting this conclusion. 2. This sorption is a maximum at $\sigma_0 = \sigma_{0m}$ (or $pAg = pAg_m$). The occurrence of a dependence of θ on σ_0 or ψ_0 has also been found with macromulecues on mercury, e.g. for polymethacrylic acid (MILLER and GRAHAME 1956), PVA (WOJCIAK and DUTKIEWICZ 1964), polyvinyl pyrrolidone (YOSHIDA et al. 1972a) and polyethylene glycol (YOSHIDA et al. 1972c).

Table 6–1 shows the positions of the common intersection points for several low and high molecular weight alcohols adsorbed on AgI in 10^{-1} M KNO_3.

The molecular interpretation of the occurrence and the position of σ_{0m} has been a matter of discussion, but this discussion did not include the AgI system (BOCKRIS et al. 1963, 1967, DAMASKIN et al. 1970, DAMASKIN and FRUMKIN 1972, TRASATTI 1974, COOPER and HARRISON 1977). An important aspect in the discussion is the structure of water at interfaces, a topic on which critical reviews have recently been given by PARSONS (1976) and CONWAY (1977). Certainly σ_{0m} depends on the nature of the adsorbate and also on the nature of the adsorbent and on the counterion (TRASATTI 1974, DE WIT and LYKLEMA 1973). For the AgI-KNO_3 system we may conclude that the various values of σ_{0m} are due to the properties of the adsorbing molecules or segments in the Stern-layer.

Returning to table 6–1, it should be noted that σ_{0m} is independent of M, but strongly connected with the acetate content of PVA. The sharpness of the intersection point indicates that σ_{0m} is also independent of θ. This means that the segment adsorption maximum as a function of σ_0 is independent of M and θ. Moreover, it suggests some kind of ideality. For instance, the PVA segments and the water molecules in the Stern-layer behave as a simple dielectric, lateral interactions are absent or fairly constant and reorientations do not clearly

TABLE 6–1. σ_0 and pAg corresponding to the common intersection point of the titration curves of a number of alcohols $cKNO_3 = 10^{-1}$mol dm^{-3}.

	σ_{0m} μC cm^{-2}	pAg_m
n-BuOH	-1.0	6.7
EG	-3.2	9.3
PVA 13–98	-1.6	7.4
PVA 48–98	-1.6	7.4
PVA 16–98	-1.6	7.4
PVA 13–88	-2.1	8.0
PVA 40–88	-2.2	8.0

occur. The large difference between σ_{0m} (PVA 98) and σ_{0m} (PVA 88) shows that quite different segments are adsorbed in the Stern-layer in both cases. To gather more insight on this point, the location of σ_{0m} is further analyzed.

Based upon the already noted similarity with low molecular weight adsorbates it is possible to construct a 'PVA equivalent' (50% BuOH + 50% EG) isotherm for p.d. ions by taking algebraic means of the experimental points of the saturated BuOH and saturated EG isotherms. The averaging can be done either at constant potential (pAg) or at constant charge. Although the difference is small, the procedure at constant charge gives the best results. In fig. 6–10 the PVA equivalent isotherm, obtained in this way, is shown together with the isotherm for PVA 13–98 at highest coverage and the curve for bare AgI.

The similarity between the hypothetical and measured curve is good. For the constructed isotherm σ_{0m} is close to -1.6 μC cm^{-2}, agreeing very well with σ_{0m} for PVA 98 and suggesting that electrochemically speaking PVA 98 can be considered as an equimolar mixture of BuOH + EG, as far as its effect on the Stern-layer is involved. From the great similarity it can be concluded that the acetate containing segments in PVA 98 play only a minor role. This is in agreement with the random distribution of these groups along the chain (sect. 4.2.).

The fact that to the left of σ_{0m} the experimental isotherm runs under the hypothetical and to the right above it, may have two explanations. Firstly, because the activity of the p.d. ions is influenced by the presence of EG (De Wit and Lyklema 1973) the titration curve of EG is not solely representative of interfacial effects, but contains also bulk contributions. For PVA bulk effects are negligible. Secondly, it might suggest that PVA is not capable of fully covering the surface.

For PVA 88 we have no means to construct an 'equivalent' isotherm for p.d. ions. However, from the comparison of σ_{0m} (PVA 88) with σ_{0m} (PVA 98), it

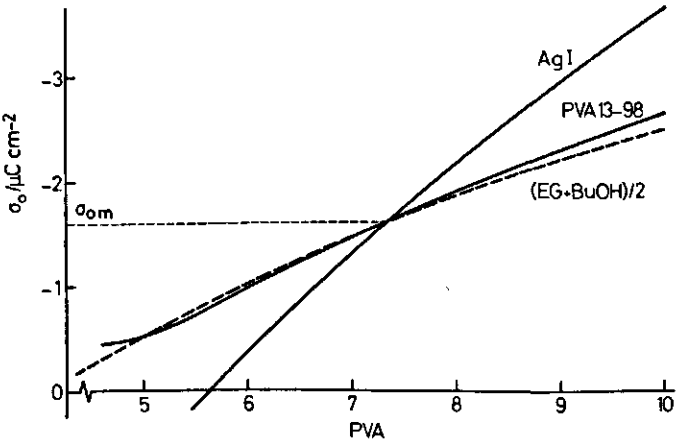

Fig. 6–10. Comparison of the PVA equivalent [(BuOH + EG)/2] titration curve with a measured (PVA 13–98) curve at highest coverage.

may be concluded that in the case of PVA 88 the Stern-layer is occupied with acetate containing segments, at least in part. This preference for acetate groups was also indicated by the difference in Δp.z.c. for both PVA's and would result from the blocky distribution of acetate groups in PVA 88. This conclusion is supported by results of SCHOLTENS (1977) and STEGERHOEK (1977) who found at the oil/water interface a much higher interfacial activity for blocky PVA 88 than for random PVA 83.

Finally, it is instructive to formulate the relation between the position of σ_{0m} and the change in p.z.c. ($\Delta\chi$) upon adsorption. To this end the integral capacitance of the double layer, K, is often introduced (FRUMKIN 1926, PARSONS 1964, FRUMKIN and DAMASKIN 1972). In doing so one may write

$$\sigma_{0m} = K_m(\theta = 0)\,\psi_{0m}\,(\theta = 0) = K_m\,(\theta = 1)\,\psi_{0m}\,(\theta = 1)$$

taking into account that

$$\psi_0(\theta = 1) = \psi_0\,(\theta = 0) - \Delta\chi_{max}$$

it follows

$$\sigma_{0m} = \frac{K_m(\theta = 0) \times K_m(\theta = 1)}{K_m(\theta = 1) - K_m(\theta = 0)}\,\Delta\chi_{max} \tag{6.6}$$

In this equation the $\Delta\chi_{max}$ term accounts for the change in polarity of the Stern-layer, whereas the capacitance factor is governed by the polarizabilities and the thicknesses of the double layer under the various conditions. Eq. (6.6) shows that a larger shift in $\Delta\chi_{max}$ results in a more negative value of σ_{0m}, provided the differential capacitance would be similar. In the case of PVA 98 and PVA 88 the capacitance factor is roughly the same and the more negative value of σ_{0m} of PVA 88 is mainly due to the larger shift of $\Delta\chi_{max}$ and hence to the lower polarity of the acetate group than the hydroxyl group.

6.4.3. *The degree of occupancy of the first layer*

Various methods of interfacial thermodynamics used to analyse double layer data in the presence of organic adsorbates (e.g. GRAHAME 1947, PARSONS 1964, CONWAY 1965, GILEADI 1967, SPARNAAY 1972, PAYNE 1973) apply only if the adsorption is a reversible process. In connection with polymer adsorption this statement requires further amplification. In many cases, including the PVA-AgI system, the adsorption as a function of the concentration is an irreversible process. However, from the great similarity with low molecular weight adsorbates and the near-reversibility of the titrations as a function of pAg, it is apparent that the adsorption is reversible with respect to 'small' changes in the pAg. Furthermore, in 10^{-1} M KNO_3 solutions only the train segments are actually 'noticed' and the issue of reversibility only applies to that part of the adsorbed layer. In conclusion, it is possible to treat the Stern-layer as being in quasi-equilibrium with the polymer outside this region and to subject $d\theta/dpAg$ to a thermodynamic analysis.

This allows us to evaluate $\theta(c_p)$ or $\theta(\Gamma_p)$ by thermodynamic means. For mercury such methods are familiar (FRUMKIN 1925, 1926, PARSONS 1959, 1964, TRASATTI 1974) but they are not directly applicable to the reversible AgI/solution interface. In our case the analysis is as follows. The Gibbs equation for the AgI/solution interface can be written as (BIJSTERBOSCH and LYKLEMA 1968, 1977)

$$d\gamma = \sigma_0 d\mu_{KI}/F + \sigma_- d\mu_s/F - \Gamma_A^w \, d\mu_A \tag{6.7}$$

where γ is the interfacial tension, F the Faraday, μ the chemical potential and Γ_A^w the surface excess relative to water of the substance A. The subscript s refers to salt (KNO_3) and A to an organic adsorbate, which is in equilibrium with the bulk. Generally Γ_A^w depends on the activity of A (this relation being the adsorption isotherm) and on the electric field at the interface, more conveniently on σ_0 or pAg.

A formal equation of the adsorption isotherm can be found relatively easy when the solvent is considered as a continuum which need not to be indicated explicitly. For the chemical potential of the adsorbate, μ_A^s, we may write

$$\mu_A^s = \mu_A^{s,0} + RT \ln f(\theta_A) \tag{6.8}$$

where $f(\theta_A)$ is some function of the coverage θ_A ($= \Gamma_A^w/\Gamma_{A,\,max}^w$) and the corresponding equation in solution reads

$$\mu_A = \mu_A^0 + RT \ln a_A \tag{6.9}$$

with a_A the activity of A in solution. The resulting isotherm equation is

$$f(\theta_A) = \beta_A a_A \tag{6.10}$$

where

$$\beta_A \equiv \exp[(\mu_A^{s,0} - \mu_A^0)/RT] = \exp(-\Delta_{ads} G_A^0/RT) \tag{6.11}$$

$\Delta_{ads} G_A^0$ being the standard Gibbs energy of adsorption of A. It includes implicitly the contribution due to the desorption of water molecules upon adsorption of A.

Eq. (6.10) is also used in mercury interfacial chemistry (see e.g. PAYNE 1973a, b, DAMASKIN et al. 1971). It is based on the rather general equation (6.8). The form of $f(\theta_A)$ is arrived at from molecular thermodynamics or from other considerations and it can cover ideal behaviour, but also corrections for intermolecular interactions and molecular size (see e.g. PARSONS 1959, DHAR et al. 1973). However, when lateral interactions occur, $RT \ln f(\theta_A)$ is not solely an entropic (configurational) term. For the system under study, $\mu_A^{s,0}$ is a characteristic, but field dependent quantity. It is to a first approximation a constant at constant charge or potential. Though it is somewhat arbitrarily, the field dependence of $\mu_A^{s,0}$ is often expressed by splitting up β_A into a 'chemical' and an 'electrical' term

$$\beta_A = \beta_{A,\mathrm{ch}}\,\beta_{A,\mathrm{el}} \tag{6.12}$$

$\beta_{A,\mathrm{el}}$ usually contains the obvious electrostatic contributions, for instance, the energies of a permanent dipole and/or an induced dipole in an electric field. It is clear that an adsorption isotherm can only be defined at a constant value of $\beta_{A,\mathrm{el}}$. A complication is that the electric field across the molecular condensor can be expressed either in terms of charge (σ_0), or in terms of potential difference across the Stern-layer. There has been much discussion on the correct choice of the electrical variable (DAMASKIN et al. 1970, PARSONS 1968, BARRADAS and SEDLAK 1972, TRASATTI 1974) but this choice does not affect the physical description of the adsorption phenomenon and is primarily a matter of best experimental fit.

The form of eq. (6.7) is suitable for constant μ_{KI} or pI analysis. If a constant charge analysis is to be carried out, we have to change variables introducing PARSONS' (1955) function

$$\xi = \gamma + \sigma_0\mu_{\mathrm{KI}}/F \tag{6.13}$$

leading to

$$\mathrm{d}\xi = -\mu_{\mathrm{KI}}\mathrm{d}\sigma_0/F + \sigma_-\mathrm{d}\mu_s/F - \Gamma^{\mathrm{w}}_A\mathrm{d}\mu_A \tag{6.14}$$

In his silver iodide work, BIJSTERBOSCH (1965) implicitly used both the constant potential and constant charge model to analyse the adsorption of BuOH. Though he erroneously used a constant surface potential instead of a constant potential (or pI), it can be concluded that for BuOH adsorption on silver iodide both treatments give similar results. In the present study the constant charge concept is preferred, because σ_{0m} (PVA) calculated on the basis of the similarity with BuOH and EG (50% BuOH + 50% EG) at constant charge agreed better with the experimental value than σ_{0m}(PVA) calculated at constant pAg. Moreover, the relation between the field strength, X, and σ_0 is somewhat less complicated than that between X and the potential decay at constant potential.

By cross differentiation of (6.14) at constant chemical potential of the salt we find

$$(\partial\mu_{\mathrm{KI}}/\partial\mu_A)_{\mu_s,\sigma_0} = F(\partial\Gamma^{\mathrm{w}}_A/\partial\sigma_0)_{\mu_s,\mu_A} \tag{6.15}$$

or when $\ln\beta_A$ is introduced as a variable and $\Gamma^{A}_{\mathrm{w}} = \theta_A\Gamma^{\mathrm{w}}_{A,\max}$

$$\left[\frac{\partial\mu_{\mathrm{KI}}}{\partial\mu_A}\right]_{\mu_s,\sigma_0} = F\Gamma^{\mathrm{w}}_{A,\max}\left[\frac{\partial\theta_A}{\partial\ln\beta_A}\right]_{\mu_s,\mu_A}\left[\frac{\partial\ln\beta_A}{\partial\sigma_0}\right]_{\mu_A,\mu_s} \tag{6.16}$$

From (6.10) it can be derived that

$$\left[\frac{\partial\theta_A}{\partial\ln\beta_A}\right]_{\mu_A} = \left[\frac{\partial\theta_A}{\partial\ln a_A}\right]\beta_A \tag{6.17}$$

furthermore

$$(\mathrm{d}\mu_{KI})_{\mu_s} = (\mathrm{d}\mu_{1^-})_{\mu_s} = -RT(\mathrm{d}pI)_{\mu_s}$$

Recalling that β_A is a function of σ_0 only, we may write

$$-(\mathrm{d}pI)_{\mu_s,\sigma_0} = F\Gamma^{w}_{A,\max}\left[\frac{\mathrm{d}\ln\beta_A}{\mathrm{d}\sigma_0}\right]_{\mu_s,\sigma_0}(\mathrm{d}\theta_A)_{\mu_s,\sigma_0} \tag{6.18}$$

This equation is easily integrated at constant σ_0 and μ_s, for under these conditions ($\mathrm{d}\ln\beta_A/\mathrm{d}\sigma_0$) is a constant

$$pI(\theta_A) - pI(\theta_A = 0) = -F\Gamma^{w}_{A,\max}\left[\frac{\mathrm{d}\ln\beta_A}{\mathrm{d}\sigma_0}\right]\theta_A \tag{6.19}$$

Substituting $\theta_A = \theta_{A,\max}$ in (6.19) and combining this with (6.19), one obtains at fixed σ_0 and μ_s

$$\theta_A = \frac{pI(\theta_A) - pI(\theta_A = 0)}{pI(\theta_A = \theta_{A,\max}) - pI(\theta_A = 0)}\theta_{A,\max} \tag{6.20}$$

Eq. (6.20) shows that θ_A can in principle be obtained from horizontal cross-sections through $\sigma_0(pAg)$ isotherms, provided $\theta_{A,\max}$ can be estimated. (Note that $\mathrm{d}pI = -\mathrm{d}pAg$ at fixed T, μ_s and μ_A). Putting $\theta_{A,\max} = 1$ gives the more familiar form of (6.20)

$$pI(\theta_A) = (1-\theta_A)\,pI(\theta_A = 0) + \theta_A\,pI(\theta_A = 1) \tag{6.21}$$

showing that $pI(\theta_A)$ can be considered as a linear combination of the $p\Gamma$s at the uncovered and fully covered surface.

Alternatively, if we would have taken β_A as a function of the potential, or for that matter, proportional to pI, we would have obtained at fixed μ_s and pI

$$\theta_A = \frac{\sigma_0(\theta_A) - \sigma_0(\theta_A = 0)}{\sigma_0(\theta_A = \theta_{A,\max}) - \sigma_0(\theta_A = 0)}\theta_{A,\max} \tag{6.22}$$

requiring vertical cross-sections through the isotherms.

The considerations given at the beginning of this section now lead us to the assumption that (6.20) and (6.22) may also be used for polymer segments adsorbed in trains. Then from θ_A it is possible to calculate $p = \Gamma^{w}_{A}/\Gamma_p$, the fraction of segments in actual contact with the surface. In order to calculate θ_A an estimate of $\theta_{A,\max}$ is needed for each polymer sample. This quantity is not directly experimentally accessible, because with polymers it is likely that there remain voids present in the Stern-layer. Moreover, $\theta_{A,\max}$ depends on the surface charge but this effect is probably small when the chosen charge is not too different from σ_{0m} (Bijsterbosch 1965, De Wit and Lyklema 1973). As a first approximation $\theta_{\max}$ (PVA 98) can be calculated by using the before mentioned similarity between a layer covered with 50% BuOH and with 50% EG and a layer of PVA segments. Comparing the experimentally observed shift of the isoelectric point (see below) with the thus calculated hypothetical $\Delta\chi_{\max}$ (sect.

6.4.2.), θ_{max} (PVA 98) is found to be 0.85. For PVA 88 only a very rough theoretical estimate of $\Delta\chi_{max}$ could be made (sect. 6.4.2.). Using +190 mV (thus assuming the Stern-layer completely made up of acetate containing segments, adsorbed in such a way that they do not contribute to the dipole moment component normal to the surface) the experimental shift of 150 mV would give θ_{max}(PVA 88) $\approx$ 0.8. In view of the uncertainty in the calculation, θ_{max} (PVA 98) and θ_{max}(PVA 88) are taken as roughly equal. For further calculations the value 0.85 is used. Similar figures have been reported by others (SILBERBERG 1967, JOPPIEN 1974, LIPATOV and SERGEEVA 1974) for other systems. MILLER and GRAHAME (1956), the first who used a double layer technique to obtain information on θ_A of a polymer, obtained for polymethacrylic acid on mercury a maximum coverage of the Stern-layer with train segments of 0.80.

Results of our calculations of θ(PVA) as a function of the adsorbed amount, Γ_p, are shown in fig. 6–11. The values given apply to the region around the c.i.p. ($0.5 < -\sigma_0/\mu C\ cm^{-2} < 3$). The bars denote the spread of the values calculated at different values of σ_0. The inaccuracy of θ(PVA) is considerable due to the fact that all uncertainties in σ_0 show up strongly in θ. It is seen that θ increases

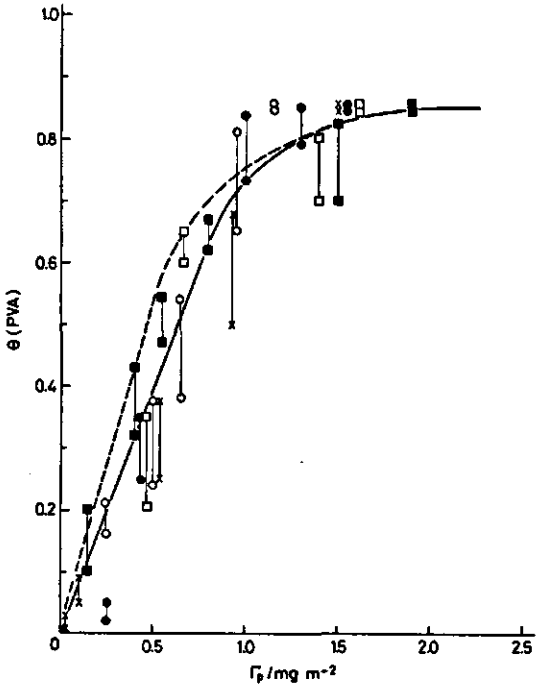

FIG. 6–11. Degree of occupancy of the first layer, θ (PVA), as a function of the adsorbed amount, Γ_p, calculated from the titration measurements. The dashed curve represents θ(PVA) as calculated from electrophoresis. ○, PVA 13–98; □, PVA 48–98; x, PVA 16–98; ●, PVA 13–88; ■, PVA 40–88.

rapidly and almost linearly up to about 0.75 mg m^{-2}, indicating that most PVA is then adsorbed in trains or flat loops. After this, θ increases more slowly and PVA adsorbed in excess of this is progressively accommodated in loops. The differences between the various PVA's are scarcely significant. Fig. 6–11 also shows θ(PVA) as obtained from Δi.e.p. measured by electrophoresis (sect. 6.4.4.). In view of the fact that two quite different double layer measurements were used, the agreement is satisfactory.

6.4.4. *Electrophoresis; degree of occupancy of the first layer and effective polymer layer thickness*

Electrophoretic mobilities in 10^{-3} M HNO_3 of silver iodide sols covered with various PVA's are shown in fig. 6–12 and fig. 6–13. The following characteristic features are observed:

1. The isoelectric point shifts to more positive values with increasing amount of adsorbed PVA, small Γ_p's being relatively more effective than larger Γ_p's.
2. The mobilities pass through a shallow maximum at the negative side: the maximum mobility is reduced upon increasing Γ_p, especially at high Γ_p.
3. The slope $d(UX^{-1})/dpAg$ at the i.e.p. decreases progressively with Γ_p.

Trends 1. and 3. are illustrated in fig. 6–14. The decrease of the maximum mobility upon increase of Γ_p was also found by SUGIURA and YABE (1970), but these authors did not study the influence of the pAg, hence their results allow no further quantitative analysis.

The shift of the i.e.p. (Δi.e.p.) may be identified with the shift of the p.z.c. measured by titration, because in 10^{-3} mol dm^{-3} HNO_3 specific adsorption is negligible, especially at the p.z.c. (LIJKLEMA 1957). The titrations and electrophoresis exhibit the same trends. The first adsorbed molecules produce a relatively large shift: at higher adsorption the i.e.p. becomes less sensitive to Γ_p and tends to a limiting value. This behaviour indicates that the first molecules adsorb to a large extent in trains, whereas at higher Γ_p the polymer accumulates predominantly in loops and tails, which do not affect the location of the i.e.p.

Quantitatively, Δi.e.p. is much better established than Δp.z.c. and it provides a more reliable tool to assess θ_A, taking

$$\theta_A = \frac{\Delta\text{i.e.p.}}{\Delta\text{i.e.p.}_{\max}}\,\theta_{A,\max} \tag{6.23}$$

which is the equivalent of (6.20). Using again $\theta_{max} = 0.85$, the occupancy was calculated. The results are shown in fig. 6–15. The agreement with θ (PVA) from the titrations is satisfactory, see fig. 6–11. For a discussion of θ we refer to sect. 6.4.3.

In sect. 6.4.2.a discussion was given on the preferential adsorption of acetate containing segments of PVA 88 in the Stern-layer. Theoretically it was found that Δp.z.c.$_{max}$(PVA 98) = +128 mV, whereas Δp.z.c.$_{max}$(PVA 88) could be

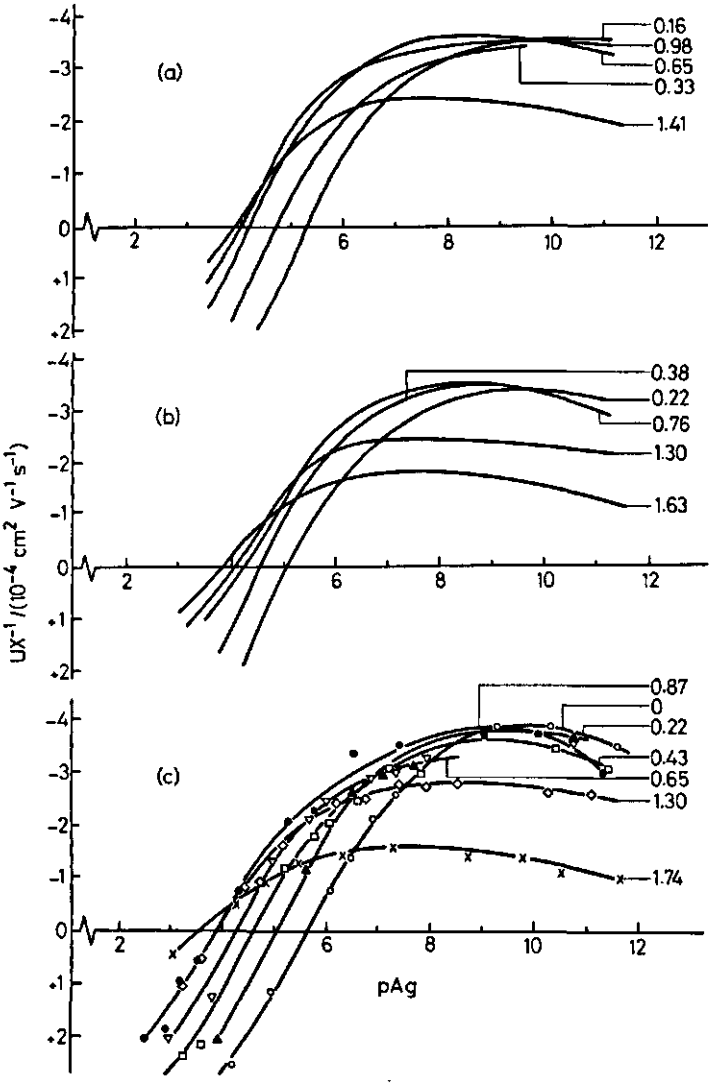

FIG. 6–12. Electrophoretic mobilities at 20.0°C of AgI sols as a function of *pAg* in the presence of adsorbed PVA of the 98-series. The absorbed amounts in mg m^{-2} are indicated. (a) PVA 3–98, (b) PVA 13–98, (c) PVA 48–98. For clarity the experimental points are shown only in the lower graph. Electrolyte: 10^{-3} M HNO_3.

+205 mV at most when preferential adsorption of the segments with an acetate group occurred, or +135 mV for random adsorption. The actual magnitude of Δi.e.p.$_{max}$(+151 mV) for PVA 88 cleary shows that acetate containing segments adsorb preferentially. As 151 mV is smaller than the theoretical shift (+190 mV) that would ensue if the acetate groups are apolar, it is not possible to

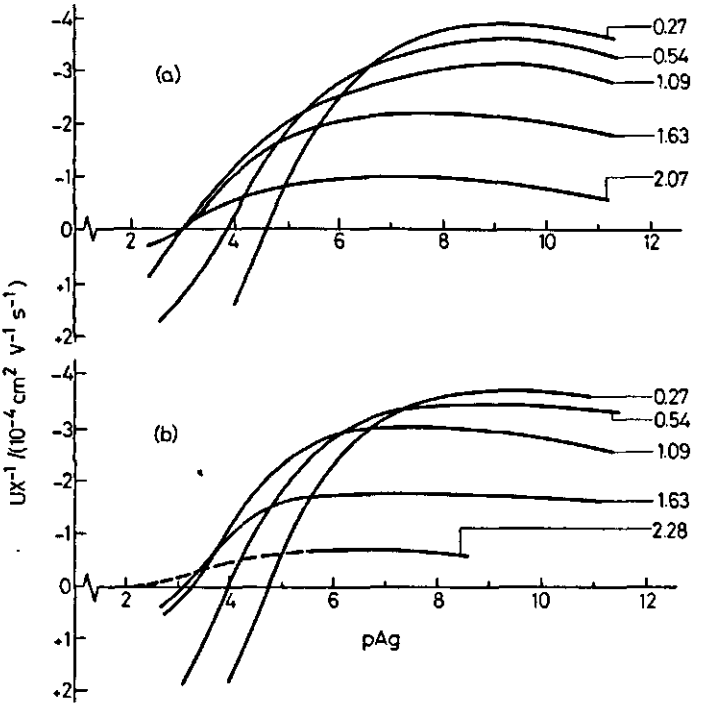

FIG. 6–13. Electrophoretic mobilities at 20.0°C of AgI sols as a function of *pAg* in the presence of adsorbed PVA of the 88-series. The adsorbed amounts in mg m^{-2} are indicated. (a) PVA 13–88; (b) PVA 40–88. Electrolyte: 10^{-3} M HNO_3.

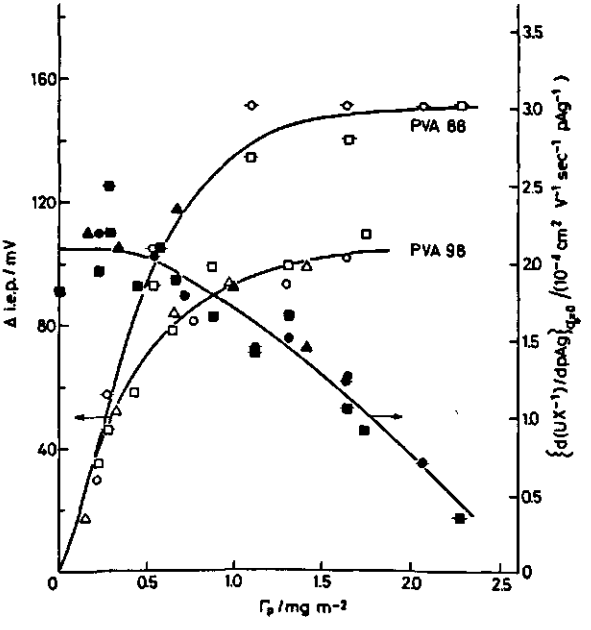

FIG. 6–14. The shift of the i.e.p., Δ i.e.p. and the slope, $d(UX^{-1})/dpAg$, in the i.e.p., for AgI sols as a function of the adsorbed amount of PVA. Electrolyte: 10^{-3} M HNO_3; $T = 20.0$°C; ▲, △, PVA 3–98; ●, ○, PVA 13–98, ■, □, PVA 48–98; ◓, ⊖, PVA 13–88; ■, ⊟, PVA 40–88.

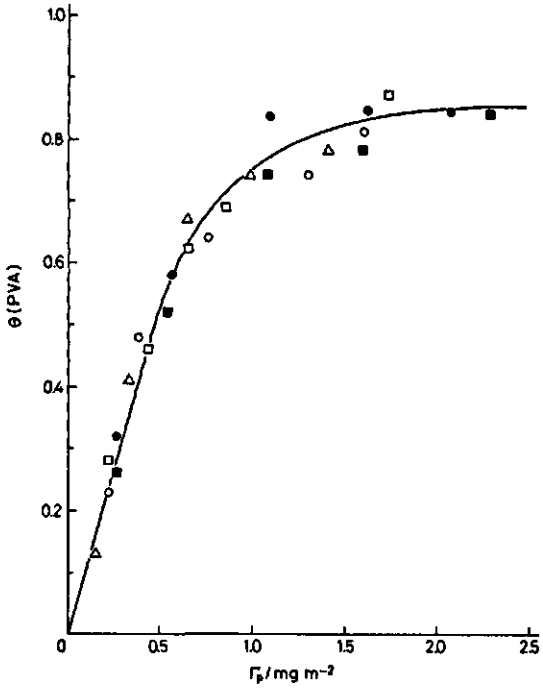

FIG. 6–15. Degree of occupancy of the first layer, θ(PVA), calculated from the shift of the i.e.p., as a function of the adsorbed amount of PVA.
△, PVA 3–98; ○, PVA 13–98; □, PVA 48–98; ●, PVA 13–88; ■, PVA 40–88.

make conclusions about the orientation of these groups on the surface. The fact that Δi.e.p.$_{max}$(PVA 88) is smaller than 190 mV can be due to either or both of two causes: (*i*) the surface is not fully covered and (*ii*) the Stern-layer also contains hydroxyl groups. In view of the general behaviour of polymers (*i*) will certainly contribute, however, its extent can only be roughly estimated. Taking θ_{max}(PVA 88) = 0.85, as is done in our calculations, would reduce the theoretical shift to +160 mV. Assuming that Δi.e.p.$_{max}$ is a linear combination of the contributions of acetate and hydroxyl containing segments, it is found that the Stern-layer is covered with about 50% of each of these segments. However, taking the lower limit θ_{max}(PVA 88) = 0.80, would yield a Stern-layer fully covered with acetate containing segments. Reality is probably between these extremes but anyway it is certain, that the Stern-layer is considerably enriched in acetate groups, as compared with the average acetate content in the chain.

The trend observable in the influence of PVA on the electrophoretic maximum at high *pAg* values is opposite to that in Δi.e.p. At low Γ_p, PVA adsorption has little effect, but at high Γ_p the electrophoretic mobility decreases progressively with Γ_p. This is obviously due to loop and tail formation and the subsequent outward displacement of the slipping zone. In this way a *qualitative* measure of the growing thickness of the adsorbed layer is obtained. However, it is not advisable to use this decrease for a *quantitative* measure of the effective

layer thickness, $\bar{\Delta}$, as was done by FLEER et al. (1972) and followed by GARVEY et al. 1976, KAVANAGH et al. (1975) and BARAN et al. (1976a, b).

The reason for caution is twofold:

(1) The conversion of mobilities into ζ-potentials is not really feasible in the plateau region because of the difficulty to account properly for the relaxation effect (WIERSMA et al. 1966). Moreover, the particles are non-spherical.

(2) In addition to ζ, the potential, ψ_d, at the boundary between the Stern-layer and the diffuse part of the double layer (and/or C_d), and the course of $\psi(x)$ in the diffuse part of the double layer has to be known to calculate $\bar{\Delta}$. Generally these items of information are not available. The potential ψ_d can be obtained from titration data only for the case that specific adsorption is zero, but under plateau conditions specific adsorption is non-zero and depends on the amount of segments adsorbed in trains.

The behaviour of $\psi(x)$ in the presence of an adsorbed polymer has been studied theoretically by BROOKS (1973) for the case of low potentials. According to BROOKS the normal Boltzmann distribution of counterions has to be corrected for two factors: (a) a purely geometrical one accounting for the volume of the adsorbed polymer and (b) a factor accounting for the interactions between ions and polymer, ions and solvent and polymer and solvent, that is: a non-ideality term. Using the FLORY (1942)-HUGGINS (1942) approximation of concentrated polymer solutions, BROOKS obtained for the distribution of counterious

$$n_i(x) = n_i(\infty) \exp\left[-\frac{z_i e\psi(x)}{kT}\right] \exp\left[-\beta(x)\right] \tag{6.24}$$

with

$$\beta(x) = \left[\phi_p(x) - \phi_p(\infty)\right]\left[1 - \chi_{sp} + \chi_{ip} - \chi_{si}\right] \tag{6.25}$$

where z_i is the valency of the ions, e is the elementary charge, ϕ_p is the volume fraction of polymer and χ a Flory-Huggins interaction parameter, the subscripts i, s, p referring to counterion, solvent and polymer respectively. The χ-term describes the interactions between the components, which ultimately result in the appearance of excluded volume effects, compare (4.26). Hence both factors in the RHS of (6.25) correspond to an excluded volume. Combining (6.24) with the Poisson equation and assuming a flat double layer with a low surface potential behaving as a simple dielectric and a step function for $\phi_p(x)$ BROOKS obtained an expression for $\psi(x)$, the potential distribution in the diffuse part of the double layer.

With respect to ζ, the potential at the plane of shear, there are two opposing trends: (a) the potential $\psi(x)$ increases for all values of x due to excluded volume effects, leading to an increase of ζ and (b) an outward displacement of the plane of shear upon polymer adsorption, resulting in a reduction of ζ. In principle it is possible to obtain an effective thickness if both trends are taken into account. However this solution, besides accurate parameter values, also

requires some insight in the segment density distribution, which is just the sought quantity. Thus, in practice, $\overline{\Delta}$ can be found only if trend (a) can be shown to be insignificant.

Comparing the theoretical computations made by BROOKS (1973, his figs. 2 and 3) with the present results, it can be concluded that (*i*) the plane of shear is shifted drastically and (*ii*) the values of $\beta(x)$ are small. The last conclusion is supported by the fact that χ_{sp} is close to 0.5 (sect. 4.4.) and that the interactions between counterions and PVA are negligible (FLEER 1971). Moreover, the polymer volume fractions in bulk ($\phi_p(\infty) \approx 10^{-4}$) and in the diffuse part of the double layer ($0.08 < \{ < \phi_p > _{\Delta} \} < 0.25$ see sect. 7.2.). are small.

The complexity of the practical situation is further illustrated by the experimental data shown in figs. 6–12 and 6–13. At a constant *pAg* close to the i.e.p. the mobility rises with increasing Γ_p, whereas at a *pAg* value in the plateau region just the opposite happens. This indicates that an in- or decrease of a ζ-potential upon adsorption should be treated with caution. The explanation of the above phenomenon is that upon adsorption the i.e.p. shifts to more positive values, making ψ_0 and ψ_d larger, so that at relatively low potentials larger values of ζ are (also) found. Moreover, it is possible, as is the case with low molecular weight adsorbates (BIJSTERBOSCH 1965, VINCENT et al. 1971), that ψ_d increases due to the displacement of counterions from the Stern-layer by adsorbing polymer trains. This feature is not covered by BROOKS' theory, at least not explicitly.

These complications lead us to the conclusion that the reduction of ζ in the plateau region is not easily related to $\overline{\Delta}$ and instead we proposed (KOOPAL and LYKLEMA 1975) to use the slope $\mathrm{d}(UX^{-1})/\mathrm{d}pAg$ in the immediate surroundings of the i.e.p. Under these conditions specific adsorption of counterions is negligible. Then ψ_d can be obtained from titration data (OVERBEEK and MACKOR 1952, LIJKLEMA 1957) and relaxation and Brooks-type corrections are absent or small. Electrophoretic mobilities, UX^{-1}, can be converted into ζ-potentials according to HENRY (1931), see WIERSMA et al. (1966). We put, at or around the i.e.p.

$$\mathrm{d}\zeta/\mathrm{d}pAg = (\mathrm{d}\zeta/\mathrm{d}\psi_d)\,(\mathrm{d}\psi_d/\mathrm{d}\sigma_d)\,(\mathrm{d}\sigma_d/\mathrm{d}\sigma_0)\,(\mathrm{d}\sigma_0/\mathrm{d}pAg) \tag{6.26}$$

where σ_d is the diffuse double layer charge, which under the preset conditions equals $-\sigma_0$. To obtain $(\mathrm{d}\zeta/\mathrm{d}\psi_d)$ we neglect Brooks-type corrections (see above) and use the Debije-Huckel approximation for spherical double layers. This is a good approximation in our case, as could be verified by comparison with the tables of LOEB et al. (1960). The following is obtained ($T = 20.0^{\circ}$C).

$$\left[\frac{\mathrm{d}\zeta}{\mathrm{d}pAg}\right]_{\sigma_0 \to 0} = 58.16 \left[\frac{a}{a + \overline{\Delta}}\right] \left[\frac{C}{C_d}\right] \exp(-\kappa\overline{\Delta}) \tag{6.27}$$

in which C_d is the diffuse double layer capacitance, a the particle radius and $\overline{\Delta}$

the distance between the Stern-plane and the effective slipping plane. We shall call $\bar{\Delta}$ the electrophoretic thickness. C is the total double layer capacitance, which can be derived from titration. For a flat double layer using the linear Poisson-Boltzmann equation (in an 1–1 electrolyte) eq. (6.27) changes to (KOOPAL and LYKLEMA 1975):

$$\left[\frac{d\zeta}{dpAg}\right]_{\sigma_0 \to 0} = 58.16 \left[\frac{\operatorname{sech}^2(e\psi_d/4kT)}{\operatorname{sech}^2(e\zeta/4kT)}\right] \left[\frac{C}{C_d}\right] \exp(-\kappa\bar{\Delta}) \tag{6.28}$$

In the Debije-Huckel approximation the factor containing ψ_d and ζ approaches unity.

Around the p.z.c. and in 10^{-3} mol dm^{-3} HNO_3 C/C_d is nearly independent of the adsorbed amount, because C is mainly determined by the diffuse part of the double layer. However, this does not mean that C/C_d is equal to unity. Around the p.z.c. we may write

$$\frac{1}{C} = \frac{1}{C_S} + \frac{1}{C_d} \tag{6.29}$$

where C_S is the capacitance of the (under the chosen conditions charge free) Stern-layer. Usually C_S is of the order of 20 μF cm^{-2}. For a flat double layer $C_d = 5.7$ μF cm^{-2}, so that C is about 4.5 μF cm^{-2} and $C/C_d \approx 0.8$. For a spherical particle with radius 42 nm $C_d = 8.8$ μF cm^{-2} and $C = 6$ μF cm^{-2}, leading to $C/C_d \approx 0.7$.

When no titration data are available, a first estimate of C/C_d can be derived from electrophoresis data, but only in the absence of polymer. From (6.27) it follows that for $\bar{\Delta} \to 0$

$$\left[\frac{d\zeta}{dpAg}\right]_{\substack{\sigma_0 \to 0 \\ \bar{\Delta} \to 0}} = 58.16 \frac{C}{C_d} \tag{6.30}$$

Using the value for C/C_d thus obtained also for the calculations in the presence of polymer, is a better approximation than equalizing this quotient to unity. Especially in 10^{-3} M salt, where C is mainly determined by the non-specific capacitance C_d, this procedure works reasonably well.

The effective thickness, $\bar{\Delta}$, was calculated using the slopes $(d\zeta/dpAg)\ \sigma_{0 \to 0}$ The increase in hydrodynamic radius of the particles, which occurs on the adsorption of the polymer, was also accounted for in the estimate of the value of $f(\kappa a)$ (HENRY 1931), to be used in the calculation of ζ-potentials from mobilities. The thus obtained $\bar{\Delta}$'s are plotted as a function of Γ_p in fig. 6–16. Within experimental error all PVA samples give the same $\bar{\Delta}$ at a given Γ_p, indicating a very similar distribution of trains, loops and tails for all samples.

The values of $\bar{\Delta}(\Gamma_p)$ found are smaller than those obtained from viscometric measurement (FLEER et al. 1972). Comparing our results with those of GARVEY

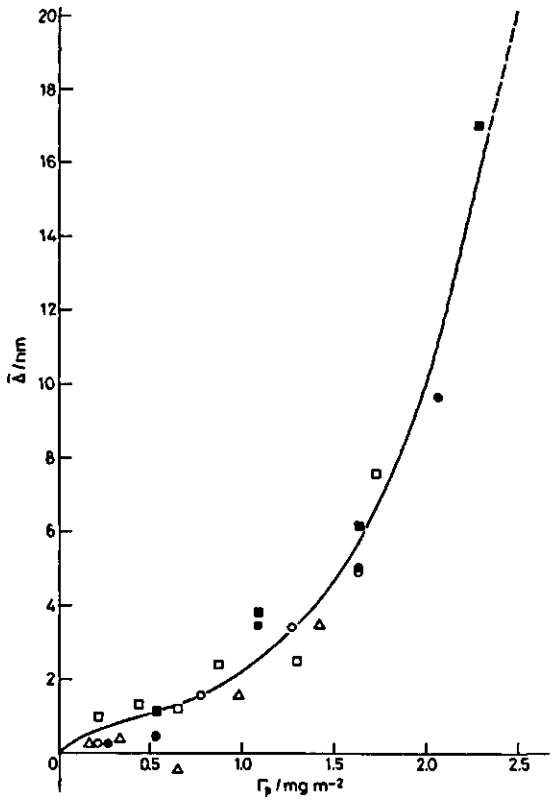

FIG. 6–16. Electrophoretic thickness, $\bar{\Delta}$, as a function of the adsorbed amount of PVA.
△, PVA 3–98; ○, PVA 13–98; □, PVA 48–98; ●, PVA 13–88; ■, PVA 40–88.

et al. (1974, 1976) who measured thicknesses of adsorbed PVA 88 layers on polystyrene latex particles with several techniques yielding hydrodynamic radii, shows also our thicknesses to be somewhat smaller, especially at low adsorption values. Though the thickness of an adsorbed layer on a large particle at fixed amount adsorbed will be somewhat greater (GARVEY et al. 1976) than that on a small particle, this difference cannot completely account for the observed discrepancy between GARVEY's results and ours.

In our calculation of $\bar{\Delta}$ it was assumed that Brooks-type corrections could be neglected. However, this may not be fully true. A first impression of the error thus introduced can be obtained by replacing $\phi_p(x)$ by a step function (SILBERBERG 1968, BROOKS 1973): $\beta(x)$ is therefore defined by

$$\phi_p(x) = <\phi_p>_\Delta, \quad \beta(x) = <\beta>, \quad \delta \leq x \leq \bar{\Delta}$$

$$\text{with} \quad <\phi_p>_\Delta = (1 - p)\Gamma_p v/\bar{\Delta} \tag{6.31}$$

$$\phi_p(x) = \phi_p(\infty), \quad \beta(x) = 0, \quad x > \bar{\Delta}$$

where δ is the first layer ($\approx$ Stern-layer) thickness. Substitution in (6.25) and (6.24) gives

$$n_i(x) = n_i(\infty) \exp(-<\beta>) \exp\left[-\frac{z_i e\psi(x)}{kT}\right] \tag{6.32}$$

The ionic space charge density is related to $\psi(x)$ by the Poisson equation. For sufficiently low potentials (the Debije-Huckel approximation) and symmetrical electrolytes it is found that

$$\nabla^2\psi = \kappa_B{}^2\psi(x), \quad \psi(x) << kT/ze \tag{6.33}$$

with

$$\kappa_B{}^2 = \kappa^2 \exp(-<\beta>) \tag{6.34}$$

and

$$\kappa^2 = 2e^2z^2n_i(\infty)/\varepsilon kT \tag{6.35}$$

where ε is the static permittivity. For a spherical colloid particle when r is the distance from the centre of the sphere eq. (6.33) can be rewritten as

$$\frac{1}{r^2}\frac{d}{dr}\left[\frac{r^2 d\psi(r)}{dr}\right] = \frac{1}{r}\frac{d^2\{r\psi(r)\}}{dr^2} = \kappa_B{}^2\psi(r) \tag{6.36}$$

The function $r\psi(r)$ is obtained by double integration, assuming a similar thickness for the diffuse layer and the polymer layer. When ψ_d is the Stern-layer potential at $r = a$ we find

$$\psi(r) = \psi_d\left[\frac{a}{r}\right] \exp\{-\kappa_B(r-a)\} \tag{6.37}$$

Substitution of $\psi(a + \bar{\Delta}) = \zeta$ gives

$$\zeta = \psi_d\left[\frac{a}{a+\bar{\Delta}}\right] \exp(-\kappa_B\bar{\Delta}) \tag{6.38}$$

and

$$\frac{d\zeta}{d\psi_d} = \left[\frac{a}{a+\bar{\Delta}}\right] \exp(-\kappa_B\bar{\Delta}) \tag{6.39}$$

Comparison with (6.26) and (6.27) shows that in this approximation, in (6.27) κ_B should be used instead of κ. Eq. (6.27) then can be written also as

$$\left[\frac{d\zeta}{dpAg}\right]_{\sigma_0\to 0} = 58.16\left[\frac{a}{a+\bar{\Delta}}\right]\left[\frac{C}{C_d}\right] \exp(-\kappa\bar{\Delta}^*) \tag{6.40}$$

where $\bar{\Delta}^*$ is the uncorrected thickness:

$$\bar{\Delta}^* = \bar{\Delta} \exp(-0.5 < \beta >) \tag{6.41}$$

As we did not apply Brooks-type corrections, fig. 6–16 in fact shows $\bar{\Delta}^*$ as a function of Γ_p instead of $\bar{\Delta}(\Gamma_p)$.

When the χ-terms in (6.25) mutually compensate and $\phi_p(\infty) \to 0$, as is possibly the case in the present study, $\bar{\Delta}$ reads

$$\bar{\Delta} = \bar{\Delta}^* \{\exp(-0.5 < \phi_p >_A)\}^{-1}$$

For low $< \phi_p >_A$

$$\bar{\Delta} = \bar{\Delta}^* (1 - 0.5 < \phi_p >_A)^{-1}$$

In the present study, $0.08 < \{< \phi_p >_A\} < 0.25$, this would result in an upward correction of 4 to 14%. The larger corrections are to be applied around $\Gamma_p = 10\ \mathrm{mg\ m^{-2}}$ (see sect. 7.2.).

The question remains, what kind of thickness is $\bar{\Delta}$? This problem is not yet solved. Its solution would require a detailed knowledge of the drainage pattern through the adsorbed polymer layer. As $\bar{\Delta}$ is a hydrodynamic thickness, presumably it is related to the root mean square distance of segments from the interface, $< d^2 >^{0.5}$, in a similar way as the hydrodynamic radius of a polymer coil is related to the radius of gyration (see TANFORD and sect. 7.1.). In eq. (6.27) or (6.39) $\bar{\Delta}$ should then be replaced by $\xi' < d^2 >^{0.5}$. Accepting this to be true and interperting ξ' as an empirical parameter, $\bar{\Delta}$ can be calculated using some theoretical segment density distribution (e.g. HOEVE 1965, ROE 1965, 1966, RUBIN 1965, HOFFMAN and FORSMAN, 1970 HESSELINK 1972, 1975) in the same way as has been done by MCCRACKIN and COLSON (1964) for the ellipsometric thickness.

6.4.5. *Influences of molecular weight, acetate content and surface charge on θ and $\bar{\Delta}$*

In chapter 5., it was found that at a given concentration, the adsorbed amount Γ_p, depends on the molecular weight and acetate content. However, the molecular weight dependence of Γ_p is small, so that for θ and $\bar{\Delta}$ an even lesser dependence on M must be expected. Figs. 6–11, 6–15 and 6–16 show that is true. As a first approximation θ and also $\bar{\Delta}$ depend solely on Γ_p. There is no influence of the molecular weight nor of the acetate content on the shape of the $\theta(\Gamma_p)$ and $\bar{\Delta}(\Gamma_p)$ curves. The only difference is that in figs. 6–15 and 6–16 higher abscissa axis values (and hence higher ordinate values) are obtainable with samples of higher M and/or greater acetate content. This unique dependence of θ and $\bar{\Delta}$ on Γ_p is the case despite the observation that with respect to σ_{0m} and Δp.z.c. (Δi.e.p.) the two polymer types differ considerably, a fact explained by the preferential adsorption of the acetate-containing segments in PVA 88. The independence of $\theta(\Gamma_p)$ of the acetate content is partly due to our choice to equalize θ_{max} for both polymer types. This may not be entirely correct, but the *shape* of the $\theta(\Gamma_p)$ curve is not affected by this choice.

If our conclusion that, as a first approximation, the distribution over trains and loops or tails is a function of the adsorbed amount *only* could be generalized, it would considerably simplify the treatment of colloidal phenomena involving particles with an adsorbed polymer layer.

Theoretically it is to be expected (SILBERBERG 1968, HOEVE 1971) that in a Θ-solvent the layer thickness increases with the square root of the number of segments per molecule, provided this number is not too large. To verify this for the present results, $\bar{\Delta}_{max}$ was plotted as a function of the square root of the degree of polymerization, $DP^{0.5}$, in fig. 6–17. Except for PVA 3–98 the result is in reasonable agreement with the prediction. Higher molecular weight species in the PVA 3–98 sample probably adsorb strongly preferentially. The same conclusion was made considering the total adsorption (see sect. 5.4.3.).

Finally, a short comment on the influence of the surface charge must be made. In chapter 5. it was found that variations in σ_0 from 0 to $-3\ \mu C\ cm^{-2}$ had no measurable effect on Γ_p. However, with respect to θ a dependence on σ_0 *is* found. As shown in sect. 6.4.2. the train segment adsorption is a maximum at $\sigma_0 = \sigma_{0m}$. Although the extent of desorption of train segments with respect to σ_{0m} is not experimentally accessible because μ_{PVA} is unknown, comparison with low molecular weight adsorbates (BIJSTERBOSCH 1965, DE WIT 1975) suggests that it is small.

Another possible way of obtaining information on the effect of σ_0 upon θ is the application (6.20) at several values for σ_0. Results of such calculations are shown in fig. 6–11. The bars denote the spread of values found at different values of σ_0 ($0.5 < -\sigma_0/\mu C\ cm^{-2} < 3$). In this case the experimental inaccuracy is such that no further conclusions can be drawn.

The thickness of the adsorbed layer can be calculated at the p.z.c. only. At other surface charges relaxation and possibly Brooks-type corrections become important, virtually preventing calculation of $\bar{\Delta}$. However, $\bar{\Delta}$ is probably independent of σ_0. Interactions between polymer segments and ions are absent

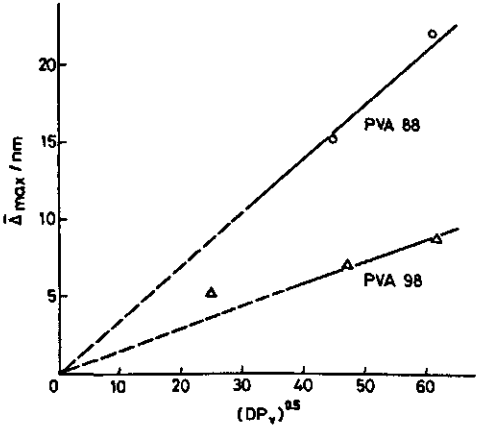

FIG. 6–17. The effective layer thickness at saturation adsorption, $\bar{\Delta}_{max}$, for the various PVA's as a function of the square root of the degree of polymerization of the samples.

or small and the total amount adsorbed is not influenced by σ_0. Hence, there are no reasons to expect a dependence of $\bar{\Delta}$ on σ_0.

6.5. Summary

Double layer and electrophoresis studies of PVA-covered AgI particles are described and interpreted to determine the effect of an adsorbing neutral polymer on the double layer properties and to investigate the mode of adsorption of PVA on AgI.

The potentiometric titrations reveal three important features upon PVA adsorption:

- the double layer capacitance decreases,
- the p.z.c. shifts to more positive values,
- the titration curves pass through a common intersection point, characteristic for the type of PVA.

These features are related to modifications in Stern-layer properties caused by adsorbing polymer segments in trains. Adsorbed polymer trains and low molecular weight organic adsorbates, having a composition comparable with that of the polymer segments, behave very similarly in this layer. From this resemblance it could be concluded that in PVA 88 the segments containing an acetate group adsorb preferentially in the Stern-layer. This is promoted by the blocky distribution of the acetate groups in PVA 88. The similarity has further been used to develop a theorem to obtain the degree of occupancy of train segments in the Stern-layer. The result obtained with the titration technique is confirmed by electrophoresis studies.

A measure for the effective layer thickness can be obtained from the slope of the electrophoretic mobility against *pAg* curve around the isoelectric point.

The main conclusion is that the fraction adsorbed in trains and the effective layer thickness are, to a first approximation, a function of the adsorbed amount *only*. The molecular weight and acetate content influence θ and $\bar{\Delta}$ only indirectly, due to the fact that higher M and greater acetate content increase the adsorption. The theoretically expected dependence of the layer thickness on the degree of polymerization is experimentally confirmed, except for PVA 3–98.

The dependence of the train segment adsorption on the surface charge is so small, that for most practical purposes it can be neglected. The same applies to the effect of σ_0 upon the layer thickness.

7. GENERAL DISCUSSION

In this last chapter the information obtained in the preceding chapters will be used to calculate some additional parameters characterizing the adsorption. A comparison will be made with theoretical predictions and where possible with similar characteristics of the PVA molecules in solution.

The combined information will be used to analyse the adsorption theory of HOEVE (1965, 1966, 1970, 1971, 1976).

7.1. FRACTION OF SEGMENTS ADSORBED IN THE FIRST LAYER AND THE AMOUNT ADSORBED IN LOOPS AND TAILS

Fig. 7–1 summarizes the main information obtained. Shown are the degree of occupancy, θ, the effective layer thickness, $\bar{\Delta}$, and the plateau adsorption values of the various PVA's. As both θ and $\bar{\Delta}$ depend solely on the amount adsorbed, other parameters derived from them need to be calculated as a function of Γ_p only.

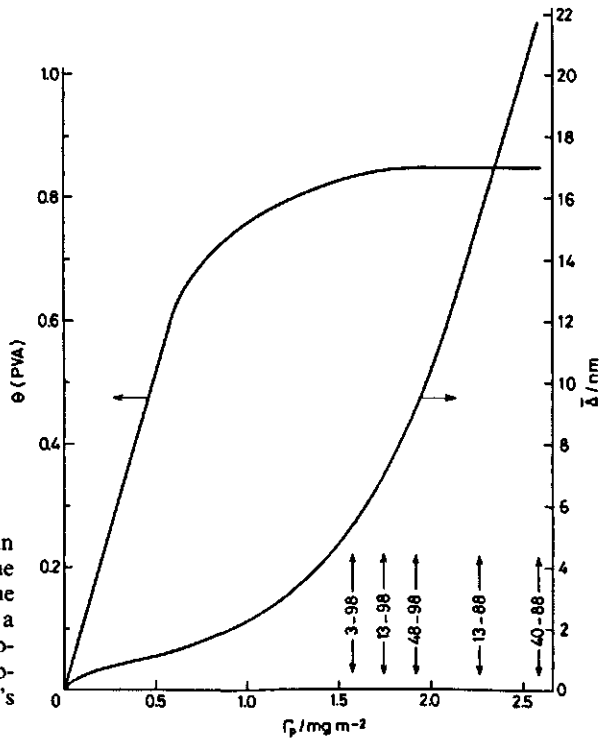

FIG. 7–1. Summary of the main adsorption data. Given are the degree occupancy, θ, and the effective layer thickness, $\bar{\Delta}$, as a function of the amount adsorbed, Γ_p. The saturation adsorption values of the various PVA's are also indicated.

A frequently used parameter is the fraction, p, of adsorbed segments in direct contact with the surface. Assuming a molecular cross section, $a_{0,s}$ per segment, θ can be transformed into p as follows

$$p = \left[\frac{10^3 M_s}{N_A a_{0,s}}\right] \frac{\theta}{\Gamma_p} \tag{7.1}$$

with Γ_p in mg m^{-2} and $a_{0,s}$ in nm. Estimates of $a_{0,s}$ can be obtained from spread monolayers (LANKVELD 1970, BARAN et al. 1976b), model calculations and comparison with other adsorbates (SMITH 1972, MCCLELLAN and HARNSBERGER 1967) or from the specific volume of PVA. Such estimates vary from 0.30 to 0.15 nm^2. The largest values are obtained from monolayer experiments and probably account for a PVA segment with two adhering water molecules (BARAN et al. 1976b). Model calculations give about 0.20 $\pm$ 0.05 nm^2. In theoretical studies the number of segments is often defined as the ratio of the specific volumes of the polymer and the solvent, in that case a cross sectional area of about 0.15 nm^2 should be used. This choice has the advantage that the volume of a train segment is equal to that of a loop or tail segment. For PVA 98 we used 0.20 and 0.15 nm^2, for PVA 88 0.22 and 0.16 nm^2. Fig. 7–2a shows p as function of Γ_p. Some p values are also tabulated in table 7–1. From p and Γ_p one easily calculates Γ_l, the amount adsorbed in loops and tails. The result is shown in fig. 7–2b.

The obtained values of p, including the reduction of p upon an increase of Γ_p, are in general agreement with other experimental findings (LIPATOV and SERGEEVA 1974, ROBB and SMITH 1974, JOPPIEN 1974, 1975).

Theoretically, it is predicted that in the case of an adsorbed *isolated* molecule ($\Gamma_p \to 0$) p would approach values of about 0.80 to 0.95 for $\chi_s^* \geq 1$ (RUBIN 1965

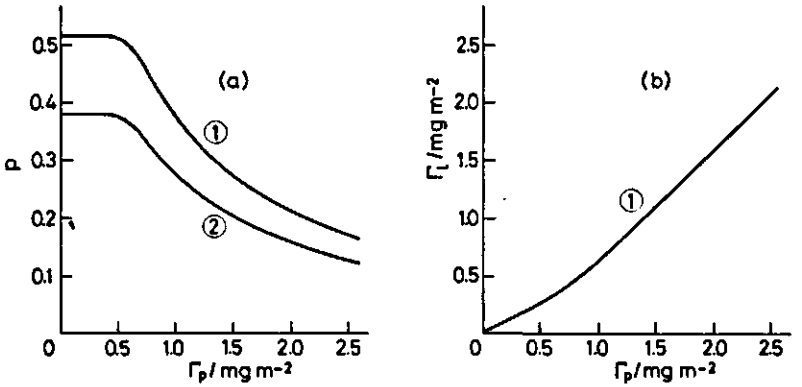

FIG. 7–2. The fraction of segments, p, adsorbed in trains (a) and the amount, Γ_l, adsorbed in loops and tails (b) as a function of the total amount adsorbed, Γ_p.
1, $M_s/a_{0,s} = 300$ mol^{-1} nm^{-2}; 2, $M_s/a_{0,s} = 225$ mol^{-1}nm^{-2}.

*χ_s = minus the free energy change, involved in the replacement of a solvent molecule by a polymer segment on the surface, in units of kT.

a, b, SILBERBERG 1967, 1968, MOTOMURA and MATUURA 1968, 1969, MOTOMURA et al. 1971), implying and effective flattening of the adsorbed molecule. For non-isolated (*interacting*) macromolecules and $\chi_s > 2$, p would be roughly 0.2 in Θ- and 0.5 in athermal solvents. Lower adsorption energies result in smaller values of p, for instance for $\chi_s \approx 1$, p equals about half the just mentioned values.

Theory also predicts p to be dependent on the polymer volume fraction in solution, ϕ_{pb}, but only for small values of ϕ_{pb}. In the range $0 < \phi_{pb} < 10^{-4}$, p would decrease from 0.9 ($\Gamma_p \rightarrow 0$) to 0.5 or 0.1, depending on the solvent quality and χ_s. Above $\phi_{pb} \approx 10^{-4}$ (or $c_p > 100$ mg dm^{-3} in case of PVA) only a slight further reduction is to be expected upon increasing ϕ_{pb}.

The cited values also depend on the flexibility of the polymer chain. The more flexible the molecules, the smaller the values of p.

At large Γ_p the agreement of our p values with these predictions is good. The actual magnitudes of p suggest that χ_s is about 2 (water being nearly a Θ-solvent for PVA). For $\Gamma_p \rightarrow 0$, p is considerably smaller than theoretically predicted. It is striking that between $\Gamma_p = 0$ and $\Gamma_p = 0.6$ mg m^{-2} p remains constant. This is equivalent to the fact that in this Γ_p range θ depends linearly on Γ_p, see fig. 6–15. (Using the data of fig. 6–11, p ($\Gamma_p \rightarrow 0$) would be even about 20% lower and stay constant up to $\Gamma_p \approx 0.8$ mg m^{-2}).

The constant value of p shows that in this part of the isotherm the conformation of the adsorbed molecules is independent of the adsorption. It can be concluded that the PVA molecules, adsorbed in an isolated position, do not completely unfold at the surface. They still have an average thickness normal to the surface of about 1.3 nm (see table 7–1), instead of the theoretically expected (RUBIN 1965b, 1966) thickness of a flat monolayer. In principle there may be two reasons for this behaviour: (a) the χ_s parameter is relatively mall (b) intramolecular interactions in the PVA chain prevent unfolding. Above we

TABLE 7–1. Some characteristics of the adsorbed PVA layer compared with those of the same molecules in solution.

adsorbed layer						solution			
Γ_p[1]) mg m^{-2}	θ	p[2])	$\bar{d}$ nm	$\langle \rho_l \rangle$ nm^{-3}	$\langle i \rangle$	PVA	$\langle r_h \rangle$[3]) nm	m_v	$\langle \rho_h \rangle$[3]) nm^{-3}
0.6	0.62	0.52	1.3	2.86	90	–	–	–	–
1.0	0.76	0.38	2.2	3.57	60	–	–	–	–
1.57	0.83	0.27	5.2	2.86	90	3–98	5.45	600	0.89
1.74	0.84	0.24	6.8	2.44	125	13–98	11.20	2180	0.37
1.92	0.85	0.22	8.8	2.13	170	48–98	16.01	3790	0.22
2.26	0.85	0.19	15.2	1.52	330	13–88	11.08	2000	0.35
2.58	0.85	0.16	22	1.22	500	40–88	15.69	3730	0.23

[1]) The five last values give the plateau adsorption of the PVA samples.
[2]) $M_s/a_{0.5} = 300$ mol^{-1}nm^{-2} ($v = 0.77$ cm^{3}g^{-1})
[3] $\xi_\eta = 0.875$.

estimated $\chi_s \approx 2$, so reason (a) is not likely to apply. Support for (b) is gained from the large values of K_0 and C for PVA (see sect. 4.4.3.). We return to this matter below.

At values of $\Gamma_p > 0.6$ mg m^{-2} the adsorbing molecules begin to form longer loops and tails. Above $\Gamma_p \approx 1.0$ mg m^{-2} the adsorption almost solely increases through the growing of loops and/or tails, see fig. 7–2b, and the adsorbed layer thickness increases strongly. Above Γ_p 0.6 mg m^{-2} the adsorbed layer is evenly distributed over the entire surface. To obtain an impression of the conformation in this Γ_p range, the effective thickness of the adsorbed layer will now be compared with the hydrodynamic radius of the PVA molecules. This radius is defined as (TANFORD 1961)

$$r_h = \xi <s^2>_0^{1/2} \tag{7.2}$$

Theoretical values of ξ can be obtained by comparing the behaviour of a polymer molecule in a velocity field (KIRKWOOD-RISEMAN 1948) with that of a rigid sphere in the same field.

In the non-free-draining* case, the *translational* friction coefficient, f_0, of a polymer molecule, moving in the direction of the applied force is given by (YAMAKAWA 1971, sec. 31.)

$$f_0 = 3.99\, \pi\, \eta_0 <s^2>_0^{1/2} \tag{7.3}$$

with η_0 the viscosity of the solvent. For a rigid sphere with radius r_h this coefficient is given by Stokes' law:

$$f_0 = 6\, \pi\, \eta_0\, r_h \tag{7.4}$$

Combining (7.3) and (7.4) gives a relation between r_h and $<s^2>_0^{1/2}$, showing $\xi = \xi_t = 0.665$. Under influence of the force field the real polymer molecule elongates, leading to a ξ value definitely smaller than unity. Hence, the above calculated value can be seen as the lower limit for ξ.

An upper limit for ξ is obtained by considering the *rotational* friction coefficient, f_r, for a polymer molecule having an angular velocity around its centre of mass. According to YAMAKAWA (1971) we may write

$$f_r = 4\pi^{3/2}\, \eta_0\, [XF(X)] <s^2>_0^{3/2} \tag{7.5}$$

where $XF(X)$ is the Kirkwood-Riseman function (see sect 4.4.1.). For the non-free-draining molecule $XF(X) = 1.259$ and (7.5) can be written as

$$f_r = 8.93\, \pi\, \eta_0\, <s^2>_0^{3/2} \tag{7.6}$$

* In the non-free-draining case the hydrodynamic interaction between the segments is so large that the effective volume is not decreased by the draining effect.

This is to be compared with Stokes' formula for rotational friction. For a rigid sphere with radius r_h

$$f_r = 8\pi \eta_0 r_h^3 \tag{7.7}$$

Equating (7.6) and (7.7) gives $\xi^3 = \xi_r^3 = 1.116$ or $\xi_r = 1.037$. It is seen that ξ_r is much higher than ξ_t. This is caused by the fact that an angular velocity hardly deforms the polymer molecule, resulting in an equivalent radius slightly exceeding the radius of gyration.

In general, both translational and rotational friction will occur in a non uniform velocity field, resulting in $0.665 < \xi < 1.037$. A well known example of such behaviour is found in viscometry, where ξ_η is obtained by combining the Einstein viscosity law (4.9) using $K_E = (2.5\ N_A)^{-1}$, with the Kirkwood-Riseman formulation given in eqs. (4.28) and (4.29), using $<s^2>_0$ instead of $<h^2>_0$ (see eq. (4.18b)). If for the non-free-draining case again $XF(X) = 1.259$ is substituted, the result is $\xi_\eta = 0.875$.

In our experiment, the effective adsorbed layer thickness is obtained from electrophoretic mobility measurements. The flow in the electrophoresis cell is laminar, and induces a shear force on the particles. Thus for comparison of $\bar{\Delta}$ with $<r_h>$ it seems reasonable to use $\xi_\eta = 0.875$ to calculate $<r_h>$. Values for $<r_h>$ based upon this value of ξ and the viscometric average radius of gyration (see table 4–4) are shown in table 7–1.

For low adsorptions and an evenly distributed surface layer ($0.6 < \Gamma_p/\mathrm{mg\,m^{-2}} < 1.0$), $\bar{\Delta}$ is much smaller than the hydrodynamic radius of the molecules in solution. Thus, although the molecules do not completely unfold, a considerable flattening occurs. This makes very small values of χ_s improbable.

Returning to the causes of incomplete unfolding of the molecules at very low adsorption values, it will be clear that reason (a), mentioned above, is invalid. It follows that intramolecular interactions in the polymer chain are present, also in the adsorbed state. These interactions, which are about the same for PVA 98 and PVA 88 judging from the C and K_0 values (see sect. 4.4.3.), possibly explain also the fact that at a given Γ_p the conformation in the adsorbed layer is independent of M and acetate content. Recalling that the acetate groups in PVA 88 adsorb preferentially, a further requirement for an equal distribution of PVA 98 and PVA 88 would be that the acetate blocks in PVA 88 are distributed at random along the chain.

The occurrence of corresponding intramolecular interactions in free and adsorbed polymer was also found for polymethacrylates (VAN VLIET 1977, Ch. 4).

7.2. Average volume fractions and segment densities in the adsorbed layer

From the amount adsorbed in loops and tails, Γ_t, the effective layer thickness and the specific volume of PVA ($v = 0.77$ cm^3 g^{-1}), the average volume fraction of polymer in the loop region, $<\phi_p>_\Delta$ and the average segment density, $<\rho_l>$, expressed in number of segments per unit volume, can be calculated. The results of these calculations are shown in fig. 7–3 and table 7–1 respectively. In addition to $<\phi_p>_\Delta$, the average volume fraction of polymer in the Stern-layer, $<\phi_{pl}>$, is also given. The latter quantity equals *0*.

It can be seen that up to $\Gamma_p \approx 1.0$ mg m^{-2} the average polymer density in the loop region increases, whereas the density in the Stern-layer approaches its limiting value. A notable feature is that the course of p (Γ_p) suggests that at about $\Gamma_p \approx 0.6$ mg m^{-2} the molecules start to interact, leading to smaller values of p at larger adsorptions. Each molecule will then have fewer segments in actual contact with the surface, leading to a smaller adsorption energy gain per molecule. This could be compensated for by a more than proportional increase in the layer thickness, rendering the entropy loss smaller. However, as said above, the density passes through its maximum at $\Gamma_p \approx 1.0$ mg m^{-2} instead of at $\Gamma_p \approx 0.6$ mg m^{-2}. This may be due to one or more of the three following reasons: 1. Experimental error in the thickness of the adsorbed layer over the range $0.7 < \Gamma_p/\text{mg m}^{-2} < 1.4$, it being systematically 15 to 25% too low. 2. Intermolecular interactions occurring in the adsorbed layer and 3. an increase in bulk volume fraction forcing more polymer to the surface region. The last mentioned effect contributes only to a minor extent, for at $\Gamma_p \approx 1.0$ mg m^{-2} the bulk concentration is still very low, about 1 mg dm^{-3}. The uncertainty in $\bar{\Delta}$ does not permit a firm conclusion regarding the remaining effects.

Comparsion of $<\rho_l>$ with the average segment density of a polymer molecule in solution will indicate what the state of compaction is of the adsorb-

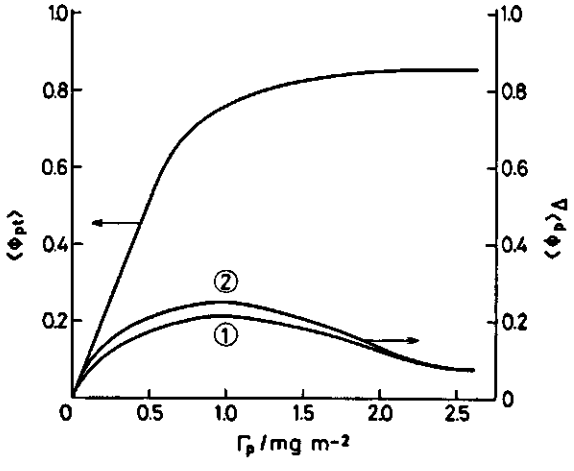

FIG. 7–3. Average volume fractions of polymer adsorbed in trains, $<\phi_{ps}>$, and in loops and tails, $<\phi_p>_\Delta$, as a function of the amount adsorbed, Γ_p.
1, $M_s/a_{0,s} = 300$ mol^{-1}nm^{-2}:
2, $M_s/a_{0,s} = 225$ mol^{-1}nm^{-2}.

ed molecules. To approximate the molecular volume in solution, the viscometric equivalent hydrodynamic sphere is again chosen. Using the viscometric average number of segments per molecule the segment density of a polymer in bulk, $<\rho_b>$, is calculated and shown in table 7–1 for various PVA's. The average segment density in the loop region is 3 to 10 times larger than $<\rho_b>$. This suggest that the average loop length is much smaller than the total chain length.

Using the effective segment length, $(2\ Cl^2)^{0.5}$, the unperturbed radius of gyration of a polymer molecule in solution can be calculated and from it the average segment density, $<\rho_b>$. Such calculations show that for chains containing 50 segments $<\rho_b> = 3.89\ \text{nm}^{-3}$ and for $m = 500$, $<\rho_b> = 1.23\ \text{nm}^{-3}$, figures comparable with the values of $<\rho_l>$. Assuming for a moment that for equal average segment densities in solution and in the adsorbed state the chain lengths are also the same, a rough approximation of the average number of segments in a loop or tail, $<i>$, can be made. The result of such calculations is shown in table 7–1. It can be seen that the average loop length in PVA 88 is two to three times as long as that in the comparable PVA 98 samples.

7.3. Comparison with a theoretical treatment

7.3.1. *Polymer adsorption models*

In the literature, a number of theories dealing with adsorption from polymer solution are reported. They can be classified into four main groups. Firstly, a group dealing with adsorption from dilute solution (e.g. Frisch-Simha-Eirich 1953a, b, Forsman and Hughes 1963a, b, c, Rubin 1965, Dimarzio and Rubin 1971, Silberberg 1962a, b, 1967, 1968, 1972, 1975, Hoeve Dimarzio and Peyser 1965, Hoeve 1965, 1966, 1970, 1971, 1976) of which the Silberberg theory is most comprehensive. These theories make detailed studies of the shapes of adsorbed polymer molecules in the isolated state or at moderate surface concentrations. They are applicable to dilute solutions from which the polymer molecules are preferentially adsorbed.

The second group of theories (e.g. Prigogine and Marechal 1952, Mackor and Van Der Waals 1952, Defay et al. 1960, Siow and Patterson 1973) confines itself to adsorbed molecules lying flat on the surface, thus largely ignoring conformational problems. They can only be applied to rodlike polymers or to flexible polymers adsorbed in the isolated state provided the adsorption energy is high.

The third group of theories is based upon the work of Everett and coworkers (Everett 1965, 1973, Ash et al. 1968, 1970) and that of Ono and Kondo (1969) and Lane (1968) concerning monomer and oligomer adsorption, and worked out explicitely for polymers by Roe (1974, 1975). Roe (1974) considers liquid mixtures consisting of monomer (solvent) and polymer molecules which are placed in a multilayer lattice, taking into account interactions with the surface and nearest neighbours. From the averaged volume fractions of poly-

mer in each lattice layer the equilibrium density distribution and the adsorption are found. The theory can be applied to the full polymer concentration range but does not discriminate between loops and tails.

The fourth group consists of the work of CHAN et al. (1975a, b), who developed a non-lattice (continuum) theory of an adsorbed polymer molecule confined in a half space by an impenetrable surface interacting with the polymer. It is applicable to adsorbed isolated molecules only.

Recently, SCHEUTJENS (1976, 1978) extended the theory of DIMARZIO and RUBIN (1971) by incorporating segment volume and segment-solvent interactions in a way which has much in common with the third group of theories. This treatment seems promising, since it is valid for large and small molecules, it covers the complete volume fraction range and takes into account both loops and tails.

The quantitative application of these theories to practical systems is thwarted by several problems, for instance:

- the identification of model parameters with experimental ones, especially the definition of a polymer segment and how its size determines the various other parameters involved,
- the experimental determination of the characteristic quantities needed,
- the fact that practical systems can be in a quasi-equilibrium state and
- the amount of computational work involved.

In this study a comparison will be made of HOEVE's model with the experimental data obtained for PVA 98 (regarded as a homopolymer). This adsorption theory is relatively attractive due to its simplicity: the equations given being soluble analytically. Moreover HOEVE considers the adsorbed layer to be built up of two regions in a way very similar to that used in this study. If the theory could explain the adsorption behaviour satisfactorily, it could be used as a basis for further work; e.g. the interpretation of polymer induced stability, see for instance FLEER (1971).

7.3.2. *The Hoeve theory*

HOEVE considers the case of polymer chains adsorbed at a homogeneous surface in equilibrium with a dilute polymer solution. The adsorbed material is distributed over loops and trains, considered as different subsystems with different partition functions. Generally the loop and train size distributions are wide. Tails are neglected. In the derivation the partition function for a single adsorbed molecule is developed first. For non interacting chains the amount adsorbed is found to be proportional to the solution concentration. When more chains are adsorbed, they start to interact both energetically and entropically and the partition function must be modified. To this end the solution phase in the vicinity of the adsorbing surface is divided in two distinct regions: a first layer with a thickness, δ, corresponding to an adsorbing segment and the region beyond that layer. In the first layer segments are attracted by the surface, leading

to a relatively high segment density, so that segment interactions in this region are manyfold. In the layers beyond the first, the attraction by the surface may be neglected and generally weaker interaction will occur. In both regions the segmental interactions are calculated on the basis of the Flory-Huggins theory.

The interactions with the surface are accounted for by a compounded parameter, σ_H, which is determined not only by the adsorption energy, but also by conformational changes occurring on adsorption. It is the ratio of the partition function of a segment adsorbed on the surface to that of a segment in solution. The free energy of adsorption per segment in contact with the surface is then $-kT \ln \sigma_H$. For non interacting chains positive values of $-\ln \sigma_H$ will result in desorption when *all* segments are adsorbed in the first layer. However, if segments are also present in loops, the overall free energy of an adsorbed molecule can still decrease due to the entropy retained in these loops, a contribution not included in $\ln \sigma_H$. Such contributions due to the presence of loops depend on the 'flexibility' of the polymer chain. In order to account for this flexibility a second parameter, c_H, is introduced, expressing the deviation from random walk statistics. It thus denotes in the case of long loops the specific character of the polymer molecule. For very stiff chains c_H equals 0, for highly flexible ones $c_H \rightarrow 1$.

Due to the various approximations made, the model can only be expected to give realistic results for large loops. A main difference with SILBERBERG's treatment is that the configuration and interaction counts are more approximate, which is ultimately compensated for in c_H and σ_H.

The final result of HOEVE's model is expressed in two basic equations governing the adsorption

$$\lambda_H + \ln \sigma_H + \ln (1+2.6c_H) + \ln (1-\theta) + 2\chi\theta = 0.5p^{-1} (0.5-\chi)K_H\theta \quad (7.8)$$

and

$$\ln \frac{N_p V}{A\delta N_s} = -m \{\lambda + 0.5 (0.5 - \chi) K_H 0\} \quad (7.9)$$

θ, χ, p and m have their usual meaning, N_p/A is the number of adsorbed molecules per unit surface, N_s/V the polymer concentration in molecules per unit volume, c_H and σ_H are the basic parameters. For a given solvent-polymer-adsorbent system at constant temperature c_H and σ_H ought to be constants. For non interacting chains ($\theta \rightarrow 0$: $\chi = 0.5$) the condition for spontaneous adsorption is $\ln \{\sigma_H(1 + 2.6\, c_H)\} > 0$. The parameter λ_H is one of the Lagrangian multipliers determined by p and c_H

$$(-\lambda_H)^{1/2} = \left[\frac{p}{1-p}\right] \left[\frac{\pi^{1/2} c_H}{1+2.6\, c_H}\right] \quad (7.10)$$

Physically, $\lambda_H kT$ may be regarded as the average adsorption free energy per

segment adsorbed. In contradistinction with ln σ_H, λ_H is a value averaged over *all* segments of the polymer chain, thus also those in loops. For adsorption to occur λ_H should always be negative. K_H is a constant. According to HOEVE (1965) the average segment density as a function of the distance normal to the surface drops discontinuously at $x = \delta$. This drop in density is given by $1-K_H$, K_H denoting the ratio between the density in the second layer and that in the first. K_H is the smaller the stiffer the chain and can be expressed as a function of c_H and the effective segment length, $(nCl^2/m)^{0.5}$ (n is the number of C-atoms in the main chain, m the number of segments):

$$K_H = \frac{(24\pi)^{1/2}\, c_H\, \delta}{(1+2.6\, c_H)\, (nCl^2/m)^{1/2}} \tag{7.11}$$

The four equations (7.8), (7.9), (7.10) and (7.11) contain four model parameters, c_H, σ_H, λ_H and K_H, thus in principle they all can be obtained, provided the parameters: m, χ, $(nCl^2/m)^{0.5}$, N_s/V, N_p/A, θ and p are known.

In his most recent article, HOEVE (1976) treats a polymer molecule using random walk statistics on a 5-choice cubic lattice, excluding immediate reversals. Incorporated are two parameters: t and w being Boltzmann factors for the first and remaining layers respectively, assigning a special weight to each step. t is related to the adsorption energy, whereas w accounts for the chain stiffness. Using the w parameter the unperturbed end-to-end distance can be expressed as

$$<h^2>_0 = (1+w/2)\, nl^2 \tag{7.12}$$

Comparison of this lattice theory with the theory discussed above enables to express c_H, K_H and σ_H into w and t:

$$c_H = 1.53\, (w^2 + 6w + 8)^{-1} \tag{7.13}$$

$$K_H = 24\, (w^2 + 6w + 12)^{-1} \tag{7.14}$$

$$\sigma_H = (w + 2)\, (w + 4)^{-1} t = (w + 2)\, (w + 4)^{-1} \exp\, (\varepsilon_a/kT) \tag{7.15}$$

ε_a is the adsorption energy per segment. For non interacting chains the critical t-value for adsorption is given by

$$t_{cr} = (w + 4)^2\, (w^2 + 6w + 12)^{-1} \tag{7.16}$$

Below this value of t no spontaneous adsorption occurs. Using $t_{cr}, \sigma_{H,cr}$ can also be found

$$\sigma_{H,cr} = (w^2 + 6w + 8)\, (w^2 + 6w + 12)^{-1} \tag{7.17}$$

For this value of σ_H the term ln $\{\sigma_H(1+2.6c_H)\}$ becomes zero. Eqs. (7.12)

to (7.17) can be used to obtain theoretical estimates for c_H, K_H, t_{cr} and ln $\sigma_{H,cr}$ when the solution properties of the polymer under study are known. For instance, comparing eq. (4.17) with (7.12) shows that

$$w = 2(C - 1) \tag{7.18}$$

In the present study m, χ and $(Cl^2)^{0.5}$ are given in chapter 4., the adsorption isotherm $\Gamma_p(c_p)$ gives N_p/A as a function of N_s/V with

$$N_p A^{-1} = 602\, \Gamma_p\, (mM_s)^{-1} \quad (\mathrm{nm}^{-2}) \tag{7.19}$$

$$N_s V^{-1} = 6.02 \times 10^{-4}\, c_p\, (mM_s)^{-1} \quad (\mathrm{nm}^{-3}) \tag{7.20}$$

θ and p follow from the double layer measurements, hence all data to solve the Hoeve equations are available.

For the calculations weight average degrees of polymerization were used, to account for the preferential adsorption of the higher molecular weight molecules. We used $M_s = 44.9$, $(2Cl^2)^{0.5} = 0.58$ nm and $\chi = 0.487$. For the molecular cross section, $a_{0,s}$, 0.15 nm^2 was taken and for $\delta = 0.4$ nm: these values correspond with the value of the specific volume, $v = 0.77$ cm^{3}g^{-1} (BRANDRUP and IMMERGUT 1965).

Firstly σ_H, c_H, λ_H and K_H are calculated, substituting various combinations of Γ_p, c_p, θ and p belonging to the plateau region of the isotherm, in the above set of equations. The plateau region is chosen because of the presence of long loops, so that the Hoeve model is expected to apply relatively satisfactory. The various sets of experimental data lead to slightly varying values for the theoretical parameters. For σ_H and c_H average values were obtained and these data in turn were used to find the theoretical isotherm.

The results of our calculations expressed as average values for K_H, c_H and σ_H are shown in table 7–2. The value of λ_H depends upon the adsorbed amount, it is tabulated for $c_p = 150$ mg dm^{-3} only. Adsorption isotherms for three PVA samples and $p(\Gamma_p)$ and $\theta(\Gamma_p)$ were calculated using c_H and ln σ_H as obtained for PVA 13–98. The results are shown in figs. 7–4 and 7–5 respectively, together with the experimentally obtained curves.

TABLE 7–2. The essential parameters of the Hoeve model for polymer adsorption calculated for the PVA-AgI system. ($M_s = 44.9$, $(2Cl^2)^{0.5} = 0.58$ nm, $\chi = 0.487$, $\delta = 0.4$ nm, $a_{0,s} = 0.15$ nm^2).

PVA	m_w	K_H	c_H	$ln\ \sigma_H$	λ_H[1])
3–98	700	1.3679	0.5562	0.1668	–0.0219
13–98	2700	1.0352	0.3110	0.5075	–0.0095
48–98	4850	1.0887	0.3414	0.4670	–0.0081

[1]) $c_p = 150$ mg dm^{-3}.

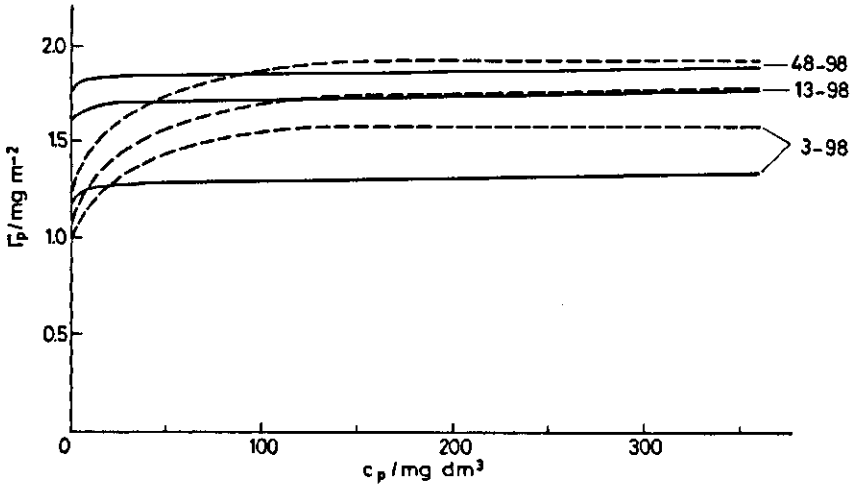

FIG. 7-4. Adsorption isotherms for PVA 98 as predicted with the Hoeve model (—), compared with experimentally obtained isotherms, (- - -).
Parameter values: $c_H = 0.3110$, $\ln \sigma_H = 0.5075$, $a_{0,s} = 0.15$ nm^2, $(2\,Cl^2)^{0.5} = 0.58$ nm, $M_s = 44.9$, $\chi = 0.487$.

Before discussing the actual values of the parameters we would like to make a few comments on the two figures.

The theoretical isotherms have a strong high-affinity character. Although the ideal experimental curves probably are somewhat steeper initially (see sect. 5.4.4.) than those shown in fig. 7-4, it seems unlikely that they become as steep as the model isotherms would predict. A similar difference is observed for

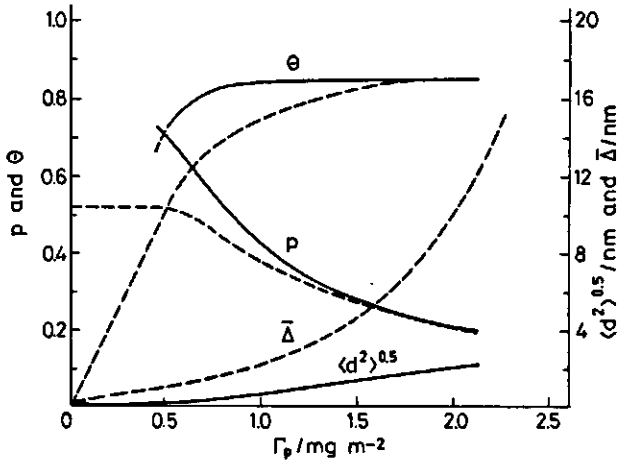

FIG. 7-5. The degree of occupancy of the first layer, θ, the fraction of segments in this layer, p, the root mean square distance of segments in loops from the surface, $<d^2>^{0.5}$, and the electrophoretic thickness, $\bar{\Delta}$, as a function of the amount adsorbed. The drawn curves are predicted by the Hoeve model, the dashed curves were obtained experimentally. In the Hoeve model the following parameter values were used: $c_H = 0.3110$, $\ln \sigma_H = 0.5075$, $a_{0,s} = 0.15$ nm^2, $(2Cl^2)^{0.5} = 0.58$ nm, $M_s = 44.9$ and $\chi = 0.487$.

p and θ. The differences can be explained by the fact that eqs. (7.8) to (7.12) only apply for large loops and low segment densities in the loop region. For small loops it becomes entropically less favourable to adsorb, taking this into account the model isotherm would bend more gradually towards its 'plateau' value: similar reasoning applies to θ.

The molecular weight dependence of the adsorption is reasonably well predicted for PVA 48–98, but only moderately for PVA 3–98. This last finding is not surprising, as discussed before we assume a strong preferential adsorption of the higher molecular weight species in this PVA sample.

A notable feature of fig. 7–5 is that the model predicts that the fraction of train segments and the degree of occupancy of the first layer are a function of the adsorbed amount *only*. This is due to the fact that c_H and σ_H are considered to be constants, independent of M and because the presence of tails is ignored in the model. Although the actual values are different, experimentally the same behaviour was found: p and θ are a function of Γ_p *only*. Our conclusion is that the model explains the trends in Γ_p, p and θ and that it is capable of predicting reasonable values for these parameters when large loops are present. Conversely, c_H and σ_H are only constants in the plateau region.

Assuming an exponential segment density distribution for the loop region (HOEVE 1965), it is also possible to calculate the root mean square distance of segments in loops from the surface, $<d^2>^{0.5}$. According to HOEVE (1966)

$$<d^2>^{1/2} = 2^{-1}3^{-1/2}\,(nCl^2/m)^{1/2}\,(-\lambda)^{-1/2} \tag{7.21}$$

or for PVA 98

$$<d^2>^{1/2} = 0.1662\,(-\lambda)^{-1/2}$$

In contradistinction with the behaviour of p or θ, the extent of the adsorbed layer is very poorly predicted by the model. From fig. 7–5 it can be seen that $<d^2>^{0.5} << \bar{\Delta}$. Apparently the values of $(-\lambda)$ are too large, or alternatively, the experimentally observed layer thickness should be determined by a few tails protruding far into the solution phase. This last possibility seems not very likely, as it would result in a very high segment density in the loop region.

Another important criterion for a model to be used is the physical reality of its basic parameters, in the present case c_H, K_H and ln σ_H. Of these parameters the easiest to interpret is K_H or rather $1-K_H$, denoting the drop in segment density at the transition from the first to the second layer. It is clear that the obtained values of K_H are too large and physically unrealistic. These large values of K_H may be due to the relatively high experimental adsorption values. In order to accommodate all that material in the adsorbed layer a large K_H is required. However, the adsorption values found, are not uncommon for PVA, similar and even larger adsorptions have been found on Sterling-FT carbon black (Koopal 1976) and on polystyrene (GARVEY et al. 1974, VAN DEN BOOMGAARD et al. 1978). Another cause for large values of K_H (PVA 98) could be the

presence of the supposed intramolecular interactions. These might give rise to a more compact segment density distribution.

Theoretically, large values of K_H reflect relatively flexible chains and in the case of high adsorption values a not too small magnitude of σ_H is expected. To verify this, the parameters c_H, K_H and σ_H of PVA have been calculated form theory, using eqs. (7.13), (7.14), (7.17) and (7.18) with $C = 7$. The results are

$$w = 12,\ c_H = 0.007,\ K_H = 0.07,\ \ln \sigma_{H,cr} = -0.02$$

The values of K_H and c_H thus obtained are considerably lower than the experimental ones. Even for very flexible chains ($w = 1$) the theoretical prediction of c_H ($= 0.102$) is much lower than the present experimental values. The value of $\ln \sigma_H$ obtained from the experiment exceeds $\ln \sigma_{H,cr}$ by about 0.5, suggesting that the adsorption energy per segment is only $0.5\,kT$ greater than the critical value. In view of the discussion given in sect. 7.1. this predicted value for the adsorption energy seems rather small.

Despite the fact that the model predicts reasonable values for the adsorption isotherm and the correct trends for p and θ, we have to conclude that the physical significance of the values obtained for the model parameters is obsure.

At first sight, a source of error might have been the choice of a CH_2-CHOH group as a segment. The model is based upon a flexible polymer chain which can be described by statistical means and each polymer segment is thought to be equal in size to a solvent molecule. With the CH_2-CHOH group as a segment none of these conditions are satisfied. The first prerequisite could be fulfilled by the introduction of a statistical chain element, s.c.e. (KUHN 1934), as suggested by HOEVE (1971). The number of s.c.e., N, and their length, L, can be calculated for each PVA sample with eqs. (4.19) and (4.20) using C and taking for the contour length, h_m, the planar zig-zag of the all-trans conformation with a distance of 0.253 nm between the alternate carbon atoms (MORAWETZ 1965, p. 120):

$$N = n(1.48\,C)^{-1} \qquad N_{\mathrm{PVA98}} = n/10.3$$
$$L = 0.187\,C \qquad L_{\mathrm{PVA98}} = 1.31 \quad \text{(nm)}$$

Apparently, this choice of a segment removes only one of the objections, a s.c.e. becomes about 5 times as big as a solvent molecule. Conversely, the ratio of molecular volumes of the polymer and the solvent could be used to define a segment. In this case, half a PVA segment would be the unit, having within 5% the same molecular volume as a water molecule. An additional advantage would be that the polymer-solvent interaction parameter, χ, is based upon the same choice. However, in doing so, the first condition is no longer fulfilled. It is difficult to decide *a priori* which violation of these assumptions will cause the worst error. Therefore c_H, K_H and $\ln \sigma_H$ were recalculated with both types of segment. However, the thus obtained values of the model parameters were not physically more significant. When a s.c.e. is used c_H, K_H and $\ln \sigma_H$ differed

strongly for the different molecular weights. In the case that half a PVA segment was used as the unit, K_H went up to about 1.6 and also c_H became larger.

A final attempt at improvement was made by adjusting the χ-parameter. In the adsorbed layer region χ may be different from its value in bulk solution due to the difference in surroundings. It is also possible that due to structuring effects by the solid the first solvent layer behaves differently. For a not complete homopolymer as PVA 98 preferential adsorption of acetate containing segments may well occur and segmental interactions may become different from those in bulk. The latter two possibilities would demand for larger values of of χ, thus a worse solvent quality or larger segment-segment interactions.

Calculating K_H, c_H and ln σ_H with $\chi = 0.5$ and $\chi = 0.52$ showed an improvement in the values of K_H and c_H, though the actual values were still much higher than the theoretically predicted ones. Also better values for ln σ_H were found. However, with these values for χ the model predicted poorly the molecular weight dependence. Introducing an enhanced value of χ in the first layer only would decrease ln σ_H, leaving the other parameters unaltered.

Overlooking the above discussion we have to conclude that the Hoeve theory does not give a physically realistic description of the adsorption of PVA on AgI. PVA may not be the best example of a flexible homopolymer, due to the presence of intramolecular interactions and 2 mole % acetate groups. However we believe that also in case of a better model polymer some problems remain unsolved, for instance, what to choose for a segment. It seems worthwile to look for ways to overcome this problem so that a better quantitative comparison of model and experiment becomes feasible.

7.4. Summary

Using the experimentally obtained adsorption paramaters, Γ_p, θ and $\bar{\jmath}$ several other characteristics of the adsorbed layer were calculated, such as: the fraction of segments in the first layer, p, the amount adsorbed in loops and tails and the volume fraction of polymer in the adsorbed layer. Molecules adsorbing in the isolated state ($\Gamma_p \rightarrow 0$) do not completely unfold, probably due to the presence of intramolecular interactions. Values of p at large Γ_p and the extent of unfolding at intermediate adsorption values suggest a free energy change of about $-2\ kT$ when adsorbed solvent molecules are replaced by a polymer segment. The average density in the loop region is relatively high, indicating that the average loop size is much smaller (1/6 to 1/20) than the total chain length.

The obtained adsorption parameters of PVA 98 allowed us to investigate the Hoeve model for polymer adsorption. The adsorbed amount at large c_p and its molecular weight dependence were reasonably well predicted. Also the qualitative trends in $p(\Gamma_p)$ and $\theta(\Gamma_p)$ were confirmed.

However, the adsorbed layer thickness is very poorly predicted and the physical significance of the values of the model parameters remains obscure.

It was not possible to obtain a consistent set of physically realistic model parameters by introducing a number of adjustments. Our general conclusion is that the Hoeve theory does not satisfactorily describe the adsorption of PVA on AgI.

SUMMARY

The purpose of this study was to investigate how the double layer properties of charged particles are modified by the presence of adsorbed polymer molecules and to obtain information on the conformation of the polymer layer from the observed alterations in the double layer properties.

In chapter 1. the use of double layer investigations to obtain insight in the adsorbed layer conformation is briefly outlined. Some theoretical and experimental aspects of the studies of polymer adsorption are shortly reviewed.

For the experiments the AgI-PVA system is chosen. Double layer charge and potential of AgI dispersed in aqueous electrolytes can be determined and controlled. Much is known about the surface area determination and the stability of AgI. PVA is a water soluble, flexible and uncharged polymer of which the concentration in solution can be determined readily. The combined AgI-PVA system is well suited for the purpose of this study. For the interpretation of the results recourse can be made to similar information previously obtained with low molecular weight alcohols.

The general procedures and the preparation of the AgI precipitates and sols are given in chapter 2.

Chapter 3. deals with the characterization of the specific surface area of the AgI samples. Several independent methods are used: capacitance measurements, N_2-adsorption, adsorption from solution and electron microscopy. Accepting an uncertainty margin of 10 to 20% the areas obtained by the last three methods compared well mutually. However, the capacitance areas were always 3 to 4 times greater. This disparity was observed before by VAN DEN HUL and LYKLEMA. Surface areas of AgI sols strongly reduce upon coagulation or precipitation. A subsequent heat treatment enhances this effect.

We used the capacitance area in electrochemical studies, whereas for the adsorption of organic molecules the methylene blue adsorption area is chosen, otherwise unrealistically low adsorption values were found.

In chapter 4. the properties and solution characteristics of PVA are described. The samples used, differing in molecular weight and acetate content, are characterized by IR and UV spectroscopy. It could be concluded that our samples are atactic, contain no or very little 1,2-glycol units and one or two conjugated carbonyl groups per molecule. The acetate groups in PVA 88 (12 mole % acetate groups) are predominantly distributed in blocks along the polymer chain, whereas in PVA 98 the distribution of these groups is probably random. Molecular weights and the molecular weight distributions were determined by viscometry and gel permeation chromatography.

The solution properties of the polymers in water have also been studied by viscometry. Unperturbed dimensions, linear expansion factors and polymer-solvent interaction parameters are calculated, taking heterodispersity into

account. The relative magnitude of the steric hindrance or the characteristic ratio, combined with the fact that water is a poor solvent for PVA suggest that intramolecular interactions occur in the polymer chain.

Chapter 5. covers the measurement of the mass of PVA adsorbed per m^2 AgI, Γ_p, as a function of the PVA concentration. Special emphasis is given to the influence of molecular weight, acetate content and of the surface charge and state of dispersion of the AgI. The adsorption isotherms show a high-affinity character, leading to a maximum amount adsorbed of 1.5 to 2.6 mg m^{-2}. The saturation adsorption increases with increasing molecular weight and acetate content. The surface charge of the AgI and its state of dispersion have no measurable influence on the adsorption. The reduction in adsorption by the addition of KNO_3 up to 10^{-1}M is due to a decrease in available surface area.

No desorption of the polymer could be detected upon dilution with solvent, but the increase in adsorption with time shows that the adsorbed segments are reversibly bound.

In chapter 6. the principles of the double layer investigations are explained, whereafter a description is given of the potentiometric titrations and electrophoresis studies. The titrations reveal three important features upon adsorption of PVA:

- the double layer capacitance decreases,
- the p.z.c. moves to more positive values,
- the curves pass through a common intersection point, characteristic for the type of PVA.

These features reflect changes in the Stern-layer, caused by adsorbing polymer trains. Adsorbed polymer trains and low molecular weight adsorbates having a composition comparable with that of the polymer segments behave very similarly in the Stern-layer. From this resemblance it could be concluded that in PVA 88 segments with an acetate group adsorbed preferentially in the first layer. This is promoted by the blocky distribution of these groups in PVA 88. The similarity has further been used to develop a theorem to obtain the degree of occupancy of train segments in the Stern-layer, θ. The obtained result is confirmed by electrophoresis studies. A measure of the effective layer thickness can be found from the slope of the electrophoretic mobility against pAg curve around the isoelectric point. It was shown that this procedure is superiour to the classical one, in which the effective layer thickness is deduced from the reduction of the mobility in the plateau region.

The main conclusion is that the fraction of polymer adsorbed in trains and the effective layer thickness are a function of the adsorbed amount only. Molecular weight and acetate content affect the adsorbed amount and thus indirectly influence the occupancy in the first layer and the effective thickness. Except for PVA 3-98, where probably preferential adsorption of higher molecular weight species occurs, the layer thickness is proportional to the square root of the degree of polymerization, as expected theoretically. The dependence of the train segment adsorption on the surface charge, though in principle present, is

too small to be practically important. The layer thickness is also independent of the surface charge.

In chapter 7. some further parameters of the adsorbed layer are calculated, such as the fraction of segments adsorbed in trains, p, and the amount adsorbed in loops and tails. It can be concluded that molecules adsorbed in the isolated state ($\Gamma_p \rightarrow 0$) do not completely unfold, probably due to the presence of intra molecular interactions. The average segment density in the loop region is relatively high, indicating that the average loop length is much shorter than the total chain length.

The obtained adsorption parameters are used for a quantitative check of the Hoeve model for polymer adsorption. The adsorbed amount at large polymer concentration is reasonably well predicted, including the molecular weight dependence. Also the trends in $p(\Gamma_p)$ and $\theta(\Gamma_p)$ were confirmed. However, the adsorbed layer thickness is very poorly predicted and the physical significance of the model parameters is obscure. Our general conclusion therefore is that the Hoeve model cannot fully describe the adsorption of AgI on PVA.

In conclusion, this study shows that double layer investigations combined with polymer adsorption measurements provide a valuable tool to investigate the conformation of adsorbed polymers. The degree of occupancy of the first layer, the effective thickness of the adsorbed layer and the kind of segments directly adsorbed onto the surface could be determined over a wide adsorption range.

ACKNOWLEDGEMENTS

This work was carried out in the Laboratory of Physical and Colloid Chemistry of the Agricultural University of Wageningen, the Netherlands.

The author is much indebted to Prof. Dr. J. LYKLEMA for his stimulating guidance and discussions during tne course of this work.

A considerable part of the experimental work was skillfully performed by miss J. HIBMA and Mr. T. C. M. BOONMAN.

Dr. D. J. GOEDHART of the AKZO research Laboratory, Arnhem, is kindly acknowledged for the GPC measurements and Dr. A. H. HERZ of Eastman Kodak research Laboratories, Rochester, for the gift of pure dye samples.

Thanks are also due to Mr. G. BUURMAN, who prepared the drawings and to the secretaries who did much of the typing of the manuscript.

Dr. R. J. AKERS was kind enough to correct the English text of this thesis.

The friendship and helpfulness of all members of the department is gratefully acknowledged and has been of great profit.

SAMENVATTING

Het doel van dit onderzoek was 1. na te gaan op welke wijze de eigenschappen van de elektrische dubbellaag rond een geladen deeltje veranderen door de aanwezigheid van geadsorbeerd polymeer en 2. deze informatie te gebruiken voor de beschrijving van de ruimtelijke structuur, of conformatie van het geadsorbeerde polymeer.

In hoofdstuk 1. is kort aangegeven hoe het onderzoek van de dubbellaag kan leiden tot inzicht in de polymeerconformatie. Daarnaast wordt een beknopt overzicht gegeven van enkele theoretische en experimentele aspecten van polymeeradsorptie.

Als model is gekozen voor het zilverjodide (AgI) – polyvinylalcohol (PVA) systeem. De eigenschappen van de elektrische dubbellaag op AgI deeltjes in waterige oplossingen in aanwezigheid van zouten en laagmolekulaire organische stoffen zijn al eerder uitvoerig onderzocht, evenals het stabiliteitsgedrag. Tevens is de bepaling van het (specifieke) oppervlak van AgI neerslagen grondig bestudeerd. PVA is een in water oplosbaar, flexibel en ongeladen polymeer, waarvan de concentratie in oplossing eenvoudig te bepalen is. Dit laatste is van belang voor het meten van adsorptie-isothermen. De combinatie AgI-PVA heeft als voordeel dat bij de interpretatie van de resultaten gebruik gemaakt kan worden van eerder gedane metingen aan AgI waarop laagmolekulaire alcoholen geadsorbeerd waren.

Algemene procedures en de bereiding van de gebruikte AgI neerslagen en solen zijn beschreven in hoofdstuk 2.

Hoofdstuk 3. behandelt de bepaling van het specifieke oppervlak van de AgI monsters. Er is gebruik gemaakt van verschillende onafhankelijke methoden zoals: capaciteitsmetingen, adsorptie van stikstofgas, adsorptie van kleurstoffen vanuit oplossing en van electronenmicroscopie. De uitkomsten van de laatste drie methoden stemden onderling redelijk overeen, de capaciteitsmethode gaf echter een oppervlak, dat 3 tot 4 maal zo groot was. Een dergelijk verschil werd al eerder gevonden door VAN DEN HUL en LYKLEMA. Het specifieke oppervlak van AgI solen is moeilijker te bepalen dan dat van AgI neerslagen. Vlokking leidt tot verkleining van het oppervlak. Dit wordt versterkt door daarna een warmtebehandeling te geven.

Bij de berekening van de wandlading van het AgI is gebruik gemaakt van net capaciteitsoppervlak. De adsorptie van PVA is echter berekend met het oppervlak verkregen uit methyleenblauw adsorptiestudies. Als ook hier het capaciteitsoppervlak werd gebruikt, zouden irreele waarden voor de adsorptie gevonden worden.

In hoofdstuk 4. is de karakterisering van het PVA beschreven. Ultraviolet en infrarood spectroscopie tonen aan, dat de monsters atactisch zijn en weinig 1,2-glycol eenheden en geconjugeerde carbonylgroepen bezitten. De acetaatgroepen in PVA 88 (12 mol % acetaat) zijn merendeels verdeeld in blokken langs

de polymeerketen, terwijl in PVA 98 deze verdeling waarschijnlijk willekeurig is. Molekuulgewichten en molekuulgewichtverdelingen van de monsters werden bepaald met viscosimetrie en gel-permeatie-chromatografie. Eveneens via viscositeitsmetingen werden de eigenschappen van PVA molekulen in oplossing bepaald, zoals: kluwenafmetingen, lineaire expansiefactoren en de χ-parameters. Hierbij werd rekening gehouden met de heterodispersiteit. De grootte van de berekende 'sterische hindering', gecombineerd met het feit dat water een zeer matig oplosmiddel is voor PVA, suggereert dat in oplossing intra-molekulaire interacties optreden.

Hoofdstuk 5. beschrijft de geadsorbeerde hoeveelheid PVA per m^2 AgI als functie van de polymeerconcentratie. Speciale aandacht is besteed aan de invloed van molekuulgewicht en acetaatgehalte van het PVA en van oppervlaktelading en dispersiegraad van het AgI. De adsorptie-isotherm stijgt in het begin zeer steil en buigt dan geleidelijk af naar een plateau bij 1,5 tot 2,6 mg m^{-2}. De maximale adsorptie neemt toe met toenemend molekuulgewicht en stijgt flink bij toenemend acetaatgehalte. De oppervlaktelading van het AgI en de dispersiegraad hebben geen duidelijke invloed op de adsorptie. Bij verdunning treedt geen desorptie op van hele polymeermolekulen. Uit de tijdsafhankelijkheid van adsorptie en het verloop van de titratie curven (H. 6.) blijkt, dat de adsorptie van segmenten wel reversible is.

In hoofdstuk 6. wordt verder uiteengezet hoe dubbellaagmetingen kunnen leiden tot gegevens omtrent de conformatie van een in die dubbellaag geadsorbeerd polymeer. Er wordt een beschrijving gegeven van de potentiometrische titraties en de electroforese metingen. De titraties, die tot het verband leiden tussen de oppervlaktelading en de wandpotentiaal, geven een drietal belangrijke veranderingen te zien ten gevolge van adsorptie van PVA:

- de capaciteit van de dubbellaag daalt bij toenemende PVA adsorptie
- het ladingsnulpunt verschuift in positieve richting
- de titratiecurven gaan door een gemeenschappelijk snijpunt, dat karakteristiek is voor het soort PVA.

Deze verschijnselen zijn terug te voeren tot veranderingen in de Stern-laag eigenschappen en worden veroorzaakt door de adsorptie van polymeer segmenten in deze laag. PVA segmenten geadsorbeerd in de Stern-laag (treinen) en vergelijkbare laagmolekulaire adsorbaten gedragen zich overeenkomstig. Uit de vergelijking van het gedrag van de adsorbaten kon geconcludeerd worden dat in PVA 88 de segmenten met een acetaatgroep bij voorkeur op het oppervlak adsorberen. Dit wordt bevorderd door de blokvormige verdeling van deze groepen langs de polymeerketen. De overeenkomst tussen hoog- en laagmolekulaire alcoholen is tevens gebruikt om een verband af te leiden, waarmee de bezetting van de eerste laag met trein segmenten kon worden berekend. De verkregen resultaten werden bevestigd door het electroforese onderzoek. Dit leverde bovendien een maat voor de dikte van de geadsorbeerde laag op. Voor de berekening hiervan is uitgegaan van de verandering van beweeglijkheid bij een variatie van de wandpotentiaal, gemeten rond het isoelectrischpunt.

De belangrijkste conclusie van het conformatie-onderzoek is, dat de fractie polymeer geadsorbeerd in de eerste laag en de effectieve laagdikte in eerste benadering beide alleen afhankelijk zijn van de geadsorbeerde hoeveelheid. Molekuulgewicht en acetaatgehalte beinvloeden deze grootheden slechts indirect. Hoewel de bezetting van de eerste laag in principe van de wandlading afhangt, is dit praktisch te verwaarlozen. Ook de laagdikte is hiervan onafhankelijk.

In hoofdstuk 7. worden nog enkele andere karakteristieke grootheden van de geadsorbeerde laag berekend, o.a. de fractie segmenten geadsorbeerd in treinen. Het blijkt, dat bij zeer lage adsorptie de molekulen niet geheel ontvouwen. Waarschijnlijk wordt dit tegengegaan door intra-molekulaire interacties. De gemiddelde segmentdichtheid in de luslaag is aanzienlijk hoger dan die in een polymeerkluwen in oplossing.

De gezamenlijke gegevens zijn tenslotte gebruikt om na te gaan of de adsorptie beschreven kon worden met het door HOEVE opgestelde model voor polymeeradsorptie. De geadsorbeerde hoeveelheid bij hoge polymeerconcentratie wordt redelijk voorspeld, evenals de molekuulgewichtsafhankelijkheid. Het verloop van de fractie segmenten in de eerste laag als functie van de geadsorbeerde hoeveelheid wordt globaal bevestigd. Slecht voorspeld wordt de geadsorbeerde laagdikte, terwijl ook de fysische betekenis van de model parameters onduidelijk is. De algemene conclusie is dan ook, dat de Hoeve-theorie de adsorptie van PVA op AgI niet bevredigend beschrijft.

Als eindconclusie kan gesteld worden, dat onderzoek van de electrische dubbellaag, gecombineerd met adsorptiemetingen, naast informatie omtrent de dubbellaagveranderingen zelf, ook waardevolle mogelijkheden biedt om de conformatie van geadsorbeerde polymeermolekulen te onderzoeken. De graad van bezetting van de eerste laag, het type segmenten aldaar geadsorbeerd en de dikte van de gehele laag konden worden bepaald in een interessant adsorptiegebied.

REFERENCES

ADELMAN, R. L., R. C. FERGUSON (1975) J. Polym. Sci. Polym. Chem. Ed. **13**, 891.
AGAR, G. A. (1961) Thesis, MIT, Cambridge, USA.
ALLEN, T. (1968) 'Particle size measurement, interpretation and application', J. Wiley and Sons, New York.
AMBLER, M. R., D. MCINTYRE (1975) J. Polym. Sci. Polym. Lett. Ed. **13**, 589.
ASH, S. G., D. H. EVERETT, G. H. FINDENEGG (1968) Trans. Faraday Soc. **64**, 2645.
ASH, S. G., D. H. EVERETT, G. H. FINDENEGG (1970) Trans. Faraday Soc. **66**, 708.
BARADAS, R. G., J. M. SEDLAK (1972) Electrochim. Acta **17**, 1901.
BARAN, A. A., I. I. KOCHERGA, I. M. SOLOMENTSEVA, O. D. KURILENKO (1976a) Kolloidn. Zh. **38**, 425 (392E).
BARAN, A. A., I. I. KOCHERGA, I. M. SOLOMENTSEVA, O. D. KURILENKO (1976b) Kolloidn. Zh. **38**, 16.
BARNETT, M. I. (1970) in 'Surface Area Determination', Proc. Int. Symp., IUPAC, Butterworth, London.
BASF (1969) Brochure Basische Analin und Soda Fabrik, Ludwigshaven, Germany.
BEACHELL, H. C., P. FOTIS, J. HUCKS (1951) J. Polym. Sci. **7**, 353.
BELTMAN, H. (1975) Dissertatie, Wageningen; Meded. Landbouwhogeschool Wageningen, 75-2.
BERESNIEWICS, A. (1959a) J. Polym. Sci. **35**, 321.
BERESNIEWICS, A. (1959b) J. Polym. Sci. **39**, 63.
BERG, H. (1937) Chemische Forschungsgesellschaft m.b.H. Ger. Pat. 673, 840.
BERGER, H. L., A. R. SCHULTZ (1965) J. Polym. Sci. A, **3**, 3643.
BERGMANN, K., C. T. O'KONSKI (1963) J. Phys. Chem. **67**, 2169.
BIJSTERBOSCH, B. H. (1965) Thesis, Utrecht; Commun. Agric. Univ. Wageningen, 65-4.
BIJSTERBOSCH, B. H., J. LYKLEMA (1965) J. Colloid Sci. **20**, 665.
BIJSTERBOSCH, B. H., J. LYKLEMA (1968) J. Colloid Interface Sci. **28**, 506.
BIJSTERBOSCH, B. H., J. LYKLEMA (1977) Adv. Colloid Interface Sci. in press.
BILLMEYER, F. W. (1966) 'Textbook of Polymer Science', Interscience Publ., New York.
BLEHA, T., L. VALKO (1976) Polymer. Vol. **17**, 298.
BLOMGREN, E., J. O'M. BOCKRIS, C. JESCH (1961) J. Phys. Chem. **65**, 200.
BOCKRIS, J. O'M., M. A. V. DEVANATHAN, K. MULLER (1963) Proc. Roy. Soc. A. **274**, 55.
BOCKRIS, J.O'M., E. GILEADI, K. MULLER (1967) Electrochim. Acta, **12**, 1301.
BOOMGAARD, VAN DEN, T., T. A. KING, T. F. TADROS, B. VINCENT (1978) J. Colloid Interface Sci. Submitted.
BOYER, S., M. C. PRETESEILLE (1966) Sci. Ind. Phot., **37**, 129.
BRANDRUP, J., E. H. IMMERGUT (1965) 'Polymer Handbook', Interscience Publ., New York.
BRASWELL, E. H. (1972) J. Phys. Chem., **76**, 4026.
BROOKS, D. E. (1973) J. Colloid Interface Sci. **43**, 687.
BROWN, A. S. (1934) J. Am. Chem. Soc. **56**, 646.
BRUNAUER, S., P. H. EMMETT, E. TELLER (1938) J. Am. Chem. Soc. **60**, 309.
BRUYN DE, H. (1942) Rec. Trav. Chim. **61**, 5, 12.
BURCHARD, W. (1961) Makromol. Chem. **50**, 20.
CHAN, D., D. J. MITCHELL, B. W. NINHAM, L. R. WHITE (1975a) J.C.S. Faraday Trans. II, **71**, 235.
CHAN, D., D. J. MITCHELL, L. R. WHITE (1975b) Faraday Discuss. Chem. Soc. **59**, 181.
CLARK, A. T., M. LAL, M. A. TURPIN, K. A. RICHARDSON (1975) Faraday Discuss. Chem. Soc. **59**, 189.
CLAYFIELD, E. J., E. C. LUMB (1974) J. Colloid Interface Sci. **47**, 6, 16.
COLL, H., D. K. GILDING (1970) J. Polym. Sci., A-2, **8**, 89.
CONWAY, B. E. (1977) Adv. Colloid Interface Sci. **8**, 91.

COOPER, I. L., J. A. HARRISON (1977) Electrochim. Acta **22**, 519.
CORRIN, M. L., N. S. STORM (1963) J. Phys. Chem. **67**, 1509.
COSGROVE, T., B. VINCENT (1978) to be published.
CRAIG, J. B., R. BAIN, P. MEARES (1967) Kolloid-Z. Z. Polym. **221**, 1.
DAMASKIN, B. B., A. N. FRUMKIN, A. CHIZHOV (1970) J. Electroanal. Chem. **28**, 93.
DAMASKIN, B. B., O. A. PETRI, V. V. BATRAKOV (1971) 'Adsorption of organic compounds on electrodes', Eng. Translation E. B. UVAROV, R. PARSONS, Ed., Plenum Press, New York.
DAMASKIN, B. B., A. N. FRUMKIN (1972) J. Electroanal. Chem. **34**, 191.
DAVIS, B. L., L. H. ADAMS (1964) Science **146**, 519.
DAWKINS, J. V. (1968) J. Macromol. Sci. Phys. B, **2**, 623.
DAWKINS, J. V., J. W. MADDOCK, D. COUPE (1970) J. Polym. Sci. A-2, **8**, 1803.
DAWKINS, J. V. (1972) British Polym. J. **4**, 87.
DEFAY, R., I. PRIGOGINE, A. BELLEMANS, D. H. EVERETT (1960) 'Surface Tension and Adsorption', Wiley, New York, Ch. 13.
DESPOTOVIC, R., V. HORVAT, S. POPOVIC, Z. SELIR (1974) J. Colloid Interface Sci. **49**, 147.
DETERMANN, H. (1968), 'Gel Chromatography', Springer Verlag, New York.
DHAR, H. P., B. E. CONWAY, K. M. JOSHI (1973) Electrochim. Acta **18**, 789.
DIALER, K., K. VOGLER, F. PATAT (1952) Helvetica Chim. Acta **35**, 869.
DIEU, H. A. (1954) J. Polym. Sci. **12**, 417.
DIMARZIO, E. A., R. J. RUBIN (1971) J. Chem. Phys. **55**, 4318.
DOI, M. (1975) J.C.S. Faraday Trans. II, **71**, 1721.
DONDOS, A. H. BENOIT (1971) Macromolecules **4**, 279.
DOUGLAS, H. W., J. BURDEN (1959) Trans. Faraday Soc. **55**, 350.
DUNCALF, B., A. S. DUNN (1973) in FINCH, Ch. 18.
ELIAS, H. G. (1972) 'Makromoleküle, Struktur-Eigenschaften-Synthesen-Stoffe', 2nd Ed., Hüthig und Wepf Verlag, Basel, Heidelberg.
EMMETT, P. H., S. BRUNAUER (1937) J. Am. Chem. Soc. **59**, 1553.
ENGEL, D. J. C. (1968) Thesis, State University, Utrecht.
ETTRE, L. S., N. BRENNER, E. W. CIERLINSKI (1962) Z. Physik. Chem. (Leipzig) **219**, 17.
EVERETT, D. H. (1965) Trans. Faraday Soc. **61**, 2478.
EVERETT, D. H. (1973) in Colloid Science **1**, A specialist Periodical Report, Chem. Soc. London, Ch. 2.
FELTER, R. E., L. N. RAY (1970) J. Colloid Interface Sci. **32**, 349.
FELTER, R. E. (1971) J. Polym. Sci. C. **34**, 227.
FINCH, C. A. (1973) 'Polyvinyl Alcohol, properties and applications' J. Wiley and Sons, London.
FINCH, C. A. (1973a) in FINCH, CH. 10.
FINCH, C. A. (1973b) in FINCH, Appendix 3.
FIXMAN, M. (1955) J. Chem. Phys. **23**, 1656.
FIXMAN, M. (1962) J. Chem. Phys. **36**, 3123.
FIXMAN, M. (1966a) J. Chem. Phys. **45**, 785.
FIXMAN, M. (1966b) J. Chem. Phys. **45**, 793.
FLEER, G. J. (1971) Thesis, Wageningen; Commun. Agric. Univ. Wageningen, 71-20.
FLEER, G. J. (1972) Unpublished results.
FLEER, G. J., L. K. KOOPAL, J. LYKLEMA (1972) Kolloid-Z. Z. Polym. **250**, 689; Kémiai Közlemények, **38**, 1.
FLEER, G. J., L. E. SMITH (1976a) Prague Meetings on Macromolecules, fifth Discuss. Conf. Lecture C 27.
FLEER, G. J., L. E. SMITH (1976b) Colloid and Interface Sci., vol. V, Acad. Press, New York.
FLEER, G. J., J. LYKLEMA (1976) J. Colloid Interface Sci. **55**, 228.
FLEMMING, J. (1973) Biopolym. **12**, 1975.
FLORY, P. J. (1942) J. Chem. Phys. **10**, 51.
FLORY, P. J., T. G. FOX (1951) J. Am. Chem. Soc. **73**, 1904.
FLORY, P. J. (1953) 'Principles of Polymer Chemistry', Cornell Univ. Press, Ithaca.
FLORY, P. J., S. FISK (1966) J. Chem. Phys. **44**, 2243.

FLORY, P. J. (1969) 'Statistical Mechanics of Chain Molecules', Wiley, New York.
FLORY, P. J. (1975) Science, **188**, 1268.
FONTANA, B. J., J. R. THOMAS (1961) J. Phys. Chem. **65**, 480.
FORBES, E. S., A. J. GROSZEK, E. L. NEUSTADTER (1970) J. Colloid Interface Sci. **53**, 629.
FORSMAN, W. C., R. E. HUGHES (1963) J. Chem. Phys. **38**, 2118, 2123, 2130.
FOX, K. K., I. D. ROBB, R. SMITH (1974) J. C. S. Faraday I, **70**, 1186.
FREED, K. F., S. F. EDWARDS (1975) J. Chem. Phys. **62**, 4032.
FRISCH, H. L., R. SIMHA, F. R. EIRICH (1953) J. Chem. Phys. **21**, 365.
FRUMKIN, A. N. (1925) Z. Phys. Chem. **116**, 466.
FRUMKIN, A. N. (1926) Z. Phys. **35**, 792.
FUJII, K., T. MOCHIZUKI, S. IMOTO, J. UKIDA, M. MATSUMOTO (1964) J. Polym. Sci. A, **2**, 2327.
FUJII, K. (1967) J. Polym. Sci. Polym. Lett. Ed. **5**, 551.
FUJII, K. (1971) Macromol. Rev. **5**, 431.
FUJIWARA, Y., S. FUJIWARA, K. FUJII (1966) J. Polym. Sci. A-1, **4**, 257.
GARVEY, M. J., T. F. TADROS, B. VINCENT (1974) J. Colloid Interface Sci. **49**, 57.
GARVEY, M. J., T. F. TADROS, B. VINCENT (1976) J. Colloid Interface Sci. **55**, 440.
GEBHARD, H., E. KILLMANN (1976) Angew. Makromol. Chem. **53**, 171.
GILEADI, E. (1967) 'Electrosorption', Plenum Press, New York.
GILES, C. H., S. N. NAKHWA (1962) J. Appl. Chem. **12**, 266.
GILES, C. H., A. P. D'SILVA, A. S. TRIVEDI (1970) in 'Surface Area Determination', Proc. Int. Symp., IUPAC, Butterworth, London.
GILES, C. H., D. SMITH, A. HUITSON (1974a) J. Colloid Interface Sci. **47**, 755.
GILES, C. H., A. P. D'SILVA, I. A. EASTON (1974b) J. Colloid Interface Sci. **47**, 766.
GILES, C. H., V. G. AGNIHOTRI, N. MCIVER (1975) J. Colloid Interface Sci. **50**, 24.
GILS VAN, G. E., H. R. KRUYT (1936) Kolloid-Beih. **45**, 60.
GOEDHART, D. J. (1975) personal communication.
GOUY, G. (1910) J. Phys. **9**, (4), 457.
GOUY, G. (1917) Ann. Phys. **7**, (9), 129.
GRAHAME, D. C. (1947) Chem. Rev. **41**, 441.
GRANATH, K. A. (1958) J. Colloid. Sci. **13**, 308.
GRAUBNER, H. (1967) Kolloid-Z. Z. Polym. **220**, 111.
GRAVES, R. E., P. I. ROSE (1975) J. Phys. Chem. **79**, 746.
GREENLAND, D. J. (1963) J. Colloid Sci. **18**, 647.
GREENLAND, D. J. (1972) Meded. Fakulteit Landbouwwetenschappen State University, Gent, Belgium **37**, 897, 915.
GREGG, S. J., K. S. W. SING (1967) 'Adsorption, Surface Area and Porosity', Acad. Press, London.
GREGG, S. J. (1972) in 'Surface Chemistry and Colloids', Phys. Chem., Ser. one, MTP. Int. Rev. Sci. **7**, M. KERKER Ed., Butterworth, London.
GRUBER, E., B. SOEHENDRA, J. SCHURZ (1974) J. Polym. Sci. Symp. Ser. **44**, 105.
GRUBISIC, Z., P. REMPP, H. BENOIT (1967) J. Polym. Sci. B, **5**, 753.
GUAITA, M., O. CHIANTORE (1975) Makromol. Chem. **176**, 185.
GULBEKIAN, E. V., G. E. J. REYNOLDS (1973) in FINCH, CH. 17.
HAAS, H. C. (1957) J. Polym. Sci. **26**, 391.
HAAS, H. C., H. HUSSEK, L. D. TAYLOR (1963) J. Polym. Sci. A, **1**, 1215.
HAAS, H. C. (1973) in FINCH, CH. 19.
HACKEL, E. (1968) in 'Properties and applications of polyvinyl alcohol', C. A. FINCH Ed., S.C.I. monograph **30**, London, CH. 1.
HAYASHI, S., C. NAKANO, T. MOTOYAMA (1964) Kobunski Kagaku **21**, 300 and 304, C.A. **62** (1965) 9249 g and 9249 h.
HAYDON, D. A., G. V. F. SEAMAN (1962) Proc. Roy. Soc. **B156**, 533.
HENRY, D. C. (1931) Proc. Roy. Soc. A. **133**, 106.
HERDAN, G. (1960) 'Small particle statistics', Butterworth, London.
HERMANN, W. O., W. HAEHNEL (1927) Ber. dt. Chem. Ges. **60**, 1658.

HERMANN, W. O., W. HAEHNEL, H. BERG (1932), Chemische Forschungsgesellschaft m.b.H. Ger. Pat. 642, 531.
HERZ, A. H., J. O. HELLING (1966) J. Colloid Interface Sci. **22**, 391.
HERZ, A. H., R. P. DANNER, G. A. JANUSONIS (1968) Adv. Chem. series **79**, Am. Chem. Soc., Washington, D.C., 173.
HERZ, A. H. (1974) personal communication.
HERZ, A. H. (1975) Photogr. Sci. Eng. **18**, 323.
HESSELINK, F. T. (1969) J. Phys. Chem. **73**, 3488.
HESSELINK, F. T. (1971) J. Phys. Chem. **75**, 65.
HESSELINK, F. T. (1975) J. Colloid Interface Sci. **50**, 606.
HEYWOOD, H. (1947) Symp. Particle Sice Analysis, Inst. Chem. Eng. Suppl. **25**, 14.
HEYWOOD, H. (1970) in 'Surface Area Determination', Proc. Int. Symp. IUPAC, Butterworth, London.
HILLSON, P. J., R. B. MCKAY (1965) Trans. Faraday Soc. **61**, 374.
HOEVE, C. A. J., E. A. DIMARZIO, P. PEYSER, (1965) J. Chem. Phys. **42**, 2558.
HOEVE, C. A. J. (1965) J. Chem. Phys. **43**, 3007.
HOEVE, C. A. J. (1966) J. Chem. Phys. **44**, 1505.
HOEVE, C. A. J. (1970) J. Polym. Sci. C, **30**, 361.
HOEVE, C. A. J. (1971) J. Polym. Sci. C, **34**, 1.
HOEVE, C. A. J. (1976) Prague Meetings on Macromolecules, fifth Discuss. Conf. Lecture C-L12.
HOFFMANN, R. F., W. C. FORSHMAN (1970) J. Polym. Sci. A-2, **8**, 1847.
HORACEK, J. (1962) Chem. Prumysl. **12**, 385; C.A. **58**, 10305f.
HUGGINS, M. L. (1942) Ann. N.Y. Acad. Sci. **43**, 1.
HUL VAN DEN, H. J. (1966) Thesis, Utrecht; Commun. Agric. Univ. Wageningen, 66-2.
HUL VAN DEN, H. J., J. LYKLEMA (1967) J. Colloid Interface Sci. **23**, 500.
HUL VAN DEN, H. J., J. LYKLEMA (1968) J. Am. Chem. Soc. **90**, 3010.
HUL VAN DEN, H. J., J. LYKLEMA (1970) in 'Surface Area Determination', Proc. Int. Symp. IUPAC, Butterworth, London.
INAGAKI, H., H. SUZUKI, M. KURATA (1966) J. Polym. Sci. C, **15**, 409.
INAGAKI, F., J. HARADA, T. SHIMANOUCHI, M. TASUNI (1972) Bull. Chem. Soc. Japan **45**, 3384.
INTERNATIONAL CRITICAL TABLES (1967) 3rd Report, contract no. CST 1265 (J. LYKLEMA).
IRANI, R. R., C. F. CALLIS (1963) 'Particle size, measurement, interpretation and application', J. Wiley and Sons, New York.
JAYCOCK, M. J., R. H. OTTEWILL, M. C. RASTOGI (1960) Proc. 3rd Int. Congr. Surface Activity **2**, 283.
JAYCOCK, M. J., R. H. OTTEWILL (1963) General Meeting, Institution of Mining and Metallurgy, 497.
JOPPIEN, G. R. (1974) Makromol. Chem. **175**, 1931.
JOPPIEN, G. R. (1975) Makromol. Chem. **176**, 1129.
KAVANAGH, B. V., A. M. POSNER, J. P. QUIRK (1975) Faraday Discuss. Chem. Soc. **59**, 242.
KAWAHARA, K., T. NORISUYE, H. FUJITA (1968) J. Chem. Phys. **49**, 4339.
KEIZER DE, A., J. LYKLEMA (1975) An Quim. **71**, 894.
KEIZER DE, A., (1977) to be published.
KENNY, J. F., G. W. WILLCOCKSON (1966) J. Polym. Sci. A-1, **4**, 690.
KILLMANN, E., R. ECKART (1971) Makromol. Chem. **144**, 45.
KILLMANN, E. (1976) Croat. Chem. Acta **48**, 463.
KIPLING, J. J. (1965) 'Adsorption from solutions of non-electrolytes', Acad. Press. London.
KIPLING, J. J., R. B. WILSON (1960) J. Appl. Chem. (London) **10**, 109.
KIRKWOOD, J. G., J. RISEMAN (1948) J. Chem. Phys. **16**, 565.
KITCHENER, J. A. (1972) Brit. Polym. J. **4**, 217.
KOOPAL, L. K. (1970) Doctoraal scriptie, Landbouwhogeschool, Wageningen.
KOOPAL, L. K., J. LYKLEMA (1975) Faraday Discuss. Chem. Soc. **59**, 230.
KOOPAL, L. K. (1976) unpublished results.

KRAGH, A. M., R. PEACOCK, G. S. REDDY (1966) J. Phot. Sci. **14**, 185.
KREVELEN VAN, D. W. (1972), 'Properties of polymers', Elsevier Sci. Publ. Comp., Amsterdam.
KUBIN, M. (1975) in 'Liquid Column Chromatography', J. Chrom. Library, **3**, Z. DEYL, K. MACEK, J. JANAK Eds., Elseviers Sci. Publ. Comp. Amsterdam.
KUHN, W. (1934) Kolloid-Z. **68**, 2.
KURARAY (1976) personal communication.
KURATA, M., H. YAMAKAWA (1958) J. Chem. Phys. **29**, 311.
KURATA, M., W. H. STOCKMAYER, (1963) Fortschr. Hochpolym. Forsch. **3**, 196.
KURATA, M., Y. TSUNASHIMA, M. IWAMA, K. KAMADA (1975) in 'Polymer Handbook', J. BRANDRUP, E. H. IMMERGUT Eds., J. Wiley and Sons, New York.
KUTA, J., I. SMOLER (1975) Collection Czechoslov. Chem. Commun. **40**, 225.
LAAR VAN J. A. W. (1952) Thesis, State University, Utrecht; see also J. T. G. OVERBEEK in 'Colloid Science' H. R. KRUYT Ed., Vol. **1**, p. 160 Elsevier, Amsterdam (1952).
LAAR VAN J. A. W. (1955) Dutch Patent 79, 472, november 15th.
LAL, M., R. T. F. STEPTO (1976) Prague Meetings on Macromolecules, fifth Discuss. Conf., Lecture C 17.
LANE, J. E. (1968) Aust. J. Chem. **21**, 827.
LANKVELD, J. M. G. (1970) Thesis, Wageningen: Commun. Agric. Univ. Wageningen, 70-21.
LANKVELD, J. M. G., J. LYKLEMA (1972a) J. Colloid Interface Sci. **41**, 454.
LANKVELD, J. M. G., J. LYKLEMA (1972b) J. Colloid Interface Sci. **41**, 466.
LANKVELD, J. M. G., J. LYKLEMA (1972c) J. Colloid Interface Sci. **41**, 475.
LIANG, C. Y., F. G. PEARSON (1959) J. Polym. Sci. **25**, 303.
LIJKLEMA, J. (1957) Dissertatie, State University, Utrecht.
LIPATOV, Y. S., L. M. SERGEEVA (1974) 'Adsorption of Polymers', Halstred Press, J. Wiley and Sons, New York.
LIPATOV, Y. S., L. M. SERGEEVA (1976) Adv. Colloid Interface Sci. **6**, 1.
LOEB, A. L., J. T. G. OVERBEEK, P. H. WIERSEMA (1960) 'The electrical double layer around a spherical colloid particle' MIT Press, Cambridge, Mass. USA.
LUTRICK, H. G., K. C. WILLIAMS, R. W. MAATMAN (1964) J. Chem. Ed. **41**, 93.
LYKLEMA, J., J. T. G. OVERBEEK (1961) J. Colloid. Sci. **16**, 595.
LYKLEMA, J. (1968) Adv. Colloid Interface Sci. **2**, 65.
LYKLEMA, J. (1977) in 'Trends in Electrochemistry', J. O'M BOCKRIS, D. A. J. RAND, B. J. WELCH Eds., Plenum. Publishing Corp. New York.
MACKOR, E. L. (1951) Rec. Trav. Chim. **70**, 663, 747, 763.
MACKOR, E. L., J. H. VAN DER WAALS (1952) J. Colloid Sci. **7**, 535.
MARK, M. B., E. N. RANDALL (1970) in 'Optical studies of adsorbed layers at interfaces', Faraday Soc. Symp. **4**, 157.
MARSZALL, L. (1974) Colloid and Polym. Sci. **252**, 335.
MATSUMOTO, M., K. IMAI (1959) J. Polym. Sci. **24**, 125.
MATSUMOTO, M., K. IMAI, Y. KAZUSA (1958) J. Polym. Sci. **28**, 426.
MATSUMOTO, M., M. MAEDA (1959) Kobunshi Kagaku **16**, 293.
MATSUMOTO, M., Y. OHYANAGI (1960) Kobunshi Kagahu **17**, 191.
MATSUZAWA, S., K. YAMAURA, H. NOGUHI (1974) Makromol. Chem. **175**, 31.
MCCAFFERTY, E. M. (1970) 'Laboratory preparation of macromolecular chemistry', McGraw-Hill, New York.
MCCLELLAN, A. L., H. F. HARNSBERGER (1967) J. Colloid Interface Sci. **23**, 577.
MCCRACKIN, F. L., J. P. COLSON (1964) Nat. Bur. Stand. Misc. Publ. **256**, 61, Washington.
MCCRACKIN, F. L. (1967) J. Chem. Phys. **47**, 1980.
MILLER, I. R., D. C. GRAHAME (1956) J. Am. Chem. Soc. **78**, 3577.
MILLER, I. R. (1971) in 'Progress in Surface and Membrane Science', J. F. DANIELLI, M. D. ROSENBERG, D. A. CADENHEAD Eds., Vol. 4, p. 299, Acad. Press. New York.
MILLER, I. R., D. BACH (1973) in 'Surface and Colloid Science', E. MATIJEVIC Ed., Vol. 6, p. 185, Wiley, New York.
MIYAMOTO, T., J. CANTON (1972) Makromol. Chem. **162**, 43.

MOORE, J. C. (1964) J. Polym. Sci. A-2, **1**, 835.
MOORE, J. C. (1967) in 'Characterization of macromolecular structure', Publ. 1573, Nat. Acad. Sci. Washington, 1968, p. 273.
MOORE, W. R. A. D., M.O'DOWD (1968) in 'Properties and Applications of polyvinyl alcohol', C. A. FINCH Ed., S.C.I. monograph, **30**, 77.
MOTOMURA, K., R. MATUURA (1968) Mem. Fac. Sci., Kyusha Univ. **C6**, 97.
MOTOMURA, K., R. MATUURA (1969) J. Chem. Phys. **50**, 1281.
MOTOMURA, K., K. SEKITA, R. MATUURA (1971a) Bull. Chem. Soc. Japan **44**, 1243.
MOTOMURA, K., K. SEKITA, R. MATUURA (1971b) Bull. Chem. Soc. Japan, **44**, 1248.
MUKERJEE, P., A. K. GOSH (1970) J. Am. Chem. Soc. **92**, 6403, 6408, 6413, 6415, 6419.
MURAHASHI, S. (1967) Pure and Appl. Chem. **15**, 435.
NAKAJIMA, A., K. FURUTATE (1949) Kobunshi Kagaku **6**, 460.
NELSEN, F. M., F. T. EGGERTSEN (1958) Anal. Chem. **30**, 1387.
NISHINO, Y. (1961) Bunseki Kagaku **10**, 656.
NORDE, W. (1976) Thesis, Wageningen: Commun. Agric. Univ. Wageningen, 76-6.
NORO, K. (1973a) in FINCH, CH. 3.
NORO, K. (1973b) in FINCH, CH. 4.
NYS, J. (1970) Dye Sensitization, Bressanova Symposium, Focal Press, London p. 26, 57.
OOMEN, J. J. C. (1965) Thesis, State University, Utrecht.
ONO, S., S. KONDO (1960) in 'Handbuch der Physik', S. FLÜGGE Ed., Springer Verlag, Berlin, Vol. 10, p. 134.
ORR, C., J. M. DALLAVALLE (1959) 'Fine particle measurement', The McMillan Comp. New York.
OVERBEEK, J. T. G. (1952) in 'Colloid science' Vol. 1, H. R. KRUYT Ed., Elsevier, Amsterdam.
OVERBEEK, J. T. G., E. L. MACKOR (1952) Compt. Rend. 3^{ieme} Réunion CITCE 1951, Milano p. 346.
OVERBEEK, J. T. G., A. WATILLON, J. M. SERRATOSA (1957) Rec. trav. Chim. **76**, 549.
PADDAY, J. F. (1964) Trans. Faraday Soc. **60**, 1325.
PADDAY, J. F., R. S. WICKHAM (1966) Trans. Faraday Soc. **62**, 1283.
PADDAY, J. F. (1968) J. Phys. Chem. **72**, 1259.
PADDAY, J. F. (1970a) in 'Surface Area Determination', Proc. Int. Symp. IUPAC, Butterworth, London, p. 331.
PADDAY, J. F. (1970b) in 'Surface Area Determination', Proc. Int. Symp. IUPAC, Butterworth, London, p. 401.
PARSONS, R. (1954) Trans. Faraday Soc. **55**, 999.
PARSONS, R. (1964) J. Electroanal. Chem. **7**, 136.
PARSONS, R. (1968) Rev. Pure Appl. Chem. **18**, 91.
PARSONS, R. (1976) Croat. Chem. Acta **48**, 597.
PATAT, F., E. KILLMANN, C. SCHLIEBENER (1964) Fortsch. Hochpolym. Forsch. **3**, 332.
PATRICK, R. L. (1967) 'Treatise on adhesion and adhesives', Marcel Dekker Inc., New York, Vol. **1**, 69.
PAYNE, R. (1973a) in 'Progress in Surface and Membrane Science', J. F. DANIELLI, M. D. ROSENBERG, D. A. CADENHEAD, Eds., Vol. **6**, 51, Acad. Press, New York.
PAYNE, R. (1973b) J. Electroanal. Chem. **41**, 277.
PEACOCK, R., A. M. KRAGH (1968) J. Phot. Sci. **16**, 229.
PERKEL, R., R. ULLMAN (1961) J. Polym. Sci. **54**, 127.
PIEPER, J. H. A., D. A. DE VOOYS (1974) J. Electroanal. Chem. **53**, 243.
PIEPER, J. H. A., D. A. DE VOOYS (1975) J. Electroanal. Chem. **65**, 429.
PIEPER, J. H. A. (1976) Thesis, State University, Utrecht.
PIERCE, C., B. EWING (1964) J. Phys. Chem. **68**, 2562.
PRIEL, Z., A. SILBERBERG (1970) Polymer Preprints **11**, 1405.
PRIGOGINE, I., J. MARECHAL (1952) J. Colloid Sci. **7**, 535.
PRITCHARD, J. G. (1970) 'Poly(vinyl alcohol), basic properties and uses', Gordon and Breach Science Publ., London.
ROBB, I. D., R. SMITH (1974) Eur. Polym. J. **10**, 1005.

ROE, R-J. (1965) J. Chem. Phys. **43**, 1591.
ROE, R-J. (1966) J. Chem. Phys. **44**, 4264.
ROE, R-J. (1974) J. Chem. Phys. **60**, 4192.
ROE, R-J. (1975) J. Chem. Phys. **62**, 490.
ROFFIA, S., G. FERROCI (1973) J. Electroanal Chem. **41**, 367.
RUBIN, R. J. (1965a) J. Chem. Phys. **43**, 2392.
RUBIN, R. J. (1965b) J. Res. Nat. Bur. Stand. (U.S.) **B69**, 301.
RUBIN, R. J. (1966) J. Res. Nat. Bur. Stand. (U.S.) **B70**, 237.
SAKAI, T. (1968a) J. Polym. Sci. A-2, **6**, 1535.
SAKAI, T. (1968b) J. Polym. Sci. A-2, **6**, 1659.
SAKAI, T. (1970) Macromolecules **3**, 96.
SAKURADA, I. (1944) Kogyo Kagaku **47**, 137.
SAKURADA, I., A. NAKAJIMA, H. FUJIWARA (1959) J. Polym. Sci. **35**, 497.
SAKURADA, I., (1968) Pure Appl. Chem. **16**, 263.
SCHEUTJENS, J. M. H. M. (1976) Doctoraal scriptie, Landbouwhogeschool, Wageningen.
SCHEUTJENS, J. M. H. M. (1978) to be published.
SCHOLTENS, B. J. R. (1977) Thesis, Wageningen; Commun. Agric. Univ. Wageningen, 77–7.
SCHRADER, M. E., A. BLOCK (1971) J. Polym. Sci. C, **34**, 281.
SENTI, F. R., N. N. HELLMAN, N. H. LUDWIG, G. E. BABCOCK, R. TOBIN, C. A. GLASS, B. L. LAMBERTS (1955) J. Polym. Sci. **17**, 527.
SHAKHOVA, E. M., S. I. MEERSON (1972) Kolloidn Zh. **34**, 579.
SHAW, D. J. (1969) 'Electrophoresis', Acad. Press, London.
SIDEBOTTOM, E. W., W. A. HOUSE, M. J. JAYCOCK (1976) J. C. S. Faraday I, **72**, 2709.
SILBERBERG, A. (1962a) J. Phys. Chem. **66**, 1872.
SILBERBERG, A. (1962b) J. Phys. Chem. **66**, 1884.
SILBERBERG, A. (1967) J. Chem. Phys. **46**, 1105.
SILBERBERG, A. (1968) J. Chem. Phys. **48**, 2835.
SILBERBERG, A. (1971) Pure Appl. Chem. **26**, 583.
SILBERBERG, A. (1972) J. Colloid Interface Sci. **38**, 217.
SILBERBERG, A. (1975) Faraday Discuss. Chem. Soc. **59**, 203.
SIMHA, R., H. L. FRISCH, F. R. EIRICH (1953) J. Phys. Chem. **57**, 584.
SIOW, K. S., D. PATTERSON (1973) J. Phys. Chem. **77**, 356.
SMITH, T. (1972) Adv. Colloid Interface Sci. **3**, 161.
SMITH, W. B., A. KOLLMANSBERGER (1965) J. Phys. Chem. **69**, 4157.
SMITH, W. R., D. G. FORD (1965) J. Phys. Chem. **69**, 3587.
SONNTAG, H. (1976) Croat. Chem. Acta **48**, 439.
SONNTAG, H. (1976) Prague Meetings on Macromolecules, fifth Discuss. Conf. Lecture C4.
SPARNAAY, H. J. (1972) 'The electrical Double Layer', Pergamon Press, Oxford.
STACY, C. J., R. L. ARNETT (1973) J. Phys. Chem. **77**, 78.
STAUDINGER, H. (1960) 'Die hochmolekularen organischen Verbindungen', Berlin 1932, 2nd ed.
STEGERHOEK, N. A. (1977) Doctoraal scriptie, Landbouwhogeschool, Wageningen.
STERN, O. (1924) Z-Electrochem. **30**, 508.
STOCKMAYER, W. H., A. C. ALBRECHT (1958) J. Polym. Sci. **32**, 215.
STOCKMAYER, W. H., M. FIXMAN (1963) J. Polym. Sci. C, **1**, 137.
STROMBERG, R. R. (1967) in 'Treatise on adhesion and adhesives', R. L. PATRICK Ed., Marcel Dekker Inc., New York, Vol 1, 69.
STROMBERG, R. R., L. E. SMITH, F. L. MCCRACKIN (1970) Discuss. Faraday Soc. **4**, 192.
SUGIURA, M., A. YABE (1970) Kogyo Kagaka Zasshi, **73**, 243.
SUGIURA, M. (1971) Bull. Soc. Phot. Sci. Tech. Japan. **21**, 22.
TADOKORO, H., K. KOZAI, S. SEKI, I. NITTA (1957) J. Polym. Sci. **26**, 379.
TADROS, T. F., J. LYKLEMA (1968) J. Electroanal. Chem. **17**, 267.
TADROS, T. F., J. LYKLEMA (1969) J. Electroanal. Chem. **22**, 1.
TANAKA, G., S. IMAI, H. YAMAKAWA (1970) J. Chem. Phys. **52**, 2639.
TANFORD, C. H. (1961) 'Physical Chemistry of Macromolecules', Wiley, New York.

TANI, T., S. KIKUCKI, K. HAYAMIZU (1967) J. Chem. Soc. Japan **70**, 1288.
TANI, T., S. KIKUCKI (1969) J. Phot. Sci. **17**, 33.
THURMOND, C. D., B. H. ZIMM (1952) J. Polym. Sci. **8**, 477.
TOYOSHIMA, K. (1973) in FINCH, CH. 2.
TRASATTI, S. (1970) J. Electroanal. Chem. **28**, 257.
TRASATTI, S. (1974) J. Electroanal. Chem. **53**, 335.
TUBBS, R. K., H. K. INSKIP, P. M. SUBRAMANIAN (1968) in 'Properties and applications of polyvinyl alcohol', C. A. FINCH Ed., S.C.I. monograph **30**, p. 95.
TUBBS, R. K., T. K. WU (1973) in FINCH, CH. 8.
TSUNEMITSU, K., H. SHOHATA (1968) in 'Properties and applications of polyvinyl alcohol', C. A. FINCH Ed., S.C.I. monograph **30**, p. 104.
TUNG, L. H. (1967) in 'Polymer fractionation', M. J. R. CANTOW Ed., Acad., Press, New York, CH. E.
VINCENT, B., J. LYKLEMA (1970) Special Discuss. Faraday Soc. **1**, 148.
VINCENT, B., B. H. BIJSTERBOSCH, J. LYKLEMA (1971) J. Colloid Interface Sci. **37**, 171.
VINCENT, B. (1974) Adv. Colloid Interface Sci. **4**, 193.
VLIET VAN, T. (1977) Thesis, Wageningen; Commun. Agric. Univ. Wageningen, 77-1.
VOOYS DE, D. A. (1976) Thesis, State University, Utrecht.
WACKER, (1975) Prospectus; personal communication.
WEN, W-Y. (1972) in 'Water and aqueous solutions', R. A. HORNE Ed., Wiley-Interscience, New York.
WEST, W., B. H. CAROLL, D. H. WHITCOMB (1952) J. Phys. Chem. **56**, 1054.
WIERSMA, P. H., A. L. LOEB, J. T. G. OVERBEEK (1966) J. Colloid Interface Sci. **22**, 78.
WINKLER, H. (1973) in FINCH, CH. 1.
WIT DE, J. N., J. LYKLEMA (1973) J. Electroanal. Chem. **41**, 259.
WIT DE, J. N. (1975) Dissertatie, Wageningen; Meded. Landbouwhogeschool Wageningen, 75-14.
WOJCIAK, W., E. DUTKIEWICZ (1964) Roczn. Chem. **38**, 271.
WOLFRAM, E., M. NAGY (1968) Kolloid-Z. Z. Polym. **227**, 86.
YACYNYCH, A. M., H. B. MARK, C. H. GILES (1976) J. Phys. Chem. **80**, 839.
YAMAKAWA, H. (1971) 'Modern theory of polymer solutions', Harper and Row Publ., New York.
YAMAKAWA, H., G. TANAKA (1971) J. Chem. Phys. **55**, 3188.
YOSHIDA, T., T. OHSAKA, S. TANAKA (1972a) Bull. Chem. Soc. Japan **45**, 326.
YOSHIDA, T., T. OHSAKA, H. YAMAMOTO (1972b) Bull. Chem. Soc. Japan **45**, 3236.
YOSHIDA, T., T. OHSAKA, M. SUZUKI (1972c) Bull. Chem. Soc. Japan **45**, 3245.
ZICHY, E. L., J. G. MORLEY, F. RODERIQUEZ (1973) Proc. VI Int. Congr. Surface Activity, Zürich 1972, **II**, 241 C, Hanser Verlag, München.
ZWICK, M. M., C. VAN BOCHOVE (1964) Text. Res. J. **34**, 417.
ZWICK, M. M. (1965) J. Appl. Polym. Sci. **9**, 2393.
ZWICK, M. M. (1966) J. Polym. Sci. A-1, **4**, 1642.

GLOSSARY OF SYMBOLS AND ABBREVIATIONS

Symbols and abbreviations that appear infrequently or in one section only are not listed.

ABBREVIATIONS

BET	Brunauer-Emmet-Teller
BuOH	n-butanol
BSF	Burchard-Stockmayer-Fixman
DEC	1,1′ diethyl 2,2′ cyanine
EG	ethylene glycol
ESBC	1 ethyl, 1′(4-sulfobutyl) 2,2′ cyanine
GPC	gel permeation chromatography
i.e.p.	isoelectric point
M	molarity
MB	methylene blue
MHS	Mark-Houwink-Sakurada
p.d.	potential determining
PVA	polyvinyl alcohol
p.z.c.	point of zero charge
s.c.e.	statistical chain element

SYMBOLS

a	exponent in the MHS equation (4.5)
a	particle radius
a_0	molecular cross section
$a_{0,s}$	*ibid.* of a PVA segment
A	polymer constant; eq (4.27)
B	polymer-solvent interaction parameter: eq (4.26)
c_i	concentration of component i
c_p	polymer concentration
C	characteristic ratio: eq. (4.17)
C	differential capacitance
C_d	*ibid.* of the diffuse part of the double layer
d	thickness of the Stern-layer
$<d^2>^{0.5}$	root mean square distance of segments in loops to the surface
F	the Faraday
$<h^2>_0^{0.5}$	unperturbed root mean square distance between the end points of a polymer chain: eq. (4.17)

$<h^2>^{0.5}$	*ibid*, perturbed
h_m	contour length of a polymer chain: eq. (4.20)
k	Boltzmann constant
k'	Huggins constant
K	constant in the MHS equation (4.5)
K_0	viscometric polymer constant: eq. (4.31)
l	length of a C–C bond
L	length of a s.c.e.: eq. (4.19)
m	number of segments in a polymer chain
M	molecular weight
M_n	*ibid.* number average
M_v, M_{va}	*ibid.* viscometric average
M_w	*ibid.* weight average
M_s	molecular weight of a polymer segment
n	number of skeletal carbon atoms in a polymer chain
N	number of s.c.e. in a polymer chain: eq. (4.19)
N_A	Avogadro's number
p	fraction of segments of a polymer chain adsorbed in the first layer
pAg	negative logarithm of the Ag^+ concentration
pAg^0	*ibid.* in the p.z.c.
pAg_m	*ibid.* in the common intersection point
pI	negative logarithm of the I^- concentration
r	distance from the centre of gravity
r_h	hydrodynamic radius
R	gas constant
$<s^2>_0^{0.5}$	unperturbed radius of gyration
$<s^2>^{0.5}$	radius of gyration
S_x	specific surface area, the subcript denotes the method
T	(absolute) temperature
UX^{-1}	electrophoretic mobility
v	partial specific volume of PVA
V_e	elution volume
V_1	molar volume of the solvent
$w(M)$	differential molecular weight distribution: eq. (4.8)
$W(M)$	integral molecular weight distribution: eq. (4.8)
x	distance to the surface
$(x/m)_s$	saturation adsorption
X	Kirkwood-Riseman draining parameter
$XF(X)$	Kirkwood-Riseman function: eq. (4.29)
X	field strength
z	excluded volume parameter: eq. (4.25)
α_h	linear expansion factor of the end-to-end distance
α_s	linear expansion factor of the radius of gyration: eq. (4.24)

α_η	linear viscosity expansion factor; eq. (4.36)
β	binary cluster integral for a pair of segments
$\beta(x)$	Brooks' excluded volume function
Γ_i^w	surface excess relative to water of component i
Γ_p	mass of polymer adsorbed per unit area
Γ_l	*ibid.* in loops
δ	thickness of a train segment
$\overline{\Delta}$	electrophoretic average thickness of the adsorbed layer: eq. (6.27)
ε	static permittivity
ε_r	relative static permittivity
ζ	electrokinetic or zeta potential
η	viscosity
$[\eta]$	intrinsic viscosity
$[\eta]_\Theta$	*ibid.* Θ-conditions
θ	fraction of the surface occupied with adsorbate
Θ	theta conditions
κ	reciprocal Debije length: eq. (6.35)
κ_B	reciprocal Debije-Brooks length: eq. (6.34)
λ	wavelength
ξ_x	proportionality factor relating the radius of gyration to the hydrodynamic radius: eq. (7.2), x denotes the type of velocity field
ρ_i	solid density of component i
$\rho(x)$	polymer segment density distribution
$<\rho_h>$	average segment density in a polymer coil in solution, based upon the hydrodynamic radius
$<\rho_l>$	average segment density in the loop region
σ_0	surface charge density; eq. (6.1)
σ_{0m}	*ibid.* at the common intersection point
σ_d	diffuse layer charge density
ϕ_{pb}	volume fraction of polymer in solution
ϕ_{pt}	average volume fraction in the train region
$<\phi_p>_\Delta$	average volume fraction in the loop region
Φ	Flory-Fox viscosity constant: eq. (4.35)
Φ_0	Flory's viscosity constant: eq. (4.29)
χ	potential at the interface originating from e.g. dipole orientation and polarization
χ	Flory-Huggins interaction parameter
ψ_0	surface potential: eq. (6.2)
ψ_d	diffuse double layer potential
$\psi(x), \psi(r)$	potential distribution

ENKELE PERSOONLIJKE GEGEVENS

Op 30 oktober 1942 ben ik geboren te Beetsterzwaag, gemeente Opsterland. De vooropleiding tot de studie aan de Landbouwhogeschool kreeg ik, na een jaar ULO school te Gorredijk, op het Drachtster Lyceum (afd. HBS-B) te Drachten.

Na vervulling van de militaire dienstplicht begon ik in 1963 de studie aan de Landbouwhogeschool te Wageningen. Het kandidaatsexamen Levensmiddelentechnologie (Chemisch-biologische specialisatie) werd afgelegd in juni 1968 en in september 1970 volgde het ingenieursexamen. De ingenieursstudie omvatte naast het hoofdvak Levensmiddelenchemie, de bijvakken Kolloidchemie (verzwaard) en Levensmiddelen microbiologie.

Sinds september 1970 ben ik werkzaam als wetenschappelijk medewerker aan het laboratorium voor Fysische en Kolloidchemie van de Landbouwhogeschool. In deze periode werd de onderwijsbevoegdheid Scheikunde behaald. In het kader hiervan heb ik o.a. ca. $1^1/_2$ jaar aktief deelgenomen aan de de werkzaamheden van de Commissie Modernisering Leerplan Scheikunde, sectie V.W.O.